VOL. 107 NO. IR1. MARCH 1981

JOURNAL OF THE IRRIGATION AND DRAINAGE DIVISION

PROCEEDINGS OF THE AMERICAN SOCIETY OF CIVIL ENGINEERS

AMERICAN SOCIETY OF CIVIL ENGINEERS FOUNDED 1852

VOL. 107 NO. IR1. MARCH 1981

JOURNAL OF THE IRRIGATION AND DRAINAGE DIVISION

PROCEEDINGS OF THE AMERICAN SOCIETY OF CIVIL ENGINEERS

ISSN 0044-7978

CONTENTS

This Journal is published quarterly by the American Society of Civil Engineers. Publications office is at 345 East 47th Street, New York, N.Y. 10017. Address all ASCE correspondence to the Editorial and General Offices at 345 East 47th Street, New York, N.Y. 10017. Allow six weeks for change of address to become effective. Subscription price to members is $7.50. Nonmember subscriptions available; prices obtainable on request. Second-class postage paid at New York, N.Y. and at additional mailing offices. IR.

DISCUSSION

Proc. Paper 16068

INFORMATION RETRIEVAL

The key words, abstract, and reference "cards" for each article in this Journal represent part of the ASCE participation in the EJC information retrieval plan. The retrieval data are placed herein so that each can be cut out, placed on a 3 × 5 card and given an accession number for the user's file. The accession number is then entered on key word cards so that the user can subsequently match key words to choose the articles he wishes. Details of this program were given in an August, 1962 article in CIVIL ENGINEERING, reprints of which are available on request to ASCE headquarters.

[a]Discussion period closed for this paper. Any other discussion received during this discussion period will be published in subsequent Journals.

16116 EMITTER DISCHARGE SENSITIVITY

KEY WORDS: **Drip irrigation; Emissions;** Pressure; Sensitivity; **Sensitivity analysis;** Temperature; Temperature effects; **Water pressure**

ABSTRACT: The discharge sensitivities to pressure and temperature of three types of emitters (helical long-path, labyrinth and vortex-type emitters) were determined in the laboratory. The measured discharge sensitivity to pressure was used to calculate the maximal permissible pressure variation in a field for the various emitters. The relative discharge distribution along an experimental pipe with helical long-path emitters was calculated on the basis of the measured temperature distribution and the computed pressure distribution. The resulting relative discharge distribution was curvilinear, in good agreement with the measured values. Under field conditions where water is heated as it flows in pipes exposed to solar radiation, emitter discharge along the second half of the pipe is determined by its specific discharge sensitivity to temperature.

REFERENCE: Zur, Benjamin, and Tal, S., "Emitter Discharge Sensitivity to Pressure and Temperature," *Journal of the Irrigation and Drainage Division,* ASCE, Vol. 107, No. IR1, **Proc. Paper 16116**, March, 1981, pp. 1-9

16115 HISTORY OF FEDERAL RESERVED WATER RIGHTS

KEY WORDS: **Federal control; Federal role;** Federal-state cooperation; History; Water allocation (policy); Water law; **Water policy; Water resources;** Water resources development; **Water rights**

ABSTRACT: The historical development of Federal reserved water rights, of interest to all who are involved in water-resource planning or use, is presented. The Federal reserved rights are those that are reserved in fact or by implication in Federal treaties, reservations, acts, or actions. Federal actions include flood-control projects and navigation improvement. The courts of the United States have developed and promulgated a system of Federal reserved water rights that can be traced from about 1850 to existing suits on water resources. A determination of Federal water rights is necessary for state water-resource planning and allocation.

REFERENCE: Bird, John W., "Origin and Growth of Federal Reserve Water Rights," *Journal of the Irrigation and Drainage Division,* ASCE, Vol. 107, No. IR1, **Proc. Paper 16115**, March, 1981, pp. 11-24

16101 AQUIFIER ESTIMATION AND KALMAN FILTERS

KEY WORDS: **Aquifers; Filters; Groundwater sources;** Parameters; **Pump tests;** Water storage; Water transfer

ABSTRACT: An iterated extended Kalman filter (IEKF) has been used for the estimation of aquifer parameters in the presence of uncertainties in the system and noise in the measurements. The technique is sequential and each additional observation reduces the error covariance of the parameter estimates. The method is computationally efficient and gives the confidence limits of the parameter estimates. Only a few observations are sufficient to provide a reasonable estimate of the aquifer parameters. Actual aquifer test data for confined nonleaky and leaky aquifers have been analyzed and the results compared with those obtained using the known technique. The IEKF method gives less residual square error and eliminates the subjectivity involved in the conventional curve matching techniques.

REFERENCE: Chander, Subhash, Kapoor, Prakash N., and Goyal, Sushil K., "Aquifer Parameter Estimation Using Kalman Filters," *Journal of the Irrigation and Drainage Division,* ASCE, Vol. 107, No. IR1, **Proc. Paper 16101**, March, 1981, pp. 25-33

16119 EFFECTS ON GROUND-WATER QUALITY

KEY WORDS: Groundwater chemistry; **Groundwater quality; Irrigation;** Irrigation effects; **Leaching;** Precipitation (chemistry); **Salinity;** Travel time; **Water types**

ABSTRACT: Increased irrigation efficiency usually reduces the degradation of groundwater resources. The effect of differences of travel times in the unsaturated zone between low and high leaching becomes more important as the depth to the groundwater table increases. Waters approaching gypsum saturation have a much greater potential for ground-water degradation at high leaching as compared to low leaching irrigation management. This is due to higher salt concentrations and, consequently, increased gypsum precipitation in the unsaturated zone in the case of low leaching.

REFERENCE: Suarez, Donald L., and van Genuchten, Martin Th., "Leaching and Water-Type Effects on Ground-Water Quality," *Journal of the Irrigation and Drainage Division*, ASCE, Vol. 107, No. IR1, **Proc. Paper 16119**, March, 1981, pp. 35-52

16145 HYDRO-SALINITY-ECONOMIC MODELING

KEY WORDS: Crop production; Crop yield; Economic factors; **Irrigation; Models; River basin planning; River basins; Salinity;** Seasonal variations; Water plans; **Water resources;** Water use

ABSTRACT: A method is presented that combines a crop yield/economic model with a hydrologic-salinity simulation model to estimate irrigation management effects of sequential water use in a river basin. Crop yields are assumed to be a function of seasonal evapotranspiration and soil solution salinities. The combined model was applied to the Hadejia River Basin in northern Nigeria. The relative efficiency of water use, with respect to crop production, is presented for selected management alternatives.

REFERENCE: Fapohunda, Henry O., and Hill, Robert W., "River Basin Hydro-Salinity-Economic Modeling," *Journal of the Irrigation and Drainage Division*, ASCE, Vol. 107, No. IR1, **Proc. Paper 16145**, March, 1981, pp. 53-69

16134 INFILTRATION EQUATIONS FOR SURFACE EFFECTS

KEY WORDS: Computer models; **Equations; Hydrology;** Infiltration capacity; Infiltration rate; **Infiltration (soils);** Mulching; Runoff; **Sealing;** Seepage; **Soil surfaces;** Surface treatment; **Water flow**

ABSTRACT: A series of equations were developed for predicting infiltration into soils with modified surfaces. The Green-Ampt approach was used in their development. They have the same functional form as the Green-Ampt and Mein-Larson two-stage infiltration equations to which they reduce for the case of a uniform soil profile. The equations were applied to coarse over-fine and fine over-coarse soil stratifications and showed good agreement with both observed infiltration rates and infiltration rates predicted by numerical solution of Richards' equation. The equations were also applied to an Ida silt loam soil to illustrate the magnitude of the predicted effect of surface sealing on infiltration. Analysis was performed for two different initial moisture contents, three different rainfall intensity ratios, and four different conductivity ratios.

REFERENCE: Moore, Ian D., "Infiltration Equations Modified for Surface Effects," *Journal of the Irrigation and Drainage Division*, ASCE, Vol. 107, No. IR1, **Proc. Paper 16134**, March, 1981, pp. 71-86

16139 HEAD LOSS OVER LONG-THROATED FLUMES

KEY WORDS: **Discharge coefficients;** Discharge measurement; **Downstream; Energy losses;** Entrances (fluid flow); **Flumes;** Laboratory tests; Submergence

ABSTRACT: Long-throated flumes, all with the same trapezoidal throat, were laboratory tested. The flume throat was first fitted with two entrance transitions with plane bottoms converged respectively 1:2, and 1:3, as measured relative to the flume center line. The 1:2 transition has no significant influence on the flume calibration. The throat was then tested with six downstream transitions of which the expansion ratio ranged from 1:0—1:10. Two flume series were tested with these transitions. The modular limits and related required energy head losses were analyzed. An equation is presented to estimate the modular limit for any long-throated flume placed in an arbitrary canal; a procedure to calculate this modular limit is also presented.

REFERENCE: Bos, Marinus G., and Reinink, Yvonne, "Required Head Loss over Long-Throated Flumes," *Journal of the Irrigation and Drainage Division,* ASCE, Vol. 107, No. IR1, **Proc. Paper 16139,** March, 1981, pp. 87-102

U.S. Customary-SI Conversion Factors

In accordance with the October, 1970 action of the ASCE Board of Direction, which stated that all publications of the Society should list all measurements in both U.S. Customary and SI (International System) units, the following list contains conversion factors to enable readers to compute the SI unit values of measurements. A complete guide to the SI system and its use has been published by the American Society for Testing and Materials. Copies of this publication (ASTM E-380) can be purchased from ASCE at a price of $3.00 each; orders must be prepaid.

All authors of *Journal* papers are being asked to prepare their papers in this dual-unit format. To provide preliminary assistance to authors, the following list of conversion factors and guides are recommended by the ASCE Committee on Metrication.

To convert	To	Multiply by
inches (in.)	millimeters (mm)	25.4
feet (ft)	meters (m)	0.305
yards (yd)	meters (m)	0.914
miles (miles)	kilometers (km)	1.61
square inches (sq in.)	square millimeters (mm^2)	645
square feet (sq ft)	square meters (m^2)	0.093
square yards (sq yd)	square meters (m^2)	0.836
square miles (sq miles)	square kilometers (km^2)	2.59
acres (acre)	hectares (ha)	0.405
cubic inches (cu in.)	cubic millimeters (mm^3)	16,400
cubic feet (cu ft)	cubic meters (m^3)	0.028
cubic yards (cu yd)	cubic meters (m^3)	0.765
pounds (lb) mass	kilograms (kg)	0.453
tons (ton) mass	kilograms (kg)	907
pound force (lbf)	newtons (N)	4.45
kilogram force (kgf)	newtons (N)	9.81
pounds per square foot (psf)	pascals (Pa)	47.9
pounds per square inch (psi)	kilopascals (kPa)	6.89
U.S. gallons (gal)	liters (L)	3.79
acre-feet (acre-ft)	cubic meters (m^3)	1,233

JOURNAL OF
THE IRRIGATION
AND DRAINAGE DIVISION

Emitter Discharge Sensitivity to Pressure and Temperature

By Benjamin Zur[1] and S. Tal[2]

Introduction

Design standards recommend a maximal 10% variation in emitter discharge along an irrigation line and over the field. In the design of an irrigation network, emitter discharge is traditionally assumed to be a function of pressure only. Discharge uniformity is assured by limiting line pressure variation over the field. The upper and lower limits of line pressure variation would depend on the discharge sensitivity to pressure of the specific emitter.

The temperature of water flowing in irrigation pipes exposed to solar radiation is expected to increase with distance. Parchomchuk (3) measured a 16° C (61° F) rise in the temperature of the water as it passed through a 37-m (121-ft) long polyethylene pipe exposed to the sun. He also measured a 6° C (43° F) rise in water temperature in a similar pipe buried 15 cm (6 in.) below the surface. Gilad et al. (1) measured the water temperature distribution along a 70-m (229-ft) long plastic pipe exposed to the sun. They report a 12° C (54° F) rise in the water temperature at the end of the line. The major part of the temperature rise was measured along the last 15 m (49 ft) of the pipe.

The sensitivity of emitter discharge to temperature was examined by Keller and Karmeli (2). They suggest that the discharge sensitivity to temperature would be minimal in emitters where the flow regime is turbulent, e.g., nozzle- , vortex- , and labyrinth-type emitters. For helical long-path emitters, Keller and Karmeli (2) assume that since the flow regime is laminar, the discharge sensitivity to temperature will be equal to the sensitivity of viscosity to temperature.

The objective of the present work was to measure the discharge sensitivity to pressure and temperature for three types of emitters, and to investigate the

[1]Sr. Lect., Dept. of Agricultural Engrg., Technion, Haifa, Israel.
[2]Grad. Research Asst., Dept. of Agricultural Engrg., Technion, Haifa, Israel.

Note.—Discussion open until August 1, 1981. To extend the closing date one month, a written request must be filed with the Manager of Technical and Professional Publications, ASCE. Manuscript was submitted for review for possible publication on June 26, 1980. This paper is part of the Journal of the Irrigation and Drainage Division, Proceedings of the American Society of Civil Engineers, ©ASCE, Vol. 107, No. IR1, March, 1981. ISSN 0044-7978/81/0001-0001/$01.00.

relative importance of pressure and temperature distribution on the discharge distribution of these emitters.

Methods and Materials

Three types of emitters, characterized by their pressure dissipation mechanism, were used in the present study. The helical long-path principle was represented by four "Netafim" emitters with nominal discharges of 1 L/h, 2 L/h, 4 L/h, and 8 L/h. The labyrinth principle was represented by the "Lego 4" emitter with a nominal discharge of 4 L/h, and two "Kochav" emitters with nominal discharges of 2 L/h and 4 L/h. The vortex principle was represented by the "Tirosh 7.5" emitter with a nominal discharge of 7.5 L/h. (Netafim, Lego 4, Kochav, and Tirosh 7.5 are all commercial names of emitters manufactured in Israel.)

The pressure and temperature sensitivity of emitter discharge was determined for each of the aforementioned emitters. These tests were conducted using 160-cm long plastic pipes on which five emitters of the same ~~kine~~ were installed at 30-cm intervals. During each test, the discharge of each emitter was measured three times. The pressure-discharge relationships of each kind of emitter were determined by measuring the discharge at six line pressures of 50 kPa, 100 kPa, 150 kPa, 200 kPa, 250 kPa, and 300 kPa. The sensitivity of emitter discharge to temperature was measured at seven water temperatures in the range of 7° C–55° C (44° F–131° F), and at three line pressures of 100 kPa, 200 kPa, and 300 kPa. Water temperatures above ambient were obtained by mixing tap water with hot water from a commercial water heater in various proportions. Water temperatures below ambient were obtained by passing tap water through a copper pipe immersed in a container filled with ice water. Water temperatures were measured at the outlets of the first, third, and fifth emitter on the plastic pipe. The temperature difference between the first and fifth emitter never exceeded 2° C.

Results and Analysis

Discharge Sensitivity to Pressure.—The pressure-discharge relationships of emitters are normally expressed by the following equation:

$$Q = aH^b \qquad (1)$$

in which Q = the discharge; H = the pressure; and a and b = constants. The values of a and b for each emitter were determined by a linear regression analysis of a logarithmic plot of the measured discharge against the applied pressure. The pressure-discharge relationships of the tested emitters are represented by the specific values of a and b in Table 1.

The results presented in Table 1 demonstrate the differences in the discharge sensitivity to pressure of the three types of emitters tested in the present study. For the helical long-path emitters, the experimental value of b was in the range of 0.86–0.66, depending on the nominal emitter discharge and therefore on the cross-sectional area of the flow path. The value of b for the labyrinth-type emitters was close to 0.5, while that for the vortex-type emitter was close to 0.43.

The experimental value of b for a given emitter determines the maximal variation in line pressure allowed in order to comply with the permissible 10% variation in emitter discharge in the field. If Q_1 and Q_2 are the maximal and minimal emitter discharge, then the following condition must be satisfied:

$$\frac{Q_1}{Q_2} = \frac{aH_1^b}{aH_2^b} = \left(\frac{H_1}{H_2}\right)^b \le 1.1 \quad \text{(2)}$$

If we define $\Delta H = H_1 - H_2$, then Eq. 2 can be rewritten as follows:

$$\frac{\Delta H}{H_2} \le \sqrt[b]{1.1} - 1.0 \quad \text{(3)}$$

The maximum allowable ratio, $\Delta H/H_2$, for the various emitters tested in the present study, are presented, as a percentage, in Table 2.

TABLE 1.—Values of a and b for Various Emitters

Emitter (1)	b (2)	a (3)	Correlation coefficient (4)
Helical; 1-L/h discharge	0.8599	0.1072	0.9976
Helical; 2-L/h discharge	0.7273	0.3933	0.9965
Helical; 4-L/h discharge	0.6869	0.7813	0.9980
Helical; 8-L/h discharge	0.6654	1.4672	0.9988
Labyrinth; 4-L/h discharge	0.5286	1.3517	0.9988
Labyrinth; 2-L/h discharge	0.5104	0.7352	0.9988
Labyrinth; 4-L/h discharge	0.4951	1.3714	0.9999
Vortex; 7.5-L/h discharge	0.4267	2.6363	0.9988

TABLE 2.—Maximum $\Delta H/H_2$ for Various Emitters, as a percentage

Emitter (1)	$\Delta H/H_2$ (2)
Helical; 1-L/h discharge	11.7
Helical; 2-L/h discharge	14.0
Helical; 4-L/h discharge	14.9
Helical; 8-L/h discharge	15.4
Labyrinth; 4-L/h discharge	19.8
Labyrinth; 2-L/h discharge	20.5
Labyrinth; 4-L/h discharge	21.2
Vortex; 7.5-L/h discharge	25.0

The results presented in Table 2 show that the requirement for a maximal 10% variability in emitter discharge results in different permissible line pressure variability for the three types of emitters. A 15% variation in line pressure could be designed for the helical long-path emitters, a 20% variability for the labyrinth-type emitters, and a 25% variability in line pressure for the vortex-type emitter.

Discharge Sensitivity to Temperature

The experimental results of emitter discharge at the various temperatures at a given line pressure suggest that the discharge temperature relationships for the tested emitters are essentially linear and could be described by the following equation:

$$Q = m + nT \quad (3)$$

in which m and n = constants; and T = the water temperature, in degrees centigrade. The constants m and n, computed by a linear regression analysis of the results, are presented in Table 3 for the various emitters.

The discharge sensitivity to temperature, as expressed by n, increased with line pressure and with the cross-sectional area of the flow path for the helical long-path emitters. For the labyrinth-type emitters, a relatively small discharge

TABLE 3.—Experimental Values of Constants *m* and *n* for Various Emitters

Line pressure, in kiloPascals (1)	*m* (2)	*n* (3)	Correlation coefficient (4)
(*a*) Helical; 1-L/h discharge			
1.0	0.0087	0.6551	0.9897
2.0	0.0116	1.2272	0.9947
3.0	0.0154	1.7186	0.9899
(*b*) Helical; 2-L/h discharge			
1.0	0.0169	1.6872	0.9946
2.0	0.0254	2.8927	0.9964
3.0	0.0303	3.9242	0.9878
(*c*) Helical; 4-L/h discharge			
1.0	0.0323	3.0612	0.9948
2.0	0.0470	5.1131	0.9964
3.0	0.0651	6.7083	0.9898
(*d*) Helical; 8-L/h discharge			
1.0	0.0543	6.2751	0.9913
2.0	0.0762	8.8801	0.9920
3.0	0.0949	11.8224	0.9819
(*e*) Labyrinth; 4-L/h discharge			
1.0	0.0079	4.8769	0.9040
2.0	0.0092	7.3293	0.8574
3.0	0.0139	9.1871	0.8594
(*f*) Vortex; 7.5-L/h discharge			
1.0	−0.0180	7.2695	0.9913
2.0	−0.0222	9.8105	0.9740
3.0	−0.0213	11.6188	0.9817

sensitivity to temperature which increased with line pressure, was measured for the Labyrinth 4-L/h emitter. The discharge of the Labyrinth 2-L/h and Labyrinth 4-L/h emitters have shown practically no sensitivity to water temperature. In contrast, the discharge of the vortex-type emitter decreased with an increase in temperature. The measured negative sensitivity decreased with an increase in line pressure.

The relative emitter discharge, Q_{RT}, as a result of changes in water temperature is defined as follows:

$$Q_{RT_{25}} = \frac{Q_T}{Q_T = 25° \text{ C}} \quad \text{(4)}$$

in which Q_T = the emitter discharge at a given temperature, T; and Q_T = 25 = the emitter discharge at a reference water temperature of 25° C (77° F).

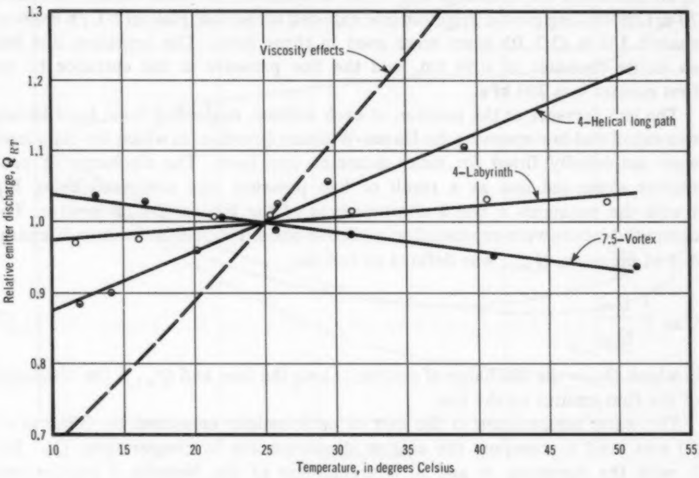

FIG. 1.—Influence of Temperature on Relative Discharge for Representative Emitters

The dependence of Q_{RT} on water temperature for representatives of the three types of emitters at a line pressure of 100 kPa is demonstrated in Fig. 1. Also included in this figure is the predicted effect of viscosity changes with temperature on Q_{RT}, characteristic of laminar flow (2).

The changes in the relative discharge due to temperature, Q_{RT}, for the Helical 4-L/h emitter were significantly less than those predicted by the dependence of the viscosity on temperature. The sensitivity of Q_{RT} to temperature is expected to equal the dependence of viscosity on temperature, as assumed by Keller and Karmeli (2), only when the flow is purely viscous. The writers (4) concluded that the flow regime in helical long-path emitters is influenced by inertial as well as viscous forces. Therefore, the reduced sensitivity of the discharge of

helical long-path emitters to temperature measured in the present study supports the conclusions drawn by the writers (4).

The measured dependence of Q_{RT} on water temperature for the labyrinth-type emitters was small or insignificant. These results were expected, since the flow regime in these emitters is turbulent as suggested by the value of 0.5 measured for the coefficient b in these emitters. The results showing a negative sensitivity of Q_{RT} to temperature for the vortex-type emitters were unexpected. The measured value of the coefficient b for these emitters was 0.43. No explanation can presently be given for these low values.

Combined Effects of Pressure and Temperature on Emitter Discharge

Results published by Gilad et al. (1) are used here to demonstrate the combined effects of pressure and temperature on emitter discharge in the field. Gilad et al. measured the discharge and water temperature for each emitter in a level 70-m (229-ft) long plastic irrigation line exposed to the sun. Helical 2-L/h emitters spaced 1.0 m (3.3 ft) apart were used in these tests. The irrigation line had an inside diameter of 0.93 cm, and the line pressure at the entrance to the first emitter was 200 kPa.

The line pressure at the position of each emitter, neglecting local head losses, was calculated in steps using the Hazen-Williams equation, in which the exponents were empirically fitted for small diameter drip lines. The discharge of each emitter along the line as a result of line pressure was computed using Eq. 1 with the constants a and b characteristic of the Helical 2-L/h emitter. The computed results were expressed on a relative basis. The relative emitter discharge due to pressure, Q_{RH}, was defined as follows:

$$Q_{RH} = \frac{Q_{Hi}}{Q_{H1}} \quad \text{(5)}$$

in which Q_{Hi} = the discharge of emitter i along the line; and Q_{H1} = the discharge of the first emitter on the line.

The water temperature at the exit of each emitter measured by Gilad et al. (1) was used to compute the emitter discharge due to temperature, Q_T. Eq. 3, with the constants m and n, characteristic of the Netafim 2 emitter was used for that purpose. The computed results were expressed on a relative basis, defining the relative emitter discharge due to temperature, Q_{RT}, as follows:

$$Q_{RT} = \frac{Q_{Ti}}{Q_{T1}} \quad \text{(6)}$$

in which Q_{Ti} = the discharge due to temperature of emitter i; and Q_{T1} = the discharge due to temperature of the first emitter along the line.

The relative emitter discharge due to the combined effects of pressure and temperature, Q_{RHT}, was computed using the following equation:

$$Q_{RHT} = Q_{RH} Q_{RT} \quad \text{(7)}$$

The computed values of Q_{RH}, Q_{RT}, and Q_{RHT}, as a function of emitter position along the irrigation line, are presented in Fig. 2. Also included in this figure

is the measured emitter discharge along the line published by Gilad et al. (1) and expressed on a relative basis, Q_{RM}.

The computed relative emitter discharge due to pressure, Q_{RH}, and the relative emitter discharge due to temperature, Q_{RT}, presented in Fig. 2, demonstrate the contrasting effects of pressure and temperature distribution on the variation in discharge of helical long-path emitters along an irrigation line. The value of Q_{RH} decreased by 10% along the first half of the pipe, and by an additional 2% along the second half of the pipe. This behavior is a direct result of the predicted pressure dissipation along an irrigation line. The value of Q_{RT} increased gradually with distance along the first two thirds of the pipe followed by a sharp increase along the remaining third of the pipe length. The temperature

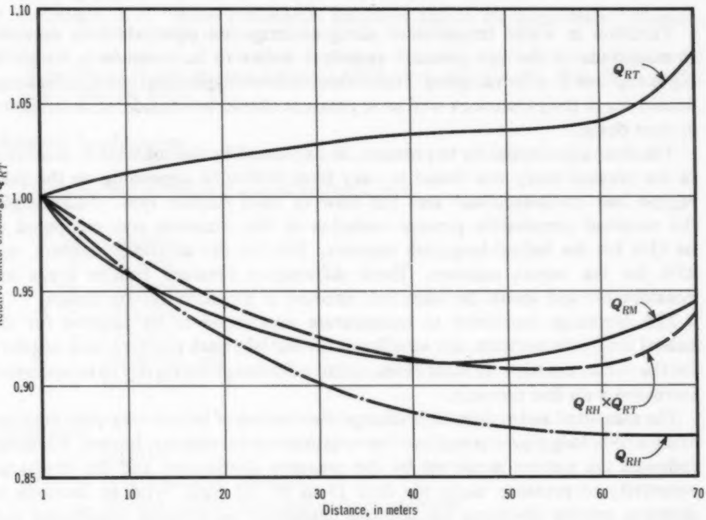

FIG. 2.—Distribution of Relative Discharge Due to Temperature, Q_{RT}, and Pressure Times Temperature, Q_{RHT}, Compared to Measured Q_{RM}, Along Irrigation Pipe

of a given volume of water would tend to increase as it moves along a pipe heated as a result of solar radiation. Its temperature at any given time would be a direct function of the duration of its presence in the pipe. The variation of the water temperature with distance along the pipe is expected to be inversely related to the water flow velocity in the pipe. Since the flow velocity drops sharply towards the end of the pipe, the water temperature would tend to increase sharply with distance.

The combined effects of the pressure and temperature variation along the pipe resulted in a curvilinear distribution of the measured relative emitter discharge, Q_{RM}. The values of Q_{RM} were close to the computed values of Q_{RH} along the first 15 m of the pipe, after which the decrease in Q_{RM} with

distance was more gradual than that of Q_{RH}. The decrease in Q_{RM} with distance ceased after about 40 m of flow. Along the last 30 m of the pipe Q_{RM} increased gradually, while Q_{RH} continued to decrease at a slower rate. The influence of line pressure on Q_{RM} was apparent along the first third of the pipe length, after which Q_{RM} became increasingly influenced by the water temperature distribution along the pipe.

The predicted relative emitted discharge, Q_{RHT}, computed by multiplying the values of Q_{RH} by Q_{RT} for each emitter, described quite well the emitter discharge distribution along the 70-m pipe. The maximal variation between the measured and computed emitter discharge was in the range of ±1.4%.

Summary and Conclusions

Variation in water temperature along an irrigation pipe which is opposite in magnitude to the line pressure variation, seems to be common in irrigation pipes exposed to solar radiation. These observations suggest that emitter discharge sensitivity to temperature as well as to pressure should be considered in irrigation system design.

The discharge sensitivity to pressure, as expressed by the constant b, measured in the present study was found to vary from 0.43–0.86 depending on the flow regime and cross-sectional area for flow of each emitter type. Accordingly, the maximal permissible percent variation in line pressure was computed to be 15% for the helical long-path emitters, 20% for the labyrinth emitters, and 25% for the vortex emitters. These differences between emitter types are considerable and should be taken into account in irrigation system design.

The discharge sensitivity to temperature was found to be positive for the helical long-path emitters, not significant for the labyrinth emitters, and negative for the vortex emitters. In most cases, emitter discharge sensitivity to temperature increased with line pressure.

The measured and computed discharge distribution of helical long-path emitters along a 70-m long pipe exposed to solar radiation was curvilinear. Emitter discharge followed the pattern predicted by the pressure distribution and the discharge sensitivity to pressure along the first 15 m of the pipe. With an increase in distance, emitter discharge became less dependent on pressure distribution and more sensitive to the temperature distribution and the discharge sensitivity to temperature. The end result was that emitter discharge along the second half of the pipe increased with distance, parallel to the rise in water temperature.

Temperature variation along an irrigation pipe exposed to solar radiation is a result of the energy balance of the pipe and the flow velocity. The energy balance of a pipe is expected to change diurnally, with the season and with the degree of shading by the crop. Therefore, it is doubtful whether the water temperature variation along an irrigation pipe could become a standard parameter in irrigation system design. However, based on the results from the present work and the results cited from the literature, some general recommendations are suggested. When emitter discharge sensitivity to temperature is positive (helical long-path emitters), the requirement for a maximal 10% variation in discharge could be limited to the first half of the pipe. Emitter discharge is expected to increase along the second half of the pipe, due to a temperature increase irrespective of line pressure variation. However, when the discharge

sensitivity to temperature is negative (vortex emitters), the decrease in emitter discharge with distance is expected to be accentuated as a result of the temperature rise, especially towards the end of the line. This calls for the design of a smaller line pressure variation than that normally required. For labyrinth-type emitters, where the discharge sensitivity to temperature is insignificant, the temperature variation along the pipe could be neglected in the design.

Appendix I.—References

1. Gilad, Y., Peleg, D., and Tirosh, G., "Irrigation Equipment Tests," *No. 81268,* ICWA, Sept., 1968.
2. Keller, J., and Karmeli, D., "Trickle Irrigation Design," Rain Bird Sprinkler Manufacturing Co., 1975.
3. Parchomchuk, J., "Water Temperature Effects on Emitter Discharge Rates," *Transactions,* ASAE, Vol. 19, 1976, pp. 690–692.
4. Tal, S., and Zur, B., "The Flow Regime in Helical Long-Path Emitters," *Journal of the Irrigation and Drainage Division,* ASCE, Vol. 106, No. IR1, Proc. Paper 15291, Mar., 1980, pp. 27–35.

Appendix II.—Notation

The following symbols are used in this paper:

a = constant;
b = constant;
H = pressure;
m = constant;
n = constant;
Q = discharge; and
T = temperature.

Subscripts

R = relative;
RH = relative due to pressure;
RHT = relative due to pressure and temperature;
RT = relative due to temperature; and
T = temperature.

[illegible]

JOURNAL OF
THE IRRIGATION
AND DRAINAGE DIVISION

Origin and Growth of Federal Reserved Water Rights

By John W. Bird,[1] F. ASCE

Introduction

Because the Federal government owns large tracts of land in the western states, it has a great potential interest in the waters available to the development of those lands. Expansion of Federal activity in those states has led to increasing Federal needs and claims for water since the turn of the century. This has led to the development of a concept of a "reserved" right, the taking of state-created water rights and a derogation of state law. Any agency such as a municipality or an irrigation district that has a need for water and a legal right to that water must carefully consider the unwritten reserved claims of the Federal government and the limitations of those claims (if they do exist). For states following the riparian doctrine, the possibility exists that there may be existing Federal reserved rights to a quantity of flow rather than the variable share in a flowing stream that is the usual rule for riparian users. In appropriation states a water user must consider the possibility that an existing senior water right may become junior to a Federal reserved right when that right is admitted. Since there is no loss of the reserved right for nonuse or because of state laws, that right may be valid, though hidden, far into the future. As a result, there have been a large number of suits concerning water rights in recent years that have been based on Winters' Doctrine or the Doctrine of Reserved Rights. It is common, in these suits, to have a state either as a principle or as an interested party that is contending against the Federal government's claims. For example, there is a suit, on appeal, of *United States of America* v. *Truckee Carson Irrigation*, State of Nevada et al., which is based on rights perceived to originate under the Winters Doctrine.

[1] Assoc. Prof., Civ. Engrg. Dept., Univ. of Nevada, Reno, Nev. 89557.

Note.—Discussion open until August 1, 1981. To extend the closing date one month, a written request must be filed with the Manager of Technical and Professional Publications, ASCE. Manuscript was submitted for review for possible publication on June 25, 1980. This paper is part of the Journal of the Irrigation and Drainage Division, Proceedings of the American Society of Civil Engineers, ©ASCE, Vol. 107, No. IR1, March, 1981. ISSN 0044-7978/81/0001-0011/$01.00.

Background

The United States Constitution is the source of Federal standing and as such the source of Federal reserved rights. Concerning water rights, this is commonly developed from Article I, Section 8, "Congress shall have the power to regulate commerce with foreign nations, and among the several states, and with Indian Tribes," and Article IV, Section 3 (2), "The Congress shall have power to dispose of and make all needful Rules and Regulations respecting the Territory or other Property belonging to the United States, ..." These are, respectively, the commerce clause and the property clause of the Constitution.

The first Federal suits regarding water were related to control over navigable waters that was reserved to the Federal government. The United States Supreme Court held that in the grant of power to Congress to regulate commerce among the several states, as given by the United States Constitution, the federal government has jurisdiction over navigable streams as far as may be necessary for commercial purposes (8). The Supreme Court expanded the concept of navigability from the thought that "a river which is navigable in fact is navigable in law," (5) to the concept that "in determining whether streams are public, navigable waters, the test is whether they are, or are capable of becoming, public highways between public places" (4).

The United States made the Louisiana Purchase in 1803, the Oregon Country Treaty in 1846, and signed the Treaty of Guadalupe Hidalgo in 1848. The acquired lands were the property of the United States and were subsequently subdivided into territories that ultimately became states with all the rights and privileges of the thirteen original states.

Until passage of the Homestead Act (32) in 1862, most of this newly acquired land was not legally open for settlement or private acquisition, or both, even though there had been a steady westward migration for a number of years. None of the first migrants could claim a riparian right to needed water since they often were not landowners and could not be until after 1862. As a result, and for some other reasons, the doctrine of prior appropriation of water was developed and adopted in some areas. The western courts usually held that, while recognizing and applying the doctrine of appropriation, they were only settling rights as between individuals and that Federal ownership of the lands prevented absolute vesting of such rights (11). There was a general judicial recognition that the Federal government, as landowner, had a superior right to the waters that were appropriated by the settlers and that there was a possibility that those appropriated rights might later be destroyed through assertion of Federal claims either by the Federal government or by private grantees with associated superior rights. The riparian patentees could claim riparian rights based on common law. During the period that territories, states, and laws concerning water were being formed, Congress debated and passed the Desert Land Act of 1866 (28) contained the provision that

> Whenever, by priority of possession, rights to the use of water for mining, agricultural, manufacturing or other purposes, have vested and accrued, and the same are recognized and acknowledged by the local customs, laws, and the decisions of the courts, the possessors and owners of such vested rights shall be maintained and protected in the same; . . .

and, in 1870, Congress clarified (33) the situation when it said

> . . . all patents granted on pre-emption or homesteads allowed shall be subject to any vested and accrued water rights, or rights to ditches and reservoirs used in conjunction with such water-right, as may have been acquired under or recognized by the preceding section

The new states interpreted the Acts of Congress in different ways, with the result that they: (1) Continued with the riparian doctrine; (2) developed the appropriation doctrine; or (3) used the "California Doctrine" with riparian rights on private lands and appropriations from the public domain forming a dual system of water rights.

California promulgated the theory (10) that prior to the creation of the western states the Federal government had proprietory rights to and sovereignty over the western lands. While sovereignty passed to the states as they were formed, the Federal government continued its proprietorship of the public domain. The water rights of the Federal government were to be determined by state law and through adoption of the common law, including the riparian system of water rights; riparian rights were created in the Federal government as a landowner. The Oregon courts (7) agreed with the California courts that the Federal government had proprietorial rights in the waters on the public domain and that these rights survived the creation of the western states. However, Oregon viewed the Desert Land Act as severing the water rights from the public lands so that subsequent Federal land grants did not convey water rights. The act was considered an exercise of the dispositive power of the Federal government to the extent that it dedicated the waters to public use by appropriation. Colorado viewed the sovereignty of the Federal government as separate from proprietary rights. Thus the transfer of sovereignty to the states as they were formed transferred all the power to control the waters. The courts interpreted the Act of 1866 along with subsequent Federal enactments to give the required consent to this interpretation.

Since Congress did not adopt any Federal laws for the disposition or determination of Federal water rights, the newly formed territories and states took the function of establishing water rights based on common law, statutes, and court decisions, and in doing so they were exercising their traditional jurisdiction over water. Each appropriation state has similar basic legal concepts: (1) Beneficial use is the measure of the existence and scope of the right; (2) ownership of the land is not considered a basis for a water right; (3) the right may, but need not necessarily, be appurtenant to the land; (4) the appropriated water may be applied at any place where it is needed, regardless of the distance from the source; (5) diversions are protected; (6) the rights of the prior appropriator must be met before a junior appropriator may take water—the burden of shortage falls on those with the latest right; (7) there is no proration in times of shortage; (8) the owner of a senior right can take no more water than was necessary for his original need; and (9) the right extends only to the use of the water, there is no right to the corpus of the water. Apparently no one at the state level considered the possibility of a Federal sovereign right or how such a right might be established. The Act of 1866 was considered to be a recognition of state law as the only valid system of acquiring water rights on the public domain.

In part, the Desert Land Act of 1877 (34) said

> . . . the water of all lakes, rivers and other sources of water supply upon the public land and not navigable, shall remain and be held free for the appropriation and use of the public for irrigation, mining, and manufacturing purposes, subject to existing rights . . .

which had been interpreted to be a dedication to the public of all interests in the waters of the public domain (7). This interpretation separated water from land and was apparently upheld later when the Supreme Court held (2) that, ". . . all non-navigable waters then a part of the public domain became publici juris [of public right], subject to the plenary control of the designated states . . ." Using these interpretations the various states passed laws and developed rules and procedures for the full development and use of water.

Rights of United States

It will be recalled that the first suits concerning water that included the Federal government were in relation to defining and determining navigable waters. This was changed and expanded in 1899 when the United States sued to restrain the building of a dam across the upper Rio Grande River based on the grounds that navigation would be impaired by that construction because of resulting diversions from the Rio Grande (23). It was the holding of the Supreme Court that, although the states have the right to adopt riparian or appropriation rules and regulations as to flowing waters for such purposes as they deem proper, a limitation must be recognized in that in the absence of specific authority from Congress, a state cannot by its legislation destroy the right of the United States, as owner of lands bordering on a stream, to the continued flow of its waters. It is well recognized that the superior power of the Federal government to secure the uninterrupted navigability of all navigable streams within the limits of the United States. Further, that power may be used to prohibit any obstruction to the navigable waters of the United States. This power was and is reserved to the United States. So, even though the proposed dam was far upstream on the non-navigable portion of the Rio Grande, the Federal government had the authority and power to extend its control from the navigable portion to the non-navigable headwaters in order to protect its sovereign rights downstream. While it was contended that the Act of 1866 and the Act of 1877 represented a Congressional grant of complete authority over non-navigable waters to the states, the Supreme Court held that Congress had not intended those acts to release that power (23). Further, even if the acts had the contended effect, the subsequent Act of 1890 (30) prohibiting obstruction to navigation must be held to control since there is no limitation on subsequent Congressional actions regarding navigation. One result of this ruling is that Congress will often claim navigation as a part of any proposed water-oriented project with the assurance that the navigation clause will strengthen federal authority for the project.

This decision that there were reserved powers in the Federal government over waters that were in fact non-navigable was extended and applied in the Winters case.

Power over Federal Property

A series of cases involving the water rights of Federally owned/administered Indian reservations illustrates Federal claims based on Federal proprietary interests and implied reservations. Indian reservations were created by treaty, proclamation, or executive order while the west was still largely federal territory. Reservations were typically established to change Indians from a nomadic to an agrarian people (26). After formation of western territories and states the available waters were usually appropriated by non-Indian settlers, leaving little water for use on the reservation. Other reservations, created for other purposes, also had little or no water available for their use after the available surface water had been appropriated for other existing needs.

To protect its program of Indian agrarian development the Federal government asserted a claim of "reserved" water rights against non-Indian appropriators beginning in 1908 with Winters' in Montana (27). In the Winters case, the United States claimed for the Indians living on the Fort Belknap Indian Reservation on the Milk River that, when the United States created the reservation, by implication, it also reserved sufficient water to carry out the purposes of the reservation a right to water for the purposes of irrigating their land, even though the treaty that reserved land for them made no mention of water. In 1899 water was diverted from the Milk River by Winters and other defendants via dams and canals. As a result of the conflict between settlers and Indians the United States Supreme Court held there was an implied reservation of the amount of water necessary for successful cultivation of the Indian lands. The reserved right had a date of priority of the formation of the reservation and was superior to later appropriations made under state law. The Supreme Court held that the Desert Land Acts of 1866 and 1877 were not applicable to the lands or waters of Indian reservations.

The reserved-rights doctrine applies to all Indian reservations, even though many of them were created after 1866 or 1877 and regardless of how the reservation in question was created. The source of the reserved waters includes waters arising upon, flowing through, or bordering Indian reservations, with the date of reservation of water coinciding with the date of creation of the reservation. The question of how the Federal water rights could be released from public lands that were later turned into reservations with implied reservations of water may need some clarification.

The Federal courts have based their decisions concerning Indian water rights on one of several theories. The theories used are: (1) The United States reserved (implied) water rights in the treaty that created the reservation (1); and (2) the Federal government reserved the land and water (implied) from the public domain for the Indians (25) (no treaty). It is unclear whether the courts, in the latter cases regarded the reservations created by the Federal government as made in the exercise of the property power or the treaty power, but either power is sufficient.

Reserved Right

Reserved water rights are only associated with lands that are reserved or withdrawn from the public domain. The public domain includes those lands

owned by the United States that are subject to entry, disposal, or private appropriation under public land laws, while reserved or withdrawn lands are taken from the public lands and are not subject to entry, disposal or private appropriation (6).

The Indians' water right is reserved for the benefit of Indians on the reservation and is not a public right but is considered to be a private right held in trust by the Federal government for the benefit of the Indians. When the reserved right was first developed it was considered by many people to be an incident associated with one suit and then, after several suits, with Indian reservations only. This has changed as a result of suits concerning reserved lands that have been determined to have reserved water rights associated with them (12,17). These other reserved water rights are public in nature, but all of the reserved rights have a priority date based upon the date of creation of the reservation. The Indians' reserved water right, when used for irrigation, appears to be appurtenant to the land, which is similar to state-created water rights. Those reserved water rights cannot be lost by nonuse under state laws, nor by legal action through condemnation or state statutory enactment, or private appropriation. While the Indians may be directed to follow state laws in some cases, that statutory language should not be construed as an abandonment of prior existing rights by the Indians unless that intent was clearly expressed in the statute. The statutes only provide for procedural filing under state law, but do not limit the reserved right. The overriding power of the federal sovereign under the supremacy clause (Art. VI, Cl. 2) of the Constitution is the source of the protection of Indian water rights from encroachment. Unless Congress clearly consents to state jurisdiction, the right cannot be set aside, overridden, denied, or otherwise be affected by state substantive law (1). The decision that the implied reservation may be for future unidentified use (1) constituted a significant departure from appropriative water law that has resulted in considerable opposition from the states and non-Indian water users as there is no well-defined measure of the amount of reserved water for Indian uses and so non-Indians have no assurance of the quality of water left for their use.

From the first cases the water reserved for use by the Indians was for agricultural purposes, uses, and needs. In *Arizona* v. *California* this was modified to be measured in terms of the "practicably irrigable acreage" on the five reservations involved and not just for the land irrigated at that time. Reservations of water were determined to have been created for the purpose of enabling Indians to develop a viable agricultural economy and other uses, such as those for industry, which might consume substantially more water than agriculture, were not contemplated at the time of the creation of the reservations. Indeed, in the middle 1800s a common aspiration in the United States was to have one's own land to farm. It was made clear that when an Indian reservation is established to provide an Indian agricultural economy, the measure of the associated reserved water right will include that amount of water necessary to irrigate the practicably irrigable acreage and to satisfy related uses. The question as to whether the reserved water is for essential uses, or convenient uses, or both, has not been answered. Furthermore, nothing has been said to date about an Indian reservation which may have not been created to establish an agricultural economy. Does the creation of a reservation that may have, as one of its original purposes, the preservation to the Indians' benefit of the fish and waters of a lake, have

the implied reservation of enough water to maintain the lake elevation and fishery? This question is currently being litigated (24).

Two standards have been promulgated for determining the uses that have reserved waters:

1. Those uses necessary to fulfill the purposes contemplated when the reservation was created (used in *Arizona* v. *California* and Winters').

2. All possible uses, including those that may appear in the future without reference to the purposes for which the reservation was created [*United States* v. *Ahtanum Irrigation District* (14)].

The first method permits a specific amount of water to be identified and protected from other users since there would be an immediate quantification of the reserved right. The Indian's rights remain uncertain with the second method and, to some extent, unprotected since the courts could conceivably require the Indians to take compensation for their claim if unappropriated water is no longer available.

The suits concerning waters for reservations, for power, and for other purposes lead to the McCarran Amendment to the Justice Appropriation Act of 1952 where the sovereign immunity of the United States was waived (35):

> in any suit . . . where it appears that the United States is the owner of or is in the process of acquiring water rights under state law, by purchase, exchange, or otherwise.

This has permitted some states to bring suit to include the United States, through its agencies, in state court water-rights adjudications to disclose and quantify any reserved rights where jurisdiction can be established under the McCarran Amendment.

In retrospect it may appear obvious that if Indian reservations had reserved water rights, then all Federal reservations should have some implied Federal reserved water right. In practice, it appears that almost everyone considered the reserved right to be confined to Indian reservations and to be, in fact, a strange quirk of law associated with Indian treaties or Indian reservations, or both, and not to be associated with any non-Indian reservations.

Pelton Dam

The difference between reserved, withdrawn, and public lands was emphasized when the Supreme Court upheld the authority of the Federal Power Commission to license construction of a private hydroelectric project on Federal reserved lands in Oregon despite state objections over the Pelton Dam (6). Since the stream involved was non-navigable, there was no assertion of the navigable servitude that is reserved to the Federal government. The Pelton Dam case is considered to be a landmark by some because the Court concluded that superior Federal authority, under the power of Congress to regulate the use and disposition of Federal property, existed to license the power project in violation of state law. The view of a lower court that the Desert Land Act constituted an irrevocable control over non-navigable waters to the state was implicitly rejected with the statement that the Desert Land Act does not apply to reserved lands.

One of the reservations involved land that had been withdrawn in 1910 for power purposes—well after the Desert Land Act enactment. It was not explained how the creation of a reservation withdrew the property reserved from the operation of the Act. In the dissent it was stated that while Congress could have revoked the Desert Land Act as far as reserved lands were concerned, it had not done so, and therefore it was congressional intention that water rights for projects on non-navigable waters were to be acquired by following state law. But this view did not prevail. Since the Supreme Court did not fully explain its decision in the Pelton Dam case, it has been speculated that the Court may have regarded the power property as giving the government a right, apart from ownership, to control the waters passing through its lands, subject to payment of compensation for interference with existing rights. Since the Desert Land Act severed the waters from the lands so that ownership of the waters did not pass to patentees of Federal lands but remained Federal property subject to state control under state law, the combination of Federal ownership of both reserved lands and unappropriated waters may have controlled the Court's decision. If this power of control exists, it must extend beyond the boundaries of the reservation to insure that waters required for the reservation continue to flow down to it [see Rio Grande (23)]. It should be noted that this view would appear to be contrary to the holding in *Kansas* v. *Colorado* (9) that the property power gives control only over Federal property and not unappropriated waters.

The uncertainty concerning the reasoning behind the Pelton decision raised concern in the western states that the Federal government was claiming plenary control over all non-navigable waters flowing through Federal reservations in the west. This was augmented by the Hawthorne Naval Reservation case (12) where the Federal court held that in maintaining a national defense reservation, a valid Federal purpose supported by both war and property powers, the United States had the right to use ground water located beneath reserved land without complying with state law. This was an application of the property power reserved right that was extended to subsurface water.

In 1956, in the State of Washington (14), it appeared that the Indian's water rights were extended when the court said that Indian rights were not limited to the use at any given date, but rather

> extended to the ultimate needs of the Indians as those needs and requirements should grow to keep pace with the development of Indian agriculture upon the reservation.

The court then upheld an agreement between white settlers and the Department of the Interior, executed in 1908, that limited the settlers to 75% of the Ahtanum waters. The water right was again expressed for irrigation purposes and implicitly limited the reserved right to irrigation and agriculture.

Arizona v. California

Since the construction of the Colorado Aqueduct, California has been diligent in appropriating water from the Colorado River. In an effort to determine and protect its water rights in the Colorado River, Arizona filed a suit against California

in 1952. Nevada, New Mexico, Utah, and the United States were added as parties to determine how much water each state has a legal right to use from the Colorado River and its tributaries. Simon H. Rifkind was appointed Special Master and reported his findings to the Supreme Court in 1961. In those proceedings the United States asserted claims to waters in the main river and in some of the tributaries not only for use on Indian reservations, but also for use in national forests, recreational and wildlife areas, and other government lands and works. The Master found both as a matter of fact and law that when the United States created those reservations, or added to them, it reserved not only land, but also the use of enough water to irrigate the irrigable portions of the reserved lands (1) or to supply other primary needs. Arizona argued that: (1) The United States had no power to make a reservation of navigable waters after Arizona became a state (1912); (2) that navigable waters could not be reserved by Executive Orders (some of the reservations were created by Executive Order); (3) that the United States did not intend to reserve water for Indian reservations; (4) that the amount of water reserved should be measured by the reasonably foreseeable needs of the Indian living on the reservation rather than by the number of irrigable acres; and (5) that the judicial doctrine of equitable apportionment should be used to divide the water between the Indians and the other citizens of Arizona.

The Supreme Court answered Arizona by stating that equitable apportionment is used to solve disputes between states and an Indian reservation that is not a state. The argument that the United States did not have the power to reserve navigable waters was based on cases that concerned only the title to lands, not waters, adjoining or underlying navigable waters. The power of the United States to regulate navigable waters is not reduced or limited. The arguments regarding the intention to reserve water and the amount reserved were rejected with reference to Winters (26) with the statement that the water rights were reserved effective as of the time the reservations were created.

For the first time the Supreme Court extended the reserved doctrine of water rights from Indian reservations to all reserved or withdrawn lands such as wildlife areas and national forests. Since the Court considered only claims on behalf of Indian reservations, it is necessary to refer to the report of the Special Master to determine the basis for extending the reserved rights doctrine to other reservations. The Special Master first determined that the United States had the power to reserve water to fulfill its purposes in creating the various reservations involved in the suit; then he determined that the circumstances surrounding their reservation demonstrated the intent of the United States to reserve water for use on the reservations involved. These reserved water rights are subject to water rights that have been previously acquired pursuant to state law, i.e., that have a priority older than the date the reservation was created.

Desert Pupfish

President H. S. Truman reserved 40 acres of land as a national monument, in 1952, under the Act for the Preservation of American Antiquities (13) which authorizes the President to proclaim as national monuments "objects of historic or scientific interest." That 40 acres included Devil's Hole, a deep limestone cavern including an underground pool inhabited by a unique species of desert

fish, about 2.5-cm long, called the Devil's Hole pupfish. The spawning area for the pupfish is a rock ledge in the pool and if the ground-water level drops significantly that rock shelf becomes exposed to air with a resultant decrease in spawning area and the potential extinction of the pupfish. As a part of the preamble to the proclamation proclaiming Devil's Hole as a national monument, President Truman said, "Whereas the said pool is of outstanding scientific importance that it should be given special importance. . . ."

In 1968, Cappaert, a local rancher, began pumping ground-water from wells located about 2-1/2 miles (4 km) from Devil's Hole. The pumping occurred during the irrigation season between March and October of each year and Cappaert was the first to appropriate ground water in the area. The National Park Service filed a protest to his ground-water application requesting that it be denied until it was determined which wells, when pumped, were causing a serious decline of water elevation in the pool. The state engineer declined to postpone his decision because there was no recorded Federal water right with respect to Devil's Hole. In a suit in Federal court the National Park Service claimed that the establishment of Devil's Hole as a National Monument reserved the unappropriated waters appurtenant to the land to the extent necessary for the purposes and requirements of the reservation. Since neither Cappaert nor anyone else had perfected water rights as of the date of the reservation, the reserved rights had first priority. An injunction was issued in Federal District Court in 1973 limiting the pumping from designated wells to control the pool elevation to an acceptable level (17). On appeal, the Ninth Circuit Court of Appeals affirmed the District Court decision (17) and held "the United States is not bound by state water laws when it reserves land from the public domain." The United States Supreme Court affirmed that decision in 1976 when it considered the water in the pool to be surface waters and not ground water; as a result, there may be a little doubt on whether or not the reserved right does extend to ground water.

Reserved Rights

In 1971 the Supreme Court declared (20) that "it is clear from our cases that the United States often has reserved water rights based on withdrawals from the public domain." As we saw in *Arizona* v. *California*, 373 U.S. 546, the Federal government had the authority both before and after a state is admitted into the Union "to reserve waters for the use and benefit of federally reserved lands." The federally reserved lands include any federal enclave. From the Eagle County (20) affirmation of *Arizona* v. *California* it is clear that water rights have been impliedly reserved to serve not only Indian reservations but also any Federal enclave created by reserving or withdrawing lands from the public domain.

Perhaps the principal question that arises is—what reserved lands? The following is a partial list of some of the reservations; it does not include Indian reservations, power site withdrawals or military installations since these have been previously mentioned. Congress specifically authorized the reservations of some public springs and water holes in 1916 in the Pickett Act (36) where "lands containing waterholes or other bodies of water needed or used by the public for watering purposes . . . maybe reserved . . ." for public purposes.

But the Bureau of Land Management is prohibited from making withdrawals under the Pickett Act by its Organic Act (40).

Many springs and water holes were reserved by an executive order for Public Water Reserve No. 107 in 1926. While numerous other specific withdrawals were made both prior and subsequent to the 1926 order, these reserves were generally local in character or otherwise minor. This withdrawal order was designed to preserve for general public use and benefit unreserved public lands containing water holes or other bodies of water needed or used by the public for watering purposes. This withdrawal reserved both land and water for public use. The quantity reserved was the total yield of each source to be used where it was needed for domestic, livestock watering, irrigation, soil, and fire and erosion control. While the 1926 order does not interfere with vested rights under state law prior to the 1926 withdrawal date, if a spring or water hole is abandoned after 1926 it does apply. Similarily, if a state water right was not acquired until after 1926, that water right is ineffective against the 1926 withdrawal.

Executive Order 5327 (April 15, 1930) reserved oil shale lands and said:

> . . . the deposits of oil shale, and lands containing such deposits owned by the United States, be, and the same are hereby, temporarily withdrawn from lease and other disposal and reserved for the purposes of investigation, examination, and classification . . .

Following the "specific purpose" test that was given in New Mexico (21) it appears that only enough water was reserved as was reasonably necessary for the "purposes of investigation, examination and classification" and not for actual oil shale development.

The Taylor Grazing Act (37) directed the Bureau of Land Management to manage the public domain for grazing purposes. It did not reserve any land from the public domain so, presumably, no reserved water rights were created by the act. Since the Classification and Multiple Use Act of 1964 (39) was to be consistent with and supplemental to the Taylor Act, it should create no reserved water rights since Taylor created none.

National parks created before 1916 were established by legislation that usually said that

> . . . shall make regulations providing for the preservation from injury or spoliation, of all timber, mineral deposits, natural curiosities, or wonders, within the park, and their retention in their national condition.

In 1916 the National Park Service Organic Act was passed (29) with the stated purpose ". . . to conserve the scenery and the natural and historic objects and the wildlife therein . . ." Whether the national park was created before or after 1916, water is reserved for the purpose of the park—protecting forest growth, watershed protection, erosion control, lawn watering, fire protection, minimum stream flows, lake levels, irrigation, wildlife and bird watering, campground uses and maintenance, public facility uses, etc. (21). If additional water is needed, or if water is needed for secondary purposes, the National Park Service may acquire additional water rights by following state law.

The Wild and Scenic Rivers Act (31)

> . . . shall not be construed as a reservation of the waters of such streams for purposes other than those specified . . . or in quantities greater than necessary to accomplish these purposes.

It may be inferred that the amount of unappropriated waters that are reserved is limited to those necessary to protect the particular esthetic, recreational, scientific, biotic, or historic features that led to the river's inclusion as a component of the system.

The Reclamation Act of 1902 (38) provided that

> . . . nothing in this Act shall be construed as affecting or intending to affect or to in any way interfere with the laws of any State or Territory relating to the control, appropriation, use, or distribution of water used in irrigation . . .

This has been recently interpreted by the United States Supreme Court (3) as requiring the United States to apply, pursuant to state law, for water rights needed for any proposed Bureau of Reclamation (now known as Water and Power Resources Service) project and to comply with conditions established by the state, unless the conditions are inconsistent with congressional directives.

In general, the implied Federal reserved right is for enough water to fulfill the specific purpose for which the land is reserved. Nonreserved rights are those for secondary uses, or for congressionally authorized management objectives on multiple-use public lands. In the case of nonreserved rights the Federal government would follow state law in acquiring a water right.

As a rule, reserved water rights were adjudicated in Federal courts until the passage of the McCarran Amendment in 1952 (35) which granted a limited waiver of Federal sovereign immunity to permit suits against the United States in stream adjudication where the United States' water rights are involved. The Supreme Court interpreted (20) the amendment to include the Federal water rights of federal non-Indian reservations and enclaves, as well as Indian reserved rights (15). From these cases it is now possible for the states to initiate adjudication for determination, extent, existence, scope, and measure of reserved rights in the state courts without having to wait for the Federal government to initiate such a suit.

Other Indian Reserved Rights

As yet, there are no standards for determining the amount of water reserved by Indian reservations for nonagricultural uses. There are, however, these pending cases that demonstrate that the measure may be that amount of water necessary to fulfill the particular purpose for which the water was impliedly reserved. First, where a water right is asserted for the purpose of sustaining a viable fishery in a desert lake and its supporting stream, the United States claims sufficient water to maintain the present level of the lake over a long period of time, along with sufficient stream flows to sustain spawning runs and to preserve the instream habitat for the fish and their fingerlings (24). This case involves Pyramid Lake, a large desert lake enclosed entirely within the Pyramid Lake Indian Reservation. Second, where coal mines exist on an Indian reservation, the claim is for sufficient water to bring the coal to a marketable state on

the Ute, Mountain Ute, and Southern Ute Indian reservation in southern Colorado (15). Third, if preservation of the ecology of a stream is the purpose of a reservation, the claim if for a minimum flow of water sufficient to maintain the environment of the stream and its wildlife values on Chamokane Creek on the Spokane Indian Reservation (16).

Nonreserved Federal Water Rights

The Solicitor's Opinion, released June 23, 1979, refers in part to Federal water rights that are not reserved. The opinion indicates that these "rights" are for the purpose of carrying out the congressionally authorized objectives of the Department of the Interior. Examination of the Solicitor's Opinion leads one to conclude that Federal nonreserved right is limited to differences between Federal and state requirements for an appropriation. Under state law the Federal government has the right to file for an appropriation of water from the unappropriated waters of the state, with a date of priority appropriate for either application or actual beneficial use. These appropriations are not to adversely affect existing rights established under state law. The procedure, then, would follow state law. The purpose or beneficial use of the right might not follow state law, since the definition of beneficial use varies from state to state and since some states may not accept instream uses as beneficial. While following basic state procedures to acquire a water right, the Solicitor's Opinion states that the Federal government will not be constrained to state limitations that may tend to constrain Federal definitions of beneficial use on public lands. The area of conflict is in determining if this right exists at all and, if it does, it will probably be limited to different interpretations of beneficial uses, with the Federal government using the broadest view of beneficial use and demanding appropriation rights that may not be able to be certificated to any other user under state laws.

Future

The doctrine of reserved water rights has grown from a concept of reserved Federal powers in both navigation rights and property rights along with its treaty-making powers. The admission of a state into the union on an "equal footing" did not divest the United States of its plenary control over the waters (1), but the Supreme Court has recognized (3) that there is a conflict because the state, upon admission to the union, should have "exclusive sovereignty" over the unappropriated waters of their streams. While it may be difficult or impossible to have agreement between the states rights and reserved-rights doctrine after statehood, the reserved-rights doctrine is nevertheless law at this time.

Reserved rights always begin as implied rights that must be quantified. There are still many unanswered questions concerning reserved rights such as: (1) Can the United States reserve water rights for acquired, rather than withdrawn lands; (2) are there reserved rights for minimum stream flows; (3) does a change in the purpose of a reservation destroy or change the date of a reserved right; (4) what limits are placed on the purpose of a reservation; and (5) does a reserved water right extend off the reserved land to a distant stream or water source?

Appendix.—References

1. *Arizona* v. *California*; 373 U.S. 546 (1963).
2. *California and Oregon Power Co.* v. *Beaver Portland Cement Co.*; 295 U.S. 142, (1935).
3. *California* v. *United States*; 438 U.S. 645 (1978).
4. *Chisolm* v. *Cains*; 67 Fed. 285, (1894).
5. *The Daniel Ball*; 77 U.S. 557, (1870).
6. *Federal Power Commission* v. *Oregon*; 349 U.S. 435, (1955).
7. *Hough* v. *Porter*; 51 Ore. 318, (1909).
8. *Jolly* v. *Terra Haute Drawbridge Co.*; Fed. Case No. 7-441, (1853).
9. *Kansas* v. *Colorado*; 206 U.S. 46, (1907).
10. *Lux* v. *Haggin*; 69 Cal. 255 (1886).
11. *Kidd* v. *Laird*; 15 Cal. 161, (1860).
12. *Nevada ex rel Shamberger* v. *United States*; 165 F. Supp. 600, (1958).
13. Proclamation No. 2961, 66 Stat. C 18, Fed. Reg. 691.
14. *United States* v. *Ahtanum Irrigation District*; 236 F. 2nd 321, (1956).
15. *United States* v. *Akin*; 504 F. 2nd 115, (1974).
16. *United States* v. *Anderson*; Civil No. 3643 (E.D. Wash. 1972).
17. *United States* v. *Cappaert*; 375 F. Supp. 456, (1974).
18. *United States* v. *Cappaert*; 508 F. 2nd 313, (1974).
19. *United States* v. *Conrad Investment Co.*; 156 Fed. 123, (1907).
20. *United States* v. *District Court for Eagle County*; 401 U.S. 520, (1971).
21. *United States* v. *New Mexico*; 438 U.S. 696, (1978).
22. *United States* v. *Powers*; 305 U.S. 527, (1939).
23. *United States* v. *Rio Grande Dam and Irrigation Co.*; 174 U.S. 690, (1899).
24. *United States* v. *Truckee-Carson Irrigation District*; Civil No. 2987 JBA.
25. *United States* v. *Walker River Irrigation District*; 104 F. 2nd 334, (1939).
26. *Winters* v. *United States*; 143 Fed. 740, (1908).
27. *Winters* v. *United States*; 207 U.S. 564, (1908).
28. Act of July 26, 1866, Ch. 262, 14 stat 251 (Desert Lands Act, 1866).
29. Act of Aug. 25, 1916, 39 stat sec. 535 (National Park Service Organic Act).
30. 265 stat. 454 (1890) (Rivers and Harbors Act).
31. 16 U.S.C. sec. 1271-1287, 82 stat 906, 1976 (Wild and Scenic Rivers Act).
32. 43 U.S.C. sec. 161 (1958) (Homestead Act).
33. 43 U.S.C.A. sec. 661.
34. 43 U.S.C.A. sec. 321 (Desert Land Act 1877).
35. 43 U.S.C. sec. 666 (1970) (McCarran Amendment).
36. 43 U.S.C. sec. 291 et seq. (Pickett Act).
37. 43 U.S.C. sec. 315 et seq. (Taylor Grazing Act).
38. 43 U.S.C. sec. 372 et seq. (Reclamation Act).
39. 43 U.S.C. 1411 et seq. (Classification and Multiple Use Act).
40. 43 U.S.C. 1714.

JOURNAL OF
THE IRRIGATION
AND DRAINAGE DIVISION

Aquifer Parameter Estimation Using Kalman Filters

By Subhash Chander,[1] Prakash N. Kapoor,[2] and Sushil K. Goyal[3]

Introduction

The quantitative evaluation of an aquifer as a potential ground-water resource depends largely on the correct determination of its two inherent characteristics: its ability to store and its ability to transmit water. In case of leaky aquifers, the leakage factor of the overlying semipervious layer must also be known. These parameters are estimated by analyzing the observed head variations in an aquifer test. The measured heads in the field do not necessarily satisfy the assumed flow equations for analysis because of the uncertainties in the system and noise in the measurements. Conventional approaches for parameter estimation from pumping test analysis (5,9) do not account for such uncertainties, and do not give any index of reliability of the parameters.

A computationally-efficient nonlinear filter, known as an iterated extended Kalman filter (IEKF) has been used to get the parameter estimates both for nonleaky and leaky aquifers, along with the confidence limits, in the presence of modeling and observational errors.

Mathematical Formulation

Nonleaky Aquifer.—Under the Dupuit-Forchheimer assumptions, the partial differential equation representing the radial flow of groundwater in a confined

[1]Prof. in Civ. Engrg., Indian Inst. of Tech., Delhi, Hauz Khas, New Delhi, 11016, India.

[2]Asst. Prof. in Civ. Engrg., Indian Inst. of Tech., Delhi, Hauz Khas, New Delhi, 11016, India.

[3]Research Scholar in Civ. Engrg., Indian Inst. of Tech., Delhi, Hauz Khas, New Delhi, 11016, India.

Note.—Discussion open until August 1, 1981. To extend the closing date one month, a written request must be filed with the Manager of Technical and Professional Publications, ASCE. Manuscript was submitted for review for possible publication on July 2, 1980. This paper is part of the Journal of the Irrigation and Drainage Division, Proceedings of the American Society of Civil Engineers, ©ASCE, Vol. 107, No. IR1, March, 1981. ISSN 0044-7978/81/0001-0025/$01.00.

nonleaky aquifer of constant depth is:

$$T\left[\frac{\partial^2 s}{\partial r^2} + \left(\frac{1}{r}\right)\frac{\partial s}{\partial r}\right] = S\frac{\partial s}{\partial t} - q \quad \text{(1)}$$

in which T = the transmissivity, in square meters per day; s = the drawdown, in meters; r = the distance, in meters, from the pumped well; S = the storage coefficient; t = the time, in days, elapsed since pumping started; and q = the rate of withdrawl per unit area, in meters per day. Eq. 1 assumes that the pumping well fully penetrates the aquifer layer during the test. Theis' solution (8) for Eq. 1 is:

$$s = \left(\frac{Q_w}{4\pi T}\right) W\left(\frac{r^2 S}{4Tt}\right) \quad \text{(2a)}$$

$$\text{or} \quad s = \left(\frac{Q_w}{4\pi T}\right)\left[-0.5772 - \ln\left(\frac{r^2 S}{4Tt}\right) + \left(\frac{r^2 S}{4Tt}\right) - \left(\frac{1}{2!}\right)\left(\frac{r^2 S}{4Tt}\right)^2 + \ldots\right] \quad \text{(2b)}$$

in which Q_w = the constant pumping rate, in cubic meters per day; and $W(\ )$ = the well function for a nonleaky aquifer. Eq. 2b may not be fully representative

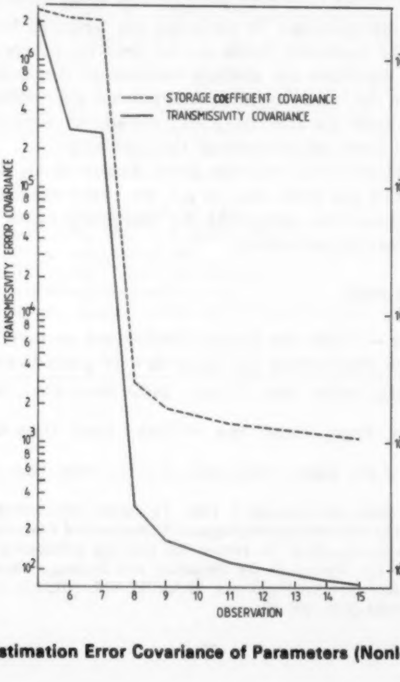

FIG. 1.—Estimation Error Covariance of Parameters (Nonleaky Aquifer)

of the ground-water system under analysis, and in addition, there may be errors in the observed drawdowns. Due to these likely errors the estimation of parameters T and S can be carried out using the IEKF (3), as in the following.

Defining the state vector as $\mathbf{X}(t_k) = [T\ S]'_{t_k}$, in which $[\ ]'$ = the transpose of the vector $[\ ]$; and taking T and S as time invariants for the short durations of the pumping test, the state equations is:

$$\mathbf{X}(t_{k+1}) = \mathbf{X}(t_k) \quad \text{(3)}$$

The measurement equation is

$$y(t_k) = \left(\frac{Q_w}{4\pi T}\right)\left[-0.5772 - \ln\left(\frac{r^2 S}{4Tt_k}\right) + \left(\frac{r^2 S}{4Tt_k}\right) - \left(\frac{1}{4}\right)\left(\frac{r^2 S}{4Tt_k}\right)^2 + v_{t_k}\right] \quad \text{(4a)}$$

$$\text{or} \quad y(t_k) = h(\mathbf{X}_{t_k}) + v_{t_k} \quad \text{(4b)}$$

in which the measurement function $h(\ )$ is nonlinear in T and S; v_{t_k} = the total error in the modeling and observation; it is white gaussian with zero mean and covariance defined as

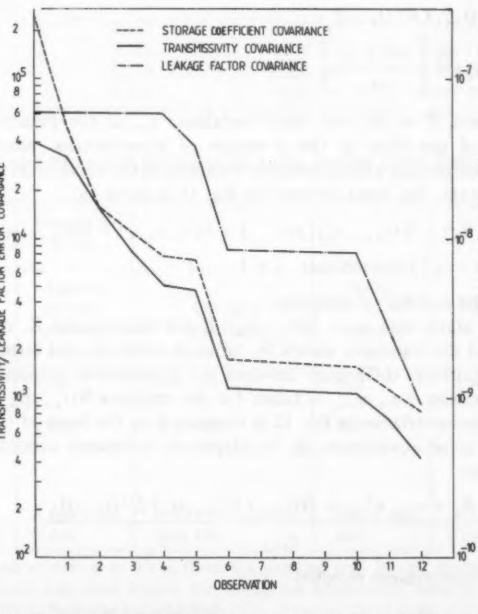

FIG. 2.—Estimation Error Covariance of Parameters (Leaky Aquifer)

$$E\{[v_{t_k}][v_{t_j}]'\} \triangleq R_{t_k}\delta_{kj} \quad (5)$$

in which **R** = the measurement noise covariance matrix; and δ = the Kronecker delta.

Starting with the initial estimates for the state as

$$\hat{X}[t_o|t_o] = \hat{X}(t_o) = E[X(t_o)] \quad (6)$$

and for the estimation error covariance as

$$P(t_o|t_o) = P(t_o) = E\{[X(t_o) - \hat{X}(t_o)][X(t_o) - \hat{X}(t_o)]'\} \quad (7)$$

the predictor-corrector algorithm for getting the filtered state estimates is given as

$$\hat{X}(t_{k+1}|t_k) = \hat{X}(t_k|t_k) \quad (8)$$

$$P(t_{k+1}|t_k) = P(t_k|t_k) \quad (9)$$

in which $P(t_{k+1}|t_k) \triangleq E\{[X(t_{k+1}) - \hat{X}(t_{k+1}|t_{k+1})][X(t_{k+1})$

$$- \hat{X}(t_{k+1}|t_k)]'\} \quad (10)$$

$$\hat{X}(t_{k+1}|t_{k+1}) = \hat{X}(t_{k+1}|t_k) + K(t_{k+1})\{y(t_{k+1}) - h[\hat{X}(t_{k+1}|t_k)]\} \quad (11)$$

in which **K**( ) = the filter gain or Kalman gain matrix

$$P(t_{k+1}|t_{k+1}) = [I - K(t_{k+1})H(t_{k+1})]P(t_{k+1}|t_k)[I - K(t_{k+1})H(t_{k+1})]'$$

$$\times [K(t_{k+1})R(t_{k+1})K'(t_{k+1})] \quad (12)$$

in which $H(t_k) \triangleq \left[\dfrac{\partial h(X_{t_k})}{\partial x_j}\right] \quad (13)$

Variables T and S = the two state variables, x_j, in the present case. The performance of the filter in the presence of measurement nonlinearities is improved by performing a local iteration, retaining at the same time, the recursive filter structure (1). The local iterator for Eq. 11 is given as:

$$\eta_{i+1} = \hat{X}(t_{k+1}|t_k) + K(t_{k+1}, \eta_i)\{y(t_{k+1}) - h(\eta_i, t_{k+1}) - H(t_{k+1}, \eta_i)$$

$$\times [\hat{X}(t_{k+1}|t_k) - \eta_i]\}, \quad \text{such that} \quad i = 1, ..., l \quad (14)$$

in which l = the number of iterations.

The iterator starts with $\eta_1 = \hat{X}(t_{k+1}|t_k)$. It reevaluates gain **K**, measurement function h, and the transition matrix **H**, on each iteration, and terminates when there is no significant difference between the consecutive iterates. The result of the last iteration, i.e., η_{l+1} is taken for the estimate $\hat{X}(t_{k+1}|t_{k+1})$, and the estimation error covariance in Eq. 12 is computed on the basis of this estimate. Measurement noise covariance, **R**, is adaptively estimated according to Sage and Husa (6) as:

$$R(t_{k+1}) = \frac{[t_k R_k + v_{t_{k+1}} v'_{t_{k+1}} + H(t_{k+1}) P(t_{k+1}|t_k) H'(t_{k+1})]}{t_{k+1}} \quad (15)$$

in which the measurement residual

$$v_{t_{k+1}} = y(t_{k+1}) - h[\hat{X}(t_{k+1}|t_k)] \quad (16)$$

Leaky Aquifer.—Under a constant head of ponding, vertical leakage, and the Dupuit-Forchheimer assumptions, the partial differential equation for groundwater flow in a confined leaky aquifer of constant depth is:

$$T\left[\frac{\partial^2 s}{\partial r^2} + \left(\frac{1}{r}\right)\frac{\partial s}{\partial r}\right] - \frac{Ts}{L^2} = S\frac{\partial s}{\partial t} - q \quad \text{(17)}$$

in which L = the leakage factor in meters. Eq. 17 assumes that the pumping well fully penetrates the aquifer layer during the test. Hantush and Jacob (2)

TABLE 1.—Aquifer Parameter Estimates for Nonleaky Aquifer Using Different Methods

Method of analysis (1)	Transmissivity, in square meters per day (2)	Storage coefficient (3)	Residual square for the data 6-30 observations (4)
Theis	2,182	0.000 724	$0.123\ 158 \times 10^{-3}$
Jacob	2,262	0.000 679	$0.311\ 713 \times 10^{-3}$
Chow	2,197	0.000 662	$0.184\ 373 \times 10^{-3}$
Kriz	1,944	0.000 648	$0.110\ 926 \times 10^{-1}$
IEKF applied to data segment:			
6–15	2,147	0.000 747	$0.117\ 728 \times 10^{-3}$
11–20	2,210	0.000 663	$0.154\ 710 \times 10^{-3}$
16–25	2,158	0.000 745	$0.121\ 447 \times 10^{-3}$
21–30	2,278	0.000 617	$0.198\ 225 \times 10^{-3}$

TABLE 2.—Aquifer Parameter Estimates for Leaky Aquifer Using Different Methods

Methods of analysis[a] (1)	Transmissivity, in square meters per day (2)	Storage coefficient (3)	Leakage factor, in meters (4)	Residual square (5)
Hantush I	1,665	0.00 170	600	$0.12\ 885 \times 10^{-4}$
Walton-type curve	1,729	0.00 190	900	$0.18\ 999 \times 10^{-4}$
Rushton's discrete numerical model	1,680 ± 50	0.00 150 + 0.0002	850 ± 100	$0.32\ 426 \times 10^{-4}$
IEKF	1,658	0.00 174	668	$0.38\ 215 \times 10^{-5}$

[a]The observation well is at 90 m from the pumped well for all methods except for Rushton's discrete numerical model, for which the observation wells are at 30 m, 60 m, 90 m, and 120 m from the pumped well.

gave the solution for Eq. 17 as:

$$s = \left(\frac{Q_w}{4\pi T}\right) W\left(\frac{r^2 S}{4Tt}, \frac{r}{L}\right) \quad (18)$$

in which $W(\, , \,)$ = the well function for a leaky aquifer. Eq. 18 is alternatively written as (4):

$$s = \left(\frac{Q_w}{4\pi T}\right)\left[2K_0\left(\frac{r}{L}\right) - W\left(\frac{Tt}{L^2 S}\right)\right] \quad (19)$$

in which $K_0(\,)$ = the modified Bessel's function of second kind and zero order. Eq. 19 is expanded as:

$$s = \left(\frac{Q_w}{4\pi T}\right) \times 2\left\{\left[1 + \left(\frac{r}{2L}\right)^2 + \left(\frac{1}{4}\right)\left(\frac{r}{2L}\right)^4 + \ldots\right] \ln\left[\frac{1.123}{\left(\frac{r}{L}\right)}\right]\right.$$

$$\left. + \left(\frac{r}{2L}\right)^2 + \left(\frac{3}{8}\right)\left(\frac{r}{2L}\right)^4 + \left(\frac{11}{216}\right)\left(\frac{r}{2L}\right)^6 + \ldots\right]\right\} - \left(\frac{Q_w}{4\pi T}\right)$$

$$\times \left[-0.5572 - \ln\left(\frac{Tt}{L^2 S}\right) + \left(\frac{Tt}{L^2 S}\right) - \left(\frac{1}{4}\right)\left(\frac{Tt}{L^2 S}\right)^2\right] \quad (20)$$

Eq. 20 is nonlinear in T, S, and L. Parameter identification problem in the presence of unknown modeling and observational noise can be solved by using the IEKF as explained earlier (Eqs. 3–16), with the state variables and the measurement function given as follows:

State vector $\mathbf{X}(t_k) = [T\,S\,L]'$ . . . . (21)

Measurement function

$$h(\mathbf{X}_{t_k}) = \left(\frac{Q_w}{4\pi T}\right) \times 2\left\{\left[1 + \left(\frac{r}{2L}\right)^2 + \left(\frac{1}{4}\right)\left(\frac{r}{2L}\right)^4\right] \ln\left[\frac{1.123}{\left(\frac{r}{L}\right)}\right.\right.$$

$$\left.\left. + \left(\frac{r}{2L}\right)^2 + \left(\frac{3}{8}\right)\left(\frac{r}{2L}\right)^4 + \left(\frac{11}{216}\right)\left(\frac{r}{2L}\right)^6\right]\right\}$$

$$- \left(\frac{Q_w}{4\pi T}\right) \times \left[-0.5772 - \ln\left(\frac{Tt}{L^2 S}\right) + \left(\frac{Tt}{L^2 S}\right) - \left(\frac{1}{4}\right) \times \left(\frac{Tt}{L^2 S}\right)^2\right] \quad (22)$$

In this case T, S, and L are the three state variables, x_j.

Application to Field Data

Aquifer test data for a nonleaky aquifer already analyzed by Sharma and Chawla (7) using Theis', Jacob's, Chow's, and Kriz' methods were selected for aquifer parameter estimation by the IEKF. The Dalem test data which have

been earlier analyzed by Kruseman and de Ridder (4), using Hantush and Walton's methods, and by Rushton and Chan (5), using a discrete numerical model, was chosen for the leaky aquifer parameter estimates.

A lithological cross section of the test site in the leaky aquifer has Holocene as the overlying semipervious layer and Kedicham (lower Pleistocene) as the impervious basis layer. During the pumping test, the screen was open only in the Kreftenheye (upper Pleistocene) which was 11 m–19 m below the ground surface. This formation is of medium coarse sand with 0%–2% clay.

Initial estimates for the parameters are normally prescribed on the basis of the geologic information of the test site. It is felt that faster convergence may be achieved by choosing the initial estimates on the basis of some information about the system behavior to pumping stresses. The initial estimates for the transmissivity and storage coefficient were found out by using the first two observations for drawdown and applying Jacob's relation (4) to the two drawdown values. The initial estimate of the leakage factor in the case of the leaky aquifer was calculated by using the last available observation and applying the approximate steady-state drawdown relationship for the leaky aquifer as used in the Hantush I method (4).

The filter provided the parameter estimates along with the estimation error covariance, and the sum of the residual squares for the difference between the observed heads and those calculated using filtered parameter estimates. Different sets of data were analyzed for estimating aquifer parameters. Successive values of estimation error covariance for the parameters for nonleaky and leaky aquifers are shown in Figs. 1 and 2, respectively. The estimated aquifer parameters and the residual squares, as obtained by using various methods, are given in Table 1 for the nonleaky aquifer, and in Table 2 for the leaky aquifer. The filtered aquifer parameter estimates along with their upper and lower limits for 95% confidence level (assuming a Gaussian distribution) are given in Table 3.

TABLE 3.—Confidence Limits of Aquifer Parameter Estimates Using IEKF

Parameter (1)	95% lower confidence limit (2)	Filtered value (3)	95% upper confidence limit (4)	Standard deviation of parameter (5)
(a) Nonleaky				
Transmissivity, in square meters per day	2,130	2,147	2,164	8.7
Storage coefficient	0.000 726	0.000 747	0.000 767	0.000 010
(b) Leaky				
Transmissivity, in square meters per day	1,620	1,658	1,696	19
Storage coefficient	0.00 168	0.00 174	0.00 180	0.000 029
Leakage factor, in meters	602	668	730	31

Analysis of Results

Comparing the aquifer parameter estimates using the IEKF method with those obtained using the known techniques, the following points are observed:

1. The sum of residual squares computed from the difference of the observed and the calculated heads is the least for the parameter estimates resulting from the IEKF method for the data segment 6–15, as compared to those obtained using various other methods.
2. Error covariance plots for the coefficients of storage and transmissibility for the nonleaky aquifer (see Fig. 1) show a rapid decrease for the first few observations, and thereafter the plots indicate only a marginal decrease with each observation. It shows that the parameter estimates tend to converge after a few observations and additional observations do not significantly change the parameter estimates.
3. Also in the case of the leaky aquifer (see Fig. 2), the error covariance for transmissivity and storage coefficient decreases rapidly for the first few observations; after that the decrease is not as rapid. The error covariance of the leakage factor decreases only marginally for the first few observations, which may be attributed to the fact that there is some time lag between the start of pumping and the leakage effects influencing the drawdown.

Conclusions

From the aforementioned analysis, it is concluded that:

1. The IEKF provides the estimates of the aquifer parameters (T and S for the nonleaky aquifer, and T, S, and L for the leaky aquifer) in the presence of system uncertainties and noisy measurements.
2. The filter also provides the confidence limits for the parameters.
3. The technique is sequential, and each additional observation reduces the error covariance of the parameter estimates, although only a few observations are sufficient to provide a reasonable estimate of the aquifer parameters.
4. The subjectivity involved in type-curve matching for the parameter estimation is eliminated using the IEKF method.

Appendix I.—References

1. Denham, W. F., and Pines, S., "Sequential Estimation When Measurement Function Nonlinearity Is Comparable to Measurement Error," *AIAA Journal*, Vol. 4, 1966, pp. 1071–1076.
2. Hantush, M. S., and Jacob, C. E., "Nonsteady Radial Flow in an Infinite Leaky Aquifer," *Transactions*, American Geophysical Union, Vol. 36, 1955, pp. 95–100.
3. Jazwinski, A. H., *Stochastic Processes and Filtering Theory*, Academic Press, New York, N.Y., 1970, pp. 272–365.
4. Kruseman, G. P., and de Ridder, N. A., "Analysis and Evaluation of Pumping Test Data," *Bulletin 11*, Institute for Land Reclamation and Improvement, Wageningen, the Netherlands, 1970, pp. 80–94.
5. Rushton, K. R., and Chan, Y. K., "A Numerical Model for Pumping Test Analysis," *Proceedings*, Institution of Civil Engineers, Vol. 61, Part 2, 1976, pp. 281–296.
6. Sage, A. P., and Husa, G. W., "Adaptive Filtering with Unknown Prior Statistics," *Proceedings*, Tenth Joint Automatic Control Conference, Aug., 1969, pp. 760–769.

7. Sharma, H. D., and Chawla, A. S., "Manual on Groundwater and Tubewells," *Technical Report No. 18*, Central Board of Irrigation and Power, New Delhi, India, 1977, pp. 44–49.
8. Theis, C. V., "The Relation between the Lowering of Piezometric Surface and the Rate and Duration of Discharges of a Well Using Groundwater Storage," *Transactions*, American Geophysical Union, Vol. 16, 1935, p. 525.
9. Walton, W. C., *Groundwater Resource Evaluation*, McGraw-Hill Book Co., Inc., New York, N.Y., 1970.

Appendix II.—Notation

The following symbols are used in this paper:

$\mathbf{H}$ = measurement transition matrix;
$h(\ )$ = measurement function;
$\mathbf{K}$ = Kalman gain matrix;
$K_0(\ )$ $\triangleq$ modified Bessel's function of second kind and zero order;
L = leakage factor in meters;
$\mathbf{P}$ = estimation error covariance matrix;
Q_w = rate of pumping, in cubic meters per day;
q = rate of withdrawal per unit area, in meters per day;
$\mathbf{R}$ = measurement noise covariance matrix;
r = distance to observation well, in meters;
S = storage coefficient;
s = drawdown in meters;
T = transmissivity, in square meters per day;
t = time, in days, since pumping started;
$W(\ )$ $\triangleq$ well function for a nonleaky aquifer;
$W(\ ,\ )$ $\triangleq$ well function for a leaky aquifer;
$\mathbf{X}$ = state vector;
x = state variable;
y = measurement;
δ $\triangleq$ Kronecker delta;
ν = measurement residual; and
$'$ $\triangleq$ transpose of a vector.

[illegible]

JOURNAL OF
THE IRRIGATION
AND DRAINAGE DIVISION

Leaching and Water-Type Effects on Ground-Water Quality

By Donald L. Suarez[1] and Martinus Th. van Genuchten[2]

Introduction

Leaching to prevent the accumulation of soluble salts in the crop rootzone is essential for sustained irrigated agriculture. Under present irrigation practices, however, many irrigated lands are leached more than is necessary to prevent yield reductions from excess salinity buildup. Reduced leaching should not result in reduced yields in many irrigation projects in the United States (10).

When leaching fractions are reduced, the total salt load of the drainage water is reduced (3,5), although the salt concentration in the lower part of the rootzone is increased. Thus, irrigation management offers a means of controlling the salt content of drainage water under certain circumstances. In a previous study, the first author and Rhoades (7) analyzed the effects of improved irrigation efficiency on ground-water salinity for closed river basins. Depending upon water chemistry, changes in irrigation efficiency at steady-state water and salt fluxes may or may not affect downstream water quality. They classified irrigation waters into three groups: Type 1—waters initially undersaturated with $CaCO_3$; Type 2—waters initially saturated with $CaCO_3$; and Type 3—waters nearing saturation with gypsum and saturated with $CaCO_3$. Improved irrigation management resulted only in a slight reduction in downstream salinity if Type 1 water was used, in no steady-state reductions in downstream salinity with Type 2 water, and in substantial steady-state reductions in downstream salinity with Type 3 water.

The effects of irrigation management on steady-state ground-water salinities have also been analyzed (6). As with surface waters, reduced leaching, at steady state, may or may not reduce degradation of ground waters receiving irrigation

[1]Geochemist, United States Salinity Lab., United States Dept. of Agr., 4500 Glenwood Drive, Riverside, Calif. 92501.

[2]Soil Scientist, United States Salinity Lab., United States Dept. of Agr., 4500 Glenwood Drive, Riverside, Calif. 92501.

Note.—Discussion open until August 1, 1981. To extend the closing date one month, a written request must be filed with the Manager of Technical and Professional Publications, ASCE. Manuscript was submitted for review for possible publication on January 17, 1980. This paper is part of the Journal of the Irrigation and Drainage Division, Proceedings of the American Society of Civil Engineers, ©ASCE, Vol. 107, No. IR1, March, 1981.

drainage waters, depending on water type and hydrologic conditions. These evaluations were made for situations in which it was assumed that no salts, other than those present in the irrigation water or those derived from the dissolution of calcium carbonates or silicates in the soil profile, contributed to ground-water salinity. If additional readily soluble salts are present in the soil, or saline waters are present in the drainage water flow path (as is often the case), then reduced leaching will always decrease the rate of ground-water salination.

These previous studies have only considered steady-state conditions without considering travel times in either the unsaturated or saturated zones. Reduced leaching substantially increases solute residence times in and below the rootzone (4) and thus influences the rate of groundwater salination. The purpose of this study is to demonstrate the important transitory effects of changes in irrigation management on ground-water salinity, including consideration of solute transport in the unsaturated zone as well as chemical precipitation.

The effect of irrigation management on water quality can best be determined by computer simulation. Although the chemical and physical components of the model have been independently tested and verified, at the present time it is not possible to verify the simulation with data from a real ground-water basin. Accurate historical data on leaching fractions, irrigation, and groundwater quality and soil CO_2 levels are not available. It is our belief that a major reason water quality implications of irrigation management have been neglected is that its effects are observable only over long time periods (often decades or longer). Because of the considerable lag between implementation and observable results, any changes in water quality could also be caused by changes in other variables within that time frame.

Procedure

The effects of changes in irrigation management (leaching fraction), travel time, and irrigation water type on ground-water quality will be demonstrated with a hydrologically very simple transport model. Although the approach taken here does not apply to any particular ground-water basin, the calculations serve to illustrate the underlying physico-chemical principles. Changes in soil type, soil layering, and depth to water table may therefore affect the numerical results of the analysis, yet they will not alter the qualitative conclusions to be drawn from these results.

Figure 1 gives a schematic diagram of the hypothetical ground-water basin used in the analysis. A water table is assumed present at a depth of 20 m below the rootzone, while the unconfined aquifer is assumed to be bounded below by an impermeable layer at a depth of 50 m. The ground-water basin is managed to maintain the water table at a depth of 20 m, with no mass flow into or out of the basin. Because of evapotranspiration, this requires importing surface water into the basin at a rate equal to the net evapotranspiration rate, E (evapotranspiration minus rainfall; E is taken as 1.00 m/yr). Water for leaching is pumped from the underlying groundwater through a series of wells which drain water uniformly from the 30 m thick saturated zone. Thus, the rate of pumping per unit surface area, Q, is equal to the average drainage flux, D. The spatially distributed wells in the basin are assumed to be sufficiently close together so that, on the average, horizontal flow is not significant in the saturated

zone. The basin is also assumed to be irrigated uniformly. Then no important areal effects are present, and the ground-water basin can be treated as a one-dimensional vertical system. Such a hydrologically simple system lends itself to analysis with relatively modest computer expenses. Although the exact simulation of an actual ground-water basin may require the use of a more complex two- or three-dimensional transport model, this will depend on the specific hydrology of that basin. The one-dimensional model will properly account for the vertical flow component, which is examined in the study.

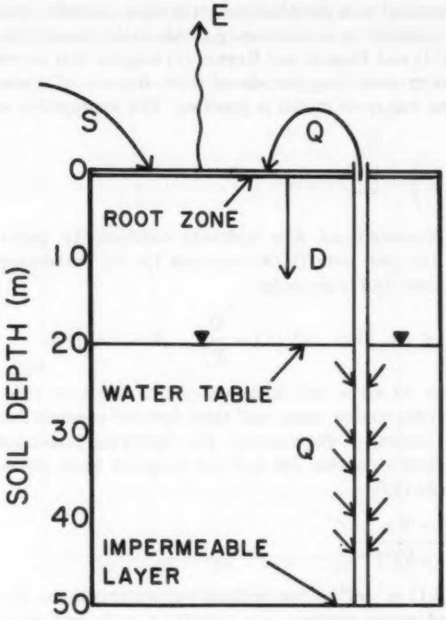

FIG. 1.—Schematic Representation of Simulated One-Dimensional Ground-Water Basin: E **= Net Evapotranspiration Rate (Set at 1.00 m/yr),** S **= Rate at Which Water is Imported (1.00 m/yr),** D **= Drainage Rate below Rootzone (0.667 m/yr for** L **= 0.4 m/yr and 0.111 m/yr for** L **= 0.1), and** Q **= Rate of Pumping from Saturated Zone (**$Q = D$**)**

Two different leaching fractions (L) are considered: $L = 0.4$ and $L = 0.1$. These values represent common inefficient practices (0.4) and a situation where management optimizes water efficiency (0.1). The leaching fraction, defined as that fraction of the applied water that leaches out of the rootzone, can be written for this study as

$$L = \frac{D}{S + Q} \quad \text{(1)}$$

in which S represents the rate at which water is imported per unit surface area ($S = E$). In the present case, $D = Q$ and $S = 1.00$ m^3/m^2 yr. One may calculate from Eq. 1 that the drainage flux for $L = 0.4$ equals 0.667 m/yr, and for $L = 0.1$ equals 0.111 m/yr. Total irrigation rates are then 1.667 m/yr for 0.4 leaching and 1.111 m/yr for 0.1 leaching.

Water and salt movement are simulated with a slightly modified version of the one-dimensional single-ion saturated-unsaturated transport model described in detail elsewhere (8). The basic transport equations however will be given here. This study analyzes the effects of different irrigation management strategies on resulting vertical salt distributions over time periods of several decades. This makes it possible to consider only steady-state water flow. Earlier studies by Wierenga (11) and Duguid and Reeves (1) suggest that to predict the quality of drainage water over long periods of time, the use of a steady state rather than a transient transport model is justified. The appropriate steady-state flow equation is

$$\frac{\partial}{\partial x}\left(K\frac{\partial h}{\partial x} - K\right) - Q_s(x) = 0 \quad \ldots \quad (2)$$

in which h = pressure head; K = hydraulic conductivity; and x = depth below the rootzone. The sink term $Q_s(x)$ accounts for the withdrawal of water from the saturated zone, and is given by:

$$Q_s(x) = 0, \quad 0 \le x < 20\ \text{m}; \quad Q_s(x) = \frac{Q}{X_s}, \quad 20 \le x \le 50\ \text{m} \quad \ldots \quad (3)$$

in which X_s (= 30 m) = the thickness of the saturated zone. Therefore, Q_s = zero in the unsaturated zone, and then remains constant between the water table and the bottom of the aquifer. The following relationship between the volumetric moisture content (θ) and the pressure head (h) was used for the unsaturated zone (10):

$$\theta = \theta_r + \frac{(\theta_s - \theta_r)}{[1 + (\alpha h)^n]^m} \quad \ldots \quad (4)$$

in which θ_r (= 0.15 m^3/m^3) = the residual soil-water content; θ_s (= 0.40 m^3/m^3) = the saturated water content; $\alpha = -0.01$; $n = 2$; and $m = 1 - 1/n$. The parameter values given here are typical for a fine sandy soil. The hydraulic conductivity of the unsaturated zone, furthermore, is described by the following predictive equation (10):

$$K = K_s \Theta^{1/2} [1 - (1 - \Theta^{1/m})^m]^2 \quad \ldots \quad (5)$$

in which K_s = 0.208 mm/s (or 75 cm/day) is the saturated hydraulic conductivity; and Θ = the dimensionless moisture content:

$$\Theta = \frac{\theta - \theta_r}{\theta_s - \theta_r} \quad \ldots \quad (6)$$

Figure 2 gives a graphical representation of Eqs. 4 and 5. It should be kept in mind that the selection of the soil-hydraulic properties will have very little effect on the results since the volumetric flux is fixed by the rate of water

application and pumping rate. These rates are in turn fixed by the aquifer depth and leaching fraction. Equation 2 is solved, subject to the boundary conditions

$$\left(-K\frac{\partial h}{\partial x}+K\right)\bigg|_{x=0}=Q \quad \text{(7a)}$$

$$\frac{\partial h}{\partial x}(X,t)=1 \quad \text{(7b)}$$

in which $X(=50\ \text{m})$ = the depth to the impermeable layer. Equation 7*b* represents a no-flow boundary condition. Note that the boundary flux at $x = 0$ is equal

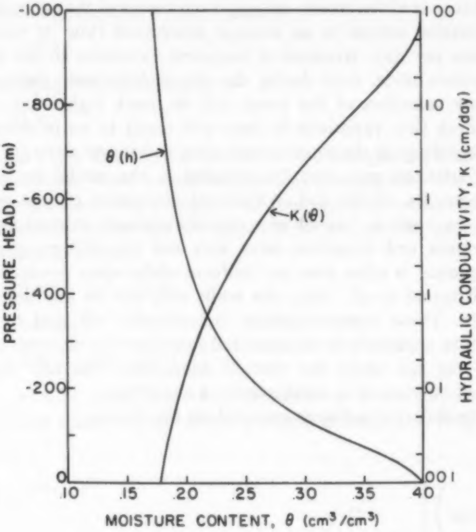

FIG. 2.—Relationship between Pressure Head (h), Volumetric Moisture Content (θ) and Hydraulic Conductivity (K) for Conditions Simulated

to the pumping rate (Q), which in turn is the same as the average drainage flux (D). The boundary at $x = 0$ corresponds to the bottom of the rootzone; the thickness of the rootzone itself is assumed to be negligible compared with the overall dimensions of the simulated system.

The governing salt-transport equation is

$$\frac{\partial \theta c}{\partial t}=\frac{\partial}{\partial x}\left(\theta \mathscr{D}\frac{\partial c}{\partial x}-qc\right)-Q_s(x)c \quad \text{(8)}$$

in which c = the total salt concentration; $\mathscr{D}$ = the dispersion coefficient; and q = the volumetric flux:

$$q = -K \frac{\partial h}{\partial x} + K \quad (9)$$

The dispersion coefficient D in Eq. 8 is evaluated by

$$\mathscr{D} = a + \lambda \left| \frac{q}{\theta} \right| \quad (10)$$

in which $a = 0.0116\ mm^2/s$; $\lambda = 1{,}000$ mm; and where $\mathscr{D}$ and q are expressed in mm^2/s and mm/s, respectively. The parameter λ is often referred to as dispersivity. The 1,000-mm value chosen for λ is much higher than is generally the case (10 mm–30 mm) in most soil physics studies. The high value of λ is necessary because of the steady-state approximation of the water flow equation. This approximation results in an average downward flow of water of only a few millimeters per day. Because of temporal variations in the irrigation and evapotranspiration rates, both during the day and between days and seasons, the actual flow velocities of the water will be much higher and often change directions. These flux variations in time will result in an increased spreading of the salt, especially in the unsaturated zone and upper parts of the saturated zone. Such variations can only be included in the model by increasing the apparent dispersivity of the soil. Additional dispersion effects are caused by the fact that the basin is treated as a one-dimensional vertical system. Actual evapotranspiration and irrigation rates may not be uniform over the basin; irrigation frequency is often also not uniform while some portions of the basin may not be irrigated at all. Also, the wells may not be distributed uniformly over the basin. These nonuniformities undoubtedly will lead to some lateral flow components, especially in the saturated zone, thereby increasing the apparent dispersion of the salt along the vertical dimension. The salt concentrations, therefore, must be viewed as areal averaged quantities.

Initial and boundary conditions imposed on Eq. 8 are:

$$c(x,0) = C_o \quad (11a)$$

$$\left(-\theta \mathscr{D} \frac{\partial c}{\partial x} + qc\right)\bigg|_{x=0} = QC_d \quad (11b)$$

$$\frac{\partial c}{\partial x}(X,t) = 0 \quad (11c)$$

in which C_d = the concentration of the drainage water leaving the rootzone.

The subsurface material is taken to be a fine sandy soil with no ion exchange potential. Two different water types are considered in this study. In each case the initial salt concentration in the soil profile (C_o) is taken to be the same as the concentration of the imported water. In the first example, C_o is taken to be 8.52 meq/L with a composition resembling that of Colorado River or Rio Grande River water equilibrated with $CaCO_3$ at 0.03 atm CO_2 pressure. Thus, this water is initially saturated with $CaCO_3$ ("Type 2" water). Its composition in milliequivalents per liter is as follows: Ca, 6.87; Mg, 0.60; Na, 1.05; Cl, 0.21; alkalinity, 7.00; and SO_4, 1.31.

Chemical equilibrium calculations, based on a procedure similar to that of

Ref. 7, showed that the salinity of the drainage water (C_d) can be linearly related to the salinity of the irrigation water (C_i) given the foregoing. This generalization is valid only for waters where Ca $\simeq$ HCO_3, such as in the water composition selected here. In addition, when Ca is not equal to HCO_3 (in milliequivalents per liter), no generalized relationship can be proposed between the concentration of the irrigation water and the concentration of the drainage water. This is because waters of the same salinity but with different Ca concentrations can be derived by mixing various proportions of different drainage waters generated from the same original water. In that case, the flow equation and the chemical equilibria model would need to be combined into a multi-ion model and solved for each of the ions in the model. Again, this was not the case for the water chosen in this paper, since Ca $\simeq$ HCO_3.

For 0.40 leaching, the linear relationship is

$$C_d = 2.50C_i - 10.3 \quad \quad (12)$$

For 0.10 leaching, the relationship is

$$C_d = 10C_i - 61.8 \quad \quad (13)$$

These equations imply that the amount of $CaCO_3$ precipitated is a linear function of the concentration, with constant chemical precipitation for each leaching fraction. Although there was a slight interrelationship between chemical precipitation and concentration, it can be neglected for our present analysis.

For 0.40 leaching we have

$$C_i = 0.4C_Q + 0.6\,C_o \quad (L = 0.4) \quad \quad (14)$$

and for 0.10 leaching

$$C_i = 0.1C_Q + 0.9\,C_o \quad (L = 0.1) \quad \quad (15)$$

in which C_o (= 8.52 meq/L) = the concentration of the imported water; and C_Q = the average concentration of the pumped groundwater (Fig. 1):

$$C_Q = \frac{1}{30}\int_{20}^{50} c(x,t)\,dx \quad \quad (16)$$

Substitution of Eq. 14 into Eq. 12 allows C_d to be expressed in terms of C_Q and C_o only. This expression is valid for any value of C_o chosen as long as C_d varies linearly with C_i.

This analysis assumes that no chemical reactions occur below the bottom of the rootzone. The partial pressure of CO_2 in an aquifer below an irrigated area with no recharge other than drainage water will be approximately the same as that of the bottom of the rootzone, if no $CaCO_3$ precipitation or dissolution occurs when mixing waters of different composition. Initially, calcite-saturated solutions can be supersaturated or undersaturated when mixed. This effect is explained in detail by Wigley and Plummer (12). As shown in their analysis, for fixed P_{CO_2} and temperature, this effect is largest when chemically dissimilar waters are mixed, e.g., water where Ca > HCO_3 mixed with water where Ca < HCO_3, and results in supersaturation. This effect is not important in our simulation. The other important potential cause of nonequilibrium is due to the nonlinearity of activity coefficients with ionic strength. This nonlinear

effect causes an undersaturation in mixtures of solutions with different ionic strengths. The effects, however, are not substantial in the present example because subsurface mixing occurs only with waters that differ at the most one order of magnitude in concentration, not between waters with orders of magnitude differences in concentration. We assumed, therefore, that no substantial chemical precipitation or dissolution reactions take place below the rootzone in the simulation described here. The ionic strength effect is more important when groundwater is mixed directly with dilute surface water; however, this is properly accounted for by precipitation in the rootzone (Eq. 12).

The other water type considered is that of a water containing only $CaSO_4$. The ground-water concentration at $t = 0$ is taken now as $C_o = 5$ meq/L, the same as the concentration of the imported water at all times. Again, from chemical equilibrium calculations, it was found that the concentration of the drainage water leaving the soil rootzone is given by

$$C_d = 2.5\,C_i \quad (L = 0.4) \qquad (17a)$$

$$C_d = 10.0\,C_i \quad (L = 0.1) \qquad (17b)$$

in which C_i, as before, is given by Eq. 13 and Eq. 16 for 0.40 and 0.10 leaching,

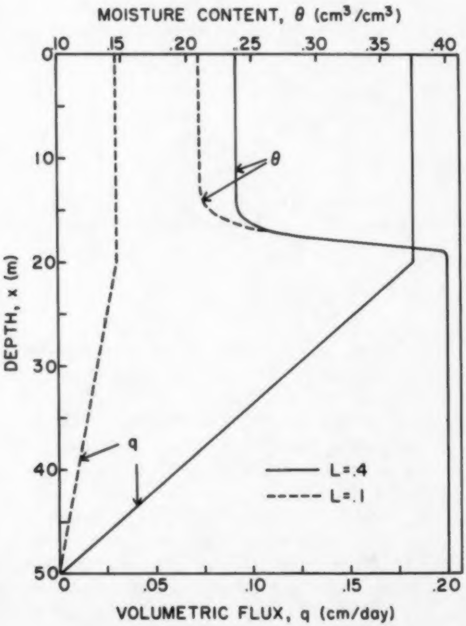

FIG. 3.—Moisture Content (θ) and Volumetric Flux (q) with Depth for 0.1 and 0.4 Leaching Fractions

respectively. The value of C_d cannot exceed 31.15 meq/L, because gypsum will precipitate at 31.15 meq/L in a pure $CaSO_4$ system (25° C). Substituting Eq. 15 into Eq. 17*b* shows that the limiting concentration occurs immediately after the start of the simulation experiment, when the leaching fraction equals 0.1.

Results

Steady-state distributions of the soil water content and the volumetric flux for both leaching fractions are shown in Fig. 3. The volumetric flux in the

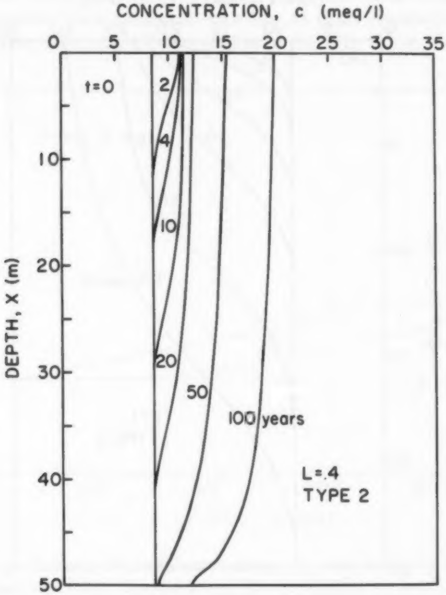

FIG. 4.—Salinity Profiles (Concentration Versus Depth) Obtained after Irrigating for 2 yr, 4 yr, 10 yr, 20 yr, 50 yr, and 100 yr with Type 2 Water ($CaCO_3$ Saturated) with Initial Solute Concentration of 8.52 meq/L and Leaching Fraction of 0.4

unsaturated zone equals the rate at which water is pumped out of the saturated zone: 0.667 m/yr for 0.40 leaching, and one-sixth of this amount or 0.111 m/yr for 0.10 leaching. As shown in Fig. 3, soil-water content in the unsaturated zone is 0.238 for 0.40 leaching and 0.210 for 0.10 leaching for the given fluxes. The volumetric flux is constant in the unsaturated zone and decreases linearly from the water table to the bottom of the aquifer where it equals zero; this results from no water being pumped from the unsaturated zone and from uniform pumping of the saturated zone.

The mean residence (or travel) time of the salt in the unsaturated zone, τ, is given by the relationship

$$\tau = \frac{\theta X_u}{q} \quad (18)$$

in which X_u (= 20 m) = the thickness of the unsaturated zone. From Eq. 18 it follows that the mean residence time in the unsaturated zone is about 7 yr for 0.40 leaching, and 38 yr for 0.10 leaching. Thus, it will take more than five times longer for the salt to travel from the rootzone (assumed to

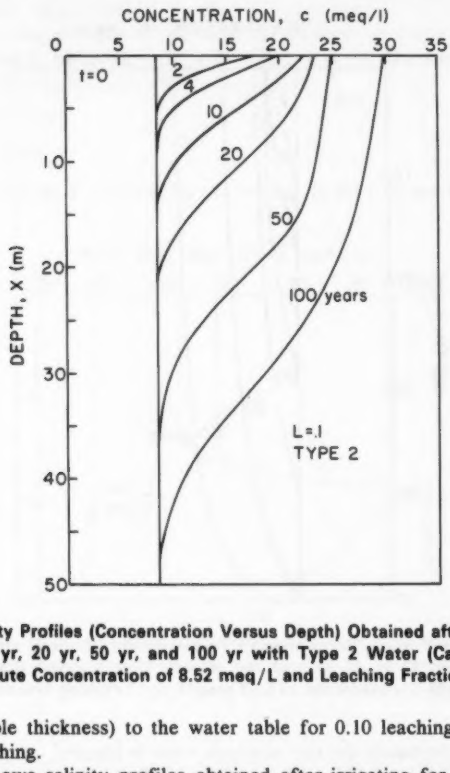

FIG. 5.—Salinity Profiles (Concentration Versus Depth) Obtained after Irrigating for 2 yr, 4 yr, 10 yr, 20 yr, 50 yr, and 100 yr with Type 2 Water ($CaCO_3$ Saturated) with Initial Solute Concentration of 8.52 meq/L and Leaching Fraction of 0.1

be of negligible thickness) to the water table for 0.10 leaching, as compared with 0.40 leaching.

Figure 4 shows salinity profiles obtained after irrigating for 2 yr, 4 yr, 10 yr, 20 yr, 50 yr, and 100 yr with Type-2 (Colorado River) water and 0.40 leaching. The concentration distributions are quite diffuse at all times, partly because of the relatively high value of the dispersivity used in the calculations, and partly because of the initially small concentration difference between groundwater and drainage water. This concentration difference will increase slowly after about 5 yr, when the concentration front reaches the water table. This occurs

a few years earlier than the mean residence time (7 yr) because of the effects of dispersion on the concentration front. At that time the average concentrations in the ground water (C_Q) begin to increase, leading to an equivalent increase in the concentration of the irrigation and drainage water (Eq. 13 and Eq. 12, respectively). The concentration distributions, however, remain quite uniform versus depth, especially in the unsaturated zone (Fig. 4). Note that the concentration front reaches the bottom of the aquifer after about 50 yr.

Similar distributions for 0.10 leaching are shown in Fig. 5. While the concentration in the unsaturated zone now increases much faster than for 0.40 leaching, the concentration front itself moves much slower towards the water table. The leading edge of the front reaches the ground-water table after about 20 yr, roughly 17 yr earlier than predicted with Eq. 18 if no dispersion were present. The most striking differences between Fig. 4 and Fig. 5 are the steepness and

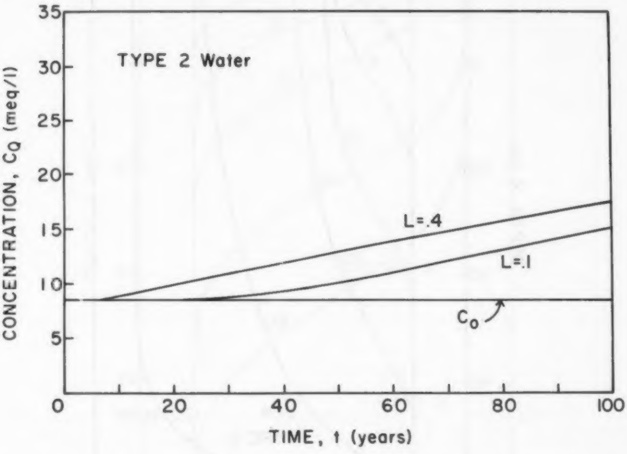

FIG. 6.—Average Ground-Water Concentration, C_Q with Time for Type 2 Water for 0.4 and 0.1 Leaching: Initial Ground-Water Concentration, C_o is 8.52 meq/L

locations of the solute fronts. Low leaching causes much more salt to be stored in the upper parts of the soil profile, leading to a slower salination of the underlying ground-water system. Especially the lower part of the saturated zone remains relatively free of salt for a much longer period of time.

Since the amount of imported water is just equal to the net evapotranspiration rate in both cases, and since this water is saturated with $CaCO_3$, the total amounts of salt precipitated in the rootzone must be the same for both leaching fractions. This can be seen by comparing Eq. 12 and Eq. 13. Precipitation accounts for a loss of 61.8 meq/L for 0.10 leaching and 10.3 meq/L for 0.40 leaching. After correcting for differences in drainage volumes (six times higher for 0.40 leaching), we obtained the same mass of salt precipitation in each case. Therefore, the total amounts of salt stored in the soil profile, including

both unsaturated and saturated zones, must also be the same. This will essentially also be true for the average concentration in the soil profile, with small differences caused only by the different soil-water contents in the unsaturated zone and thus slightly different total volumes of water for the two leaching situations. The most important difference between high and low leaching is a more uneven distribution of salt for low leaching. Because less salt is stored in the unsaturated zone, the average ground-water salinity, C_Q, should be higher for 0.40 leaching than for 0.10 leaching. Figure 6 shows that this is indeed the case. The difference in average ground-water concentration for the $CaCO_3$ saturated (Type 2) water

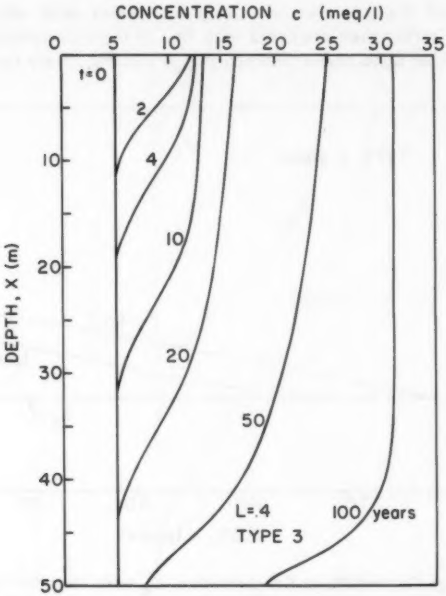

FIG. 7.—Salinity Profiles (Concentration Versus Depth) Obtained after Irrigating for 2 yr, 4 yr, 10 yr, 20 yr, 50 yr, and 100 yr with Type 3 Water ($CaSO_4$ Water) with Initial Concentration of 5.0 meq/L and Leaching Fraction of 0.4

is only about 2.5 meq/L, and remains fairly constant in time. This concentration difference, however, is expected to increase as depth to the water table increases because the mean residence time of the salt in the unsaturated zone increases (see Eq. 18).

Calculated salt distributions for Type 3 waters (those capable of precipitating gypsum) are shown in Fig. 7 and Fig. 8 for 0.40 and 0.10 leaching, respectively. The curves for 0.40 leaching (Fig. 7) are shaped similar to those for 0.40 leaching with $CaCO_3$ saturated water (Fig. 4). This was expected because the travel times in the unsaturated zone are exactly the same for both water types. The

most important difference between Fig. 4 and Fig. 7 is the larger concentration gradient for most time intervals in Fig. 7. This is due to the greater amount of precipitation for the gypsum precipitating water (Fig. 7) than for the $CaCO_3$ precipitating water (Fig. 4). The concentration of a pure gypsum water, furthermore, cannot exceed the concentration of a saturated pure gypsum solution (31.15 meq/L). This upper limit on the salt concentration in the profile leads to a constant concentration between the 0 m–37 m depth after 100 yr (Fig. 7). Gypsum saturation of the drainage water was reached after 75 yr of irrigation for 0.40 leaching. This point was reached immediately for 0.10 leaching, leading

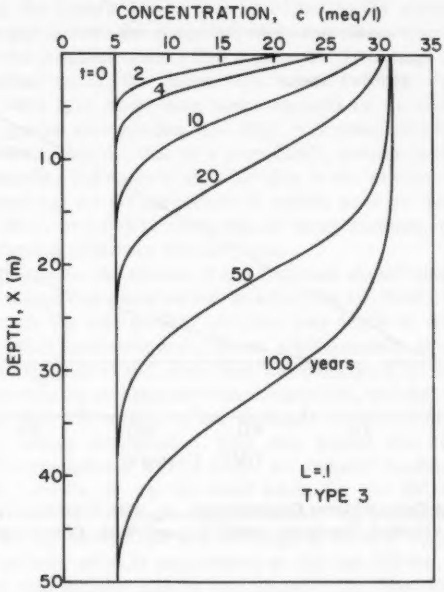

FIG. 8.—Salinity Profiles (Concentration Versus Depth) Obtained after Irrigating for 2 yr, 4 yr, 10 yr, 20 yr, 50 yr, and 100 yr with Type 3 Water ($CaSO_4$ Water) with Initial Solute Concentration of 5.0 meq/L and Leaching Fraction of 0.1

to considerably more gypsum precipitation in the rootzone. The concentration in the upper parts of the unsaturated zone does not reach saturation immediately because of the diffusion-dispersion effects on the salt distribution (Fig. 8). Increased precipitation from high to low leaching causes the differences in salinity distributions between the two leaching fractions to become more pronounced for Type 3 (gypsum precipitating) water. This is more clearly shown in Fig. 9, where the average ground-water salt concentrations are plotted versus time. The average ground-water salt concentration for 0.40 leaching increases nearly linearly from 5 meq/L (the initial concentration) after about 6 yr, to nearly

27 meq/L after 80 yr. The increase in concentration slows down after 75 yr, since it can never exceed the gypsum saturation value of 31.15 meq/L. In contrast, the average ground-water concentration for 0.10 leaching does not appreciably increase during the first 30 yr of irrigation. After 30 yr, the rate of increase in ground-water salinity is also much slower than that for 0.40 leaching. The average concentration reached 25 meq/L after 75 yr for 0.40 leaching (Fig. 9), whereas this point was reached only after 200 yr for 0.10 leaching (not shown in figure). The maximum difference in ground-water salinity between high and low leaching was reached after 90 yr (28 meq/L versus 14 meq/L). Eventually, both cases will result in gypsum-saturated ground water;

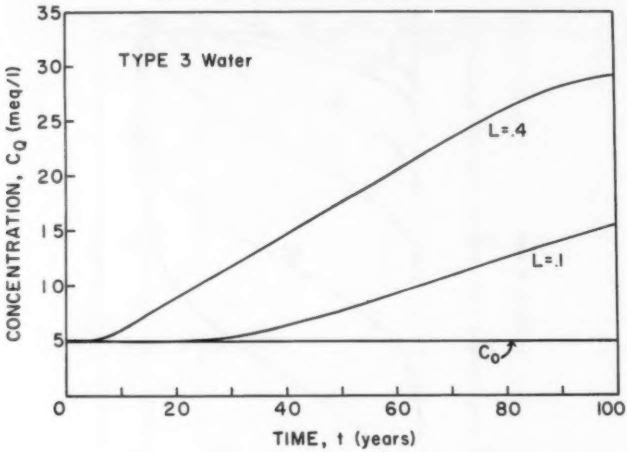

FIG. 9.—Average Ground-Water Concentration, C_Q with Time for Type 3 Water, and for 0.4 and 0.1 Leaching Fractions: Initial Ground-Water Concentration, C_o, is 5.0 meq/L

the steady-state value obviously will be reached much later for the lower leaching fractions.

Analysis

Any analysis of the type given in this paper is highly site specific and depends upon the unique conditions prevalent in each ground-water basin considered. For the closed, shallow ground-water system considered here, it is apparent that the benefit of low versus high leaching depends very much upon the type of water used for irrigation. Reduced leaching with Type 2 ($CaCO_3$ saturated) water has only a small effect on the calculated average ground-water salinity. The effect of low leaching would have been more pronounced if the depth to the ground-water table were greater than the 20 m assumed in the present calculations. The degradation of the ground water would be delayed in time

and, additionally, a larger quantity of dissolved salts would then be stored in the unsaturated, rather than the saturated, zone. The main effect of increased irrigation efficiency in the case of Type 2 water is the increased travel time in the unsaturated zone. This can be of considerable benefit whenever the depth to water table is large or if the irrigation water salinity is greater than the ground-water salinity. The considerably slower travel times for low leaching means that the saline drainage front takes much longer to mix with and degrade the higher quality ground water.

From Figs. 7, 8, and 9 it is evident that low leaching can be of considerable benefit in reducing salinity when Type 3 waters are used for irrigation. The degree to which the benefit occurs is proportional to the amount of gypsum precipitated in and below the rootzone, and, therefore, depends upon the composition of the irrigation water. The greater the percentage of precipitable salts in the applied water, the greater this benefit will be. For example, a predominantly NaCl type water with lesser amounts of Ca and SO_4 will not result in much gypsum precipitation, and, thus, not reduce salinity to any great extent. The present example, that of a pure $CaSO_4$ system, represents a case of maximum benefit. The main reason for this is the increased precipitation with reduced leaching. As the proportion of soluble salts (or imbalance in Ca, HCO_3, or Ca, SO_4, or both) in the irrigation water increase, the benefits of an improved irrigation efficiency will decrease.

In any actual analysis, the effects of ion exchange should also be taken into account. Ion exchange decreases the rate at which the salt front of the adsorbing ion moves through the soil profile, and also may result in the precipitation of additional calcium carbonate and gypsum. Unfortunately, the effects of ion exchange cannot be generalized, since they depend greatly on the exact water composition, the existing exchangeable-ion composition, and the cation exchange capacity of the soil. For example, the exchange of Na or Mg for Ca does not necessarily induce precipitation. One may expect that the quantity of exchangeable Ca precipitated will be larger for reduced leaching when $HCO_3 >> Ca$ or $SO_4 >> Ca$. If, on the other hand, $Ca >> HCO_3$ and $Ca >> SO_4$, then relatively less of the exchanged calcium will precipitate. In a recent study, Jury et al. (2) showed that the exchange of Na and Mg for Ca doubled the predicted quantity of salts precipitated in the top 150 cm of a particular soil profile that was initially high in exchangeable Ca. They also showed the importance of the water-uptake distribution in the rootzone on the time necessary to achieve steady-state salt flow in the soil rootzone. These latter effects are probably less important for the type of analysis given in this paper, since the rootzone generally comprises only a small portion of the unsaturated zone. In fact, in the present analysis, the spatial effect of the rootzone was omitted altogether. If the rootzone were included in the simulation model, it would serve only to increase the travel time in the unsaturated zone and would not significantly affect the calculated salinity of the ground water.

This paper considers a ground-water basin which is a closed hydrological unit, and in which the ground-water table remained at its initial position. If the hydrological system were to be altered by not introducing water, or by significantly reducing the amount of imported water from outside the basin, then overdrafting would be simulated, provided of course that the entire basin is irrigated with the same amount of water. Then the salinity front would never

reach the ground-water table, since the decline of the water table would exceed the rate of propagation of the solute front through the unsaturated zone. In this instance, salinity buildup in the ground water is not a factor. Maximum utilization of the available groundwater, however, would still require that high efficiency irrigation practices be applied.

In many cases, the ground-water basin will not be hydrologically isolated, but rather be connected hydrologically with another basin, a river, or other surface or subsurface flow system. The analysis will then become much more complex and probably not lend itself to a one-dimensional analysis of the type given in this paper. Nevertheless, we can still make some qualitative remarks, partly based upon the foregoing analysis. For example, if the applied irrigation water is imported *surface* water, then high leaching will probably result in a lower ground-water salinity because a greater volume of water and, thus, salts are being discharged from the basin.

Many basins are underlain by saline ground waters, with better quality waters being located at much greater depths. The objective in this case would be to cause as little displacement of the saline water as possible. Mixing of the saline ground water with the better quality ground water could result in a rapid degradation of a valuable water resource. The important variable now is not the drainage water composition but rather its volume. Low leaching here would be of considerable benefit.

An optimal irrigation management strategy also requires judgment as to which water resource is the most valuable. For example, in regions with inadequate surface water storage, but with a potential for good quality ground water, priority should be given to maintaining or improving the ground-water resources. If, however, the ground water is unsuitable or only marginally suitable for use, then the downstream river salinity would probably by the most important consideration in deciding which irrigation practice to adopt.

Conclusions

A one-dimensional numerical analysis of water and salt movement in a 50 m deep unsaturated-saturated soil profile showed the importance of leaching fraction and water type on ground-water salinity. For $CaCO_3$ saturated water, the effects of reduced leaching are relatively minor, especially if the depth to the water table is small. With increasing thickness of the unsaturated zone, the mean residence time of the salt in the unsaturated zone increases, leading to more salt storage in the upper part of the soil profile and less in the ground water. The average ground-water concentration in that case will be smaller with reduced leaching.

For waters approaching gypsum saturation, improved leaching efficiency will significantly improve ground-water salinity, even in shallow aquifer systems. For the case examined herein, salinity levels were up to 14 meq/L lower for 0.10 leaching as compared with those for 0.40 leaching. The long-term benefits of reduced leaching are the increased storage of precipitated gypsum and soluble salts in the unsaturated zone, and a lower salinity of the underlying groundwater system.

Appendix I.—References

1. Duguid, J. O., and Reeves, M., "A Comparison of Mass Transport Using Average

and Transient Rainfall Boundary Conditions," *Finite Elements in Water Resources,* W. G. Gray, G. F. Pinder, and C. A. Brebbia, eds., Pentech Press, London, England, 1977, pp. 2.25–2.35.
2. Jury, W. A., Frenkel, H., and Stolzy, L. H., "Transient Changes in the Soil-Water System from Irrigation with Saline Water: I. Theory," *Soil Science Society of America Journal,* Vol. 42, 1978, pp. 579–584.
3. Oster, J. D., and Rhoades, J. D., "Calculated Drainage Water Compositions and Salt Burdens Resulting from Irrigation with River Waters in the Western United States," *Journal of Environmental Quality,* Vol. 4, 1975, pp. 73–79.
4. Raats, P. A. C., "Convective Transport of Solutes In and Below the Rootzone, Managing Saline Water for Irrigation," *Proceedings of the International Salinity Conference,* 1976, pp. 290–298.
5. Rhoades, J. D., Oster, J. D., Ingvalson, R. D., Tucker, J. M., and Clark, M., "Minimizing the Salt Burdens Resulting from Irrigation with River Waters in the Western United States," *Journal of Environmental Quality,* Vol. 4, 1974, pp. 311–316.
6. Rhoades, J. D., and Suarez, D. L., "Reducing Water Quality Degradation Through Minimized Leaching Management," *Agriculture Water Management,* Vol. 1, 1977, pp. 127–142.
7. Suarez, D. L., and Rhoades, J. D., "Effect of Leaching Fraction on River Salinity," *Journal of the Irrigation and Drainage Division,* ASCE, Vol. 103, No. IR2, Proc. Paper 13017, June, 1977, pp. 245–257.
8. van Genuchten, M. Th., "Mass Transport in Saturated-Unsaturated Media, I. One-Dimensional Solutions," *Research Report 78-WR-11,* Water Resources Program, Princeton University, Princeton, N.J., 1978.
9. van Genuchten, Rien, "Calculating the Unsaturated Hydraulic Conductivity with a New, Closed-Form Analytical Model," *Research Report 78-WR-09,* Water Resources Program, Princeton University, Princeton, N.J., 1978.
10. van Schilfgaarde, J., Bernstein, L., Rhoades, J. D., and Rawlins, S. L., "Irrigation Management for Salt Control," *Journal of the Irrigation and Drainage Division,* ASCE, Vol. 100, No. IR3, Proc. Paper 10822, 1974, pp. 321–338.
11. Wierenga, P. J., "Solute Distribution Profiles Computed with Steady-State and Transient Water Movement Models," *Soil Science Society of America Journal,* Vol. 41, 1977, pp. 1050–1055.
12. Wigley, T. M. L., and Plumer, L. N., "Mixing of Carbonate Waters," *Geochimica et Cosmochimica Acta,* Vol. 40, 1976, pp. 989–995.

Appendix II.—Notation

The following symbols are used in this paper:

a = soil characteristic parameter used in Eq. 10, in square millimeters per second;
c = total salt concentration;
C_d = concentration of drainage water leaching rootzone, in milliequivalents per liter;
C_o = initial groundwater concentration, in milliequivalents per liter;
C_Q = average concentration of pumped groundwater, in milliequivalents per liter;
$\mathscr{D}$ = dispersion coefficient, in square millimeters per second;
D = drainage;
E = evaporation per unit surface area, in cubic meters per square meter year;
h = pressure head;
K = hydraulic conductivity, in millimeters per second;
K_s = saturated hydraulic conductivity, in millimeters per second;

L = fraction of applied irrigation water that leaches out of rootzone;
m = soil characteristics parameter used in Eq. 4;
n = soil characteristics parameter used in Eq. 4;
q = volumetric flux, in millimeters per second;
Q = rate of pumping per unit surface area, in cubic meters per square meter year;
S = rate at which water is imported into basin per unit surface area, in cubic meters per square meter year;
t = time;
x = depth below rootzone;
X = depth of impermeable layer;
X_s = thickness of saturated zone;
X_u = thickness of unsaturated zone;
α = soil characteristic parameter used in Eq. 4;
θ = volumetric moisture content;
θ_r = residual moisture content;
θ_s = saturated moisture content;
Θ = dimensionless moisture content;
λ = dispersivity, in millimeters; and
τ = mean residence or travel time.

JOURNAL OF
THE IRRIGATION
AND DRAINAGE DIVISION

River Basin Hydro-Salinity-Economic Modeling

By Henry O. Fapohunda[1] and Robert W. Hill,[2] A. M. ASCE

Introduction

The increasing use of water for irrigation, industry, and municipal water supplies has led to an increasing need for careful planning for the usable water resources. Efficiency in water use requires skilled planning and careful management of water. Efficient use considerations in a dynamic system such as a river basin implies that the physical and economic systems be described with sufficient accuracy to quantitatively and qualitatively predict the system-wide effects of depletions resulting from water use anywhere in the system. Unfortunately, such depletions for irrigation and industry concentrates and adds nondegradable substances that produce a decrease of water quality. Thus, in every hydrologic system, each upstream use has some effects on the quantity, quality, and timing of flow occurring at downstream points. An accurate assessment of the net benefits of various upstream changes or management alternatives can lead to increased use and better efficiency of available water resources within the basin. An appropriate description of a water resource system, therefore, includes the hydrologic system, the salinity flow system, the economic system, and those functions which relate them.

This paper presents a method by which an economic simulation model can be combined with an existing hydrologic salinity model in order to predict management effects of sequential water use in a river basin. The hydrologic, salinity, and economic systems are closely interrelated in any water resource project. Comprehensive planning is difficult if the three systems are analyzed independently; thus, it is advantageous to incorporate all three systems into a working model. The combined model can then be applied to river system

[1]Lect., Dept. of Agricultural Engrg., Univ. of Ife, Ife, Nigeria.

[2]Assoc. Prof., Dept. of Agricultural and Irrigation Engrg., Utah State Univ., Logan, Utah 84322.

Note.—Discussion open until August 1, 1981. To extend the closing date one month, a written request must be filed with the Manager of Technical and Professional Publications, ASCE. Manuscript was submitted for review for possible publication on June 3, 1980. This paper is part of the Journal of the Irrigation and Drainage Division, Proceedings of the American Society of Civil Engineers, ©ASCE, Vol. 107, No. IR1, March, 1981. ISSN 0044-7978/81/0001-0053/$01.00.

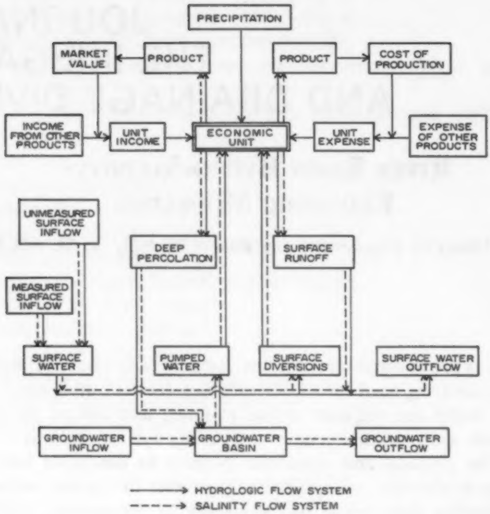

FIG. 1.—General Flowchart of Typical Hydro-Salinity Economic System (9)

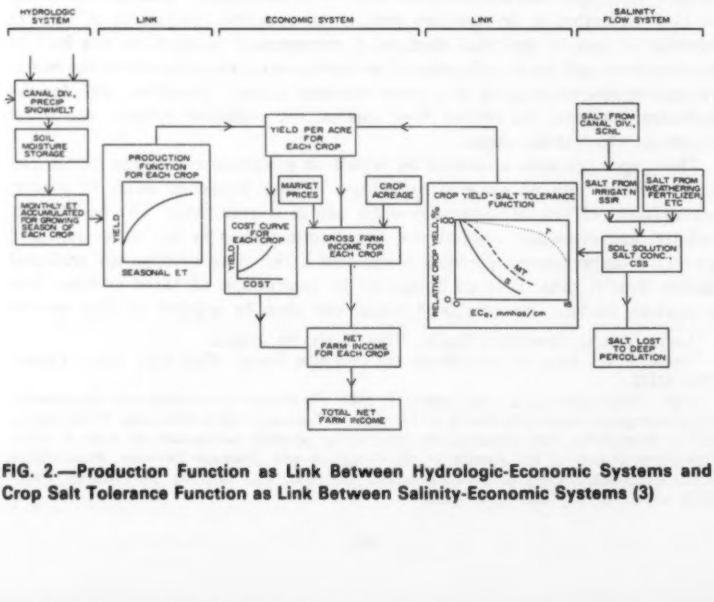

FIG. 2.—Production Function as Link Between Hydrologic-Economic Systems and Crop Salt Tolerance Function as Link Between Salinity-Economic Systems (3)

subbasins in a sequential manner moving downstream. The model provides a means of determining the relative efficiency of water with respect to production or net returns for several management alternatives.

The hydrologic, salinity, and economic flow systems are dynamic in nature and can be related through the concepts of continuity of mass and momentum. Continuity of momentum may be considered negligible in this case since velocities are low. A proper accounting of the physical hydrologic quantities is obtained

TABLE 1.—Salt Tolerance of Agricultural Crops (7)

Crop (1)	Salinity at initial yield decline (threshold) A, in millimhos per centimeter (decisiemens per meter) (2)	Yield decrease per unit increase in salinity beyond threshold B, as a percentage (3)	Salt tolerance rating (4)
Bean	1.0	19	S
Corn (grain)	1.7	12	MS
Cotton	7.7	5.2	T
Cowpea	1.3	14	MS
Millet			MS
Onion	1.2	16	S
Peanut	3.2	29	MS
Pepper	1.5	14	MS
Rice	3.0	12	MS
Safflower			MT
Sorghum			MT
Soybean	5.0	20	MT
Sugar cane	1.7	5.9	MS
Tomato	2.5	9.9	MS
Wheat	6.0	7.1	MT

as water is translated or routed through the system with respect to both space and time, as described by the following expression (adapted from Ref. 5):

$$(P_r + Q_{is} + Q_{ig}) - (\mathrm{ET} + Q_{so} + Q_{go}) = \Delta S \quad \ldots \ldots \ldots \quad (1)$$

in which P_r = the precipitation on the area; Q_{is} = the total surface inflow; Q_{ig} = the subsurface inflow; ET = the evapotranspiration from the area; Q_{so} = the total surface outflow; Q_{go} = the subsurface outflow; and ΔS = the change in water storage including snow, soil moisture, surface reservoirs, and ground water. With the exceptions of precipitation, snowmelt, and evapotranspiration, all of the water quantities described as the hydrologic model in Eq. 2 have quality parameters associated with them. If all these quantity and quality components making up Eq. 2 can be identified, then the general salt simulation model can be expressed in equation form as:

$$Q_{so} C_{so} = \sum_{j=1}^{n} Q_{isj} C_{isj} + \sum_{k=1}^{t} Q_{igk} C_{igk} \pm \sum_{p=1}^{m} \Delta S_p C_{scp} \quad \ldots \ldots \ldots \ldots \quad (2)$$

in which C_{so} = the salt concentration of outflow water; C_{isj} = the salt concentration of surface source, j; C_{igk} = the salt concentration of ground-water source, k, in outflow; and C_{scp} = the salt concentration associated with storage element, p.

Combining Hydrologic, Salinity and Economic Systems

Careful consideration should be given to the nature of the relationships existing among the hydrologic, salinity, and economic systems within a river basin. The hydrologic and salinity flow systems are physical and quantitative processes,

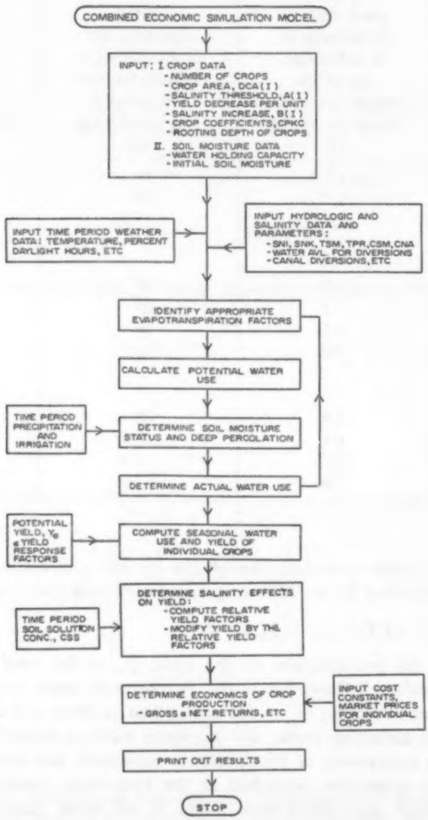

FIG. 3.—Flow Diagram of Combined Economic Simulation Model (3)

while the economic model is simply a quantitiative phenomenon. When combined, these three systems form an integrated unit since there exists a strong interrelationship between the physical and economic systems. Fig. 1 presents the basic components of the hydrologic, salinity, and economic systems and the relationships existing among them. The economic system includes the crops produced on irrigated farm land and their relationship to the hydrosalinity system, but does not directly consider livestock or municipal uses. The basic economic unit of the study is a river subbasin.

The connecting links between the hydrologic, salinity, and economic flow systems of an agricultural enterprise are dependent upon such factors as water availability (supply), water requirements (demand), salinity levels of irrigation

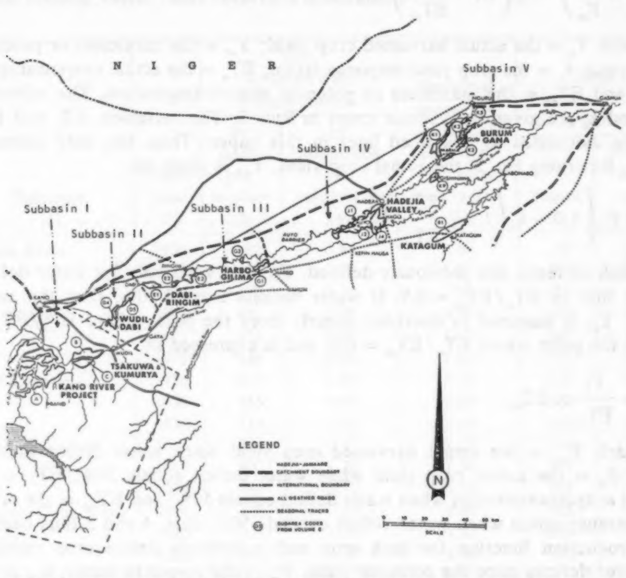

FIG. 4.—Map of Hadejia River Basin Showing Subbasins Used in Study

water and soil solution, crop salt tolerance level, and production per unit of water consumed. However, water and salinity levels are not the only factors that influence production in agriculture. Production is also a function of management, capital, labor, crop variety, weather, and soil type and fertility. By maintaining these other factors at relatively constant levels, production (yield) can be estimated at known water and salinity levels. The link between the hydrologic and the economic systems is the production function for each crop (8). A production function determines the relationship between the variation in yields of several crops resulting from a variable input of water as influenced by salinity levels of the soil, while all other factors are assumed held constant. The link between the salinity and economic systems is the crop salt tolerance function described later in this paper. Fig. 2 presents a schematic diagram of

how the hydrologic, salinity, and economic systems are linked together by their respective functions.

Production Function.—An estimate of the production function is the relationship between the crop yield and the seasonal evapotranspiration of the crop, for the assumed constant or near constant levels of fertility, management, and other conditions. The concept, as used by Doorenbos et al. (2), that relative yield decrease is a function of relative evapotranspiration deficit through an empirical yield response factor, was adopted for this study. Their approach, a simple linear model, is described by Eq. 3 as follows:

$$\left(1.0 - \frac{Y_a}{Y_m}\right) = k_y\left(1.0 - \frac{\mathrm{ET}_a}{\mathrm{ET}_m}\right) \quad (3)$$

in which Y_a = the actual harvested crop yield; Y_m = the maximum or potential crop yield; k_y = the crop yield response factor; ET_a = the actual evapotranspiration; and ET_m = the maximum or potential evapotranspiration. The values of Y_m and k_y are given for various crops in Ref. 2. The variables, ET_a and ET_m can be calculated as described later in this paper. Thus, the only unknown is Y_a. Rewriting Eq. 3, the actual crop yield, Y_a, is given as:

$$Y_a = Y_m\left[1.0 - k_y\left(1.0 - \frac{\mathrm{ET}_a}{\mathrm{ET}_m}\right)\right] \quad (4)$$

in which all terms are previously defined. Eq. 4 is valid only for water deficits up to 50% or $\mathrm{ET}_a/\mathrm{ET}_m = 0.5$. If water deficits exceed 50%, then the actual yield, Y_a, is assumed to decrease linearly from the point where $\mathrm{ET}_a/\mathrm{ET}_m$ = 0.5 to the point where $\mathrm{ET}_a/\mathrm{ET}_m = 0.0$, and is expressed as:

$$Y_{aL} = \frac{Y_b}{\mathrm{ET}_b} \times \mathrm{ET}_{aL} \quad (5)$$

in which Y_{aL} = the actual harvested crop yield when water deficit exceeds 50%; Y_b = the actual crop yield when water deficit equals 50%; ET_b = the actual evapotranspiration when water deficit equals 50%; and ET_{aL} = the actual evapotranspiration when water deficit exceeds 50%. Eqs. 4 and 5 thus become the production function for each crop and completely define crop yields at all water deficits once the potential yield, Y_m, yield response factor, k_y, actual and potential evapotranspiration, ET_a and ET_m, respectively, are known for each crop.

This approach is good as initial input into the model and is especially helpful in countries where data on crop water use and yield relationships are usually sparse. Where complete and accurate data are available on crop water use, such data should be used.

Because of its simplicity, low data requirements (only surface air temperature is needed), and applicability to most of the irrigated arid regions of the world, the modified Blaney-Criddle equation (9) has been adopted for the calculation of actual and potential evapotranspiration in this model. The equation is expressed as:

$$\mathrm{PET} = \frac{k_c k_t \mathrm{TP}}{100} \quad (6)$$

in which PET = the potential evapotranspiration; k_c = the monthly crop growth coefficient; and k_t = the monthly temperature coefficient determined from the following equation:

$$k_t = (0.0173\,T - 0.314) \quad (7)$$

$$\text{subject to} \quad k_t \geq 0.3 \quad (8)$$

in which T = the mean monthly temperature, in degrees Fahrenheit; and P = the monthly daylight hours of the year, as a percentage.

TABLE 2.—Summary of Subbasins Seasonal Water Diverted and Salinity Effects on Net Returns, Water Years 1976–1978 (calibration)

Subbasin (1)	Water year (2)	Soil Solution Salt Concentration: In parts per million (3)	Soil Solution Salt Concentration: In millimhos per centimeter (4)	Seasonal water diverted, in acre-feet per acre of land (5)	Total Net Returns, in Naira per acre[a]: Water (6)	Total Net Returns, in Naira per acre[a]: Water and salt (7)
Kano River	1976	91	0.14	1.10	160	160
	1977	114	0.18	1.27	166	166
	1978	92	0.14	1.07	158	158
Wudil-Dabi	1976	481	0.75	0.96	149	149
	1977	676	1.06	1.02	144	144
	1978	446	0.70	1.03	147	147
Dabi-Marke	1976	629	0.98	1.15	126	126
	1977	955	1.49	1.37	120	120
	1978	714	1.12	1.33	118	118
Hadejia Valley	1976	396	0.62	1.12	196	196
	1977	807	1.26	1.38	207	207
	1978	461	0.72	1.18	182	182
Burum Gana River	1976	468	.73	1.08	102	102
	1977	1,074	1.68	1.23	103	102
	1978	815	1.27	1.12	92	92

[a] 1 Nigerian Naira = 1.77 United States dollars.
Note: 1 mmho/cm = 1 ds/m. Multiply acre-feet per acre by 304.8 to obtain millimeters.

Gardner and Ehlig (4), among others, have indicated that transpiration occurs at the full potential rate through approximately the first one-third of the available soil moisture range and that thereafter the actual evapotranspiration rate lags the potential rate. This phenomena is determined in the model by the following relationships:

$$\text{ET} = \text{PET}; \quad (\text{CSM} < \text{SM} \leq \text{SMC}) \quad (9)$$

$$\text{and} \quad \text{ET} = \text{PET}\,\frac{\text{SM}}{\text{CSM}}; \quad (0 \leq \text{SM} \leq \text{CSM}) \quad (10)$$

in which ET = the estimated actual evapotranspiration, in inches; CSM = the

TABLE 3.—Summary of Subbasins Seasonal Water Diverted and Salinity

Subbasin crop area (1)	Acres				Water Diverted, in acre-feet per acre of irrigated land		
	CALIB[a] (2)	MNG[b] (3)	Change, as a percentage (4)	Water year (5)	CALIB[a] (6)	MNG[b] (7)	Change, as a percentage (8)
Kano River	71,660	140,848	+97	1976	1.10	1.15	+5
				1977	1.27	1.28	+1
				1978	1.07	1.11	+4
Wudil-Dabi	41,724	66,298	+59	1976	0.96	0.79	−18
				1977	1.02	1.22	+20
				1978	1.03	0.97	−6
Dabi-Marke	26,640	52,612	+97	1976	1.15	0.62	−46
				1977	1.37	1.30	−5
				1978	1.33	0.85	−36
Hadejia Valley	53,150	87,000	+64	1976	1.12	0.59	−47
				1977	1.38	0.81	−41
				1978	1.18	0.86	−27
Burum Gana River	16,588	33,176	+100	1976	1.08	0.73	−32
				1977	1.23	0.82	−33
				1978	1.12	1.01	−10

[a]CALIB = Calibration run results.
[b]MNG = Results from increased crop areas.
[c]1 Nigerian Naira = 1.77 United States dollars.
Note: Divide acres by 2.47 to obtain hectares. Multiply acre-feet per acre by 304.8

critical soil moisture level below which ET is less than PET (in inches), determined during the calibration process of the model; SM = the soil moisture level, in inches; and SMC = the soil moisture capacity, in inches (root zone water storage available to the plant). The estimated actual evapotranspiration is then accumulated for the growing season and for each crop and is introduced as the basic input to the economic model from the hydrologic system.

Crop Salt Tolerance Function.—Crop salt tolerance has usually been expressed as the yield decrease expected for a given level of soluble salts in the root medium compared with yields under nonsaline conditions (1). The most common method of measuring salinity is to determine the electrical conductivity of saturation extract, EC_e, from the active root zone. The salt concentration of the soil solution was calculated through an accounting process at the end of each model time period. This process can be expressed by:

$$CSS = f(SSIR, SSWF, SSDP) \quad (11)$$

in which CSS = the soil solution concentration; SSIR = the salt applied from irrigation waters; SSWF = salt added from weathering or fertilizer application; and SSDP = salt lost by deep percolation. Weathering rate of mineral is considered significant only in the ground-water system in contact with the parent geologic strata (6).

Effects on Net Returns: Comparison of Calibration and Management (Option I)

NET RETURNS, in Naira per acre[c]					
Water			Water and Salt		
CALIB[a] (9)	MNG[b] (10)	Change, as a percentage (11)	CALIB[b] (12)	MNG[b] (13)	Change, as a percentage (14)
160	164	+3	160	164	+3
166	167	+1	166	167	+1
158	163	+3	158	163	+3
149	136	−9	149	136	−9
144	155	+8	144	155	+8
147	149	+2	147	149	+2
126	100	−20	126	100	−20
120	119	−1	120	119	−1
118	112	−5	118	112	−5
196	127	−35	196	127	−35
207	151	−27	207	148	−29
182	137	−25	182	136	−25
102	85	−17	102	85	−17
103	87	−15	102	84	−18
92	84	−9	92	74	−20

to obtain millimeters.

Maas and Hoffman (7) compiled and normalized all available salt tolerance data from an extensive review of literature. Their findings were adapted into linear equations which relate the relative yield to soil saturation extract, EC_e, as:

$$Y = 100.0 - B(EC_e - A); \quad EC_e > A \qquad (12)$$

$$\text{and} \quad Y = 100; \quad EC_e \leq A \qquad (13)$$

in which Y = the relative yield for any given soil salinity exceeding the threshold, as a percentage; A = the salinity threshold, in millimhos per centimeter (in decisiemens per meter); B = yield decrease per unit salinity increase, as a percentage; and EC_e = the soil saturation extract, in millimhos per centimeter (in decisiemens per meter). The values of A and B were provided in the Maas and Hoffman report for several crops; some of their data relevant to this study were extracted and are presented as Table 1.

Eqs. 12 and 13, subsequently referred to as the crop salt tolerance function, can be used in conjunction with the values of A and B from Table 1 to determine the relative yield when the soil solution concentration is known. Thus, when the yield of each crop is determined by the seasonal evapotranspiration, further modification (reduction) of yield is done by the relative yield factor, only if the maximum threshold salinity is exceeded.

TABLE 4.—Summary of Subbasin Seasonal Water Diverted and Salinity Effects on

Subbasin (1)	Phreatophyte Area, in acres MNG I[a] (2)	MNG II[b] (3)	Change, as a percentage (4)	Water year (5)	Water Diverted, in acre-feet per acre of irrigated land MNG I[a] (6)	MNG II[b] (7)	Change, as a percentage (8)
Kano River	7,551	3,775	−50	1976	1.15	1.18	+3
				1977	1.28	1.28	0
				1978	1.11	1.13	+2
Wudil-Dabi	8,940	4,470	−50	1976	0.79	0.84	+6
				1977	1.22	1.17	−4
				1978	0.97	1.03	+7
Dabi-Marke	4,541	2,270	−50	1976	0.62	0.84	+36
				1977	1.30	1.38	+6
				1978	0.85	1.07	+25
Hadejia Valley	12,233	6,116	−50	1976	0.59	0.68	+15
				1977	0.81	1.15	+42
				1978	0.86	0.87	+1
Burum Gana River	7,640	3,820	−50	1976	0.73	0.84	+14
				1977	0.82	1.02	+24
				1978	1.01	1.29	+28

[a]MNG I = Results from increased crop areas.
[b]MNG II = Results from increased crop areas plus reduced phreatophyte areas.
[c]1 Nigerian Naira = 1.77 United States dollars.
Note: Divide acres by 2.47 to obtain hectares. Multiply acre-feet per acre by 304.8

Computer Programming: Combined Economic Simulation Model.—The hydrologic and salinity systems have been programmed on the computer in Fortran IV language by Hill et al. (5), and further modifications on these have been done by Huber et al. (6). The combined economic simulation model is presented as a conceptual mathematical model in Fig. 3 in which data on crops—costs and returns (economics), water supply (hydrology), and water quality (salinity) are combined into a single working model.

The model, hereafter referred to as the Sequential Water Use Model (SWUM), has as its main objective the evaluation of the marginal primary benefits of water by computing the incremental changes in net returns to the farm unit as a result of changes in the water supply. It also answers questions concerning the effects of upstream depletions on water quantity and quality to the downstream users.

The model requires crop, soil, temperature, daylight percent, hydrologic and salinity data, and calibration parameters as input (see Fig. 3). The model output includes monthly and seasonal values of: potential and actual evapotranspiration, irrigation water diverted and applied to each crop, and soil and streamflow salt levels. It also computes the total irrigation water diverted and applied during the growing season, the total water shortages and reservoir storage capacity required to meet such shortages. Finally, the model calculates yields and estimated net return per unit area for each crop and for the entire subbasin.

Net Returns: Comparison of Management Option I with Management Option II

NET RETURNS, in Naira per acre[c]					
Water			Water and Salt		
MNG I[a] (9)	MNG II[b] (10)	Change, as a percentage (11)	MNG I[a] (12)	MNG II[b] (13)	Change, as a percentage (14)
164	166	+1	164	166	+1
167	167	0	167	167	0
163	165	+1	163	165	+1
136	138	+1	136	138	+1
155	155	0	155	155	0
149	151	+1	149	151	+1
100	113	+13	100	113	+13
119	122	+3	119	120	+1
112	117	+5	112	116	+4
127	137	+8	127	137	+8
151	173	+14	148	173	+17
137	148	+8	136	148	+9
85	90	+5	85	87	+2
87	96	+10	84	90	+8
84	94	+12	74	93	+26

to obtain millimeters.

Application to Hadejia River Basin, Nigeria

The relationships proposed in the preceding sections of this paper were applied to the Hadejia River Basin, located in Northern Nigeria. To account for spatial differences in climate and basin characteristics, the drainage area was divided into five subbasins, as shown in Fig. 4. Data on streamflow, water quality, meteorology, crops, and economics were taken or estimated from published sources. Water and salt outflows from the upstream subbasin became the inflow for the next one downstream in a sequential manner.

The parameter set of the hydrologic and salinity processes must first be determined by calibration before the sequential use model can be used. Then the calibration parameters become inputs into the sequential use model. A mathematical programming approach used to determine the parameter vector which satisfactorily describes the model involves selecting an objective function of the form:

$$\mathrm{OBJ} = \Sigma\,(\mathrm{DIFF})^2 \qquad (14)$$

in which DIFF = the numerical difference between computed value and measured value of a given hydrologic (streamflow) or salinity (e.g., tons of salt) data.

Thus, the object of the calibration process is to adjust the various parameters in such a manner as to cause DIFF to approach zero. When this is achieved,

TABLE 5.—Summary of Subbasin Seasonal Water Diverted and Salinity Effects on 1976-1978

Subbasins (1)	Crop area, in acres (2)	Water year (3)	Change in soil solution salt concentration as a percentage (4)	Water Diverted, in acre-feet per acre of irrigated land		
				CALIB[a] (5)	MNG III[b] (6)	Change, as a percentage (7)
Kano River	71,660	1976	+198	1.10	0.92	−16
		1977	+701	1.27	0.92	−28
		1978	+1,323	1.07	0.85	−21
Wudil-Dabi	41,724	1976	+69	0.96	1.01	+5
		1977	+176	1.02	1.05	+3
		1978	+448	1.03	1.01	−2
Dabi-Marke	26,640	1976	+92	1.15	0.81	−30
		1977	+95	1.37	1.17	−15
		1978	+298	1.33	1.04	−22
Hadejia Valley	53,150	1976	+295	1.12	0.82	−27
		1977	+114	1.38	1.09	−21
		1978	+507	1.18	0.91	−23
Burum Gana River	16,588	1976	+83	1.08	0.89	−18
		1977	+49	1.23	0.83	−32
		1978	+197	1.12	1.15	+3

[a]CALIB = Results from calibration runs.
[b]MNG III = Results from drought simulation.
[c]1 Nigerian Naira = 1.77 United States dollars.
Note: Divide acres by 2.47 to obtain hectares. Multiply acre-feet per acre by 304.8

the model is said to be calibrated. The model can then be used with relative confidence in subsequent management studies of the basin.

The program's capability to model water quantity and quality effects from different management alternatives and subsequent predictions of net returns resulting from such changes in management is of tremendous importance to river basin planning and implementation. Some of the management options evaluated in this study are:

1. Increasing crop acreages to projected values.
2. Reducing phreatophyte acreages as a better management practice after the increase in crop acreages.
3. Simulated drought conditions. The main purpose of this trial was to observe the effect of low water supply and an induced highly saline soil condition on crop yield economics of the subbasins.

The results and analyses of calibration and management studies follow. A summary of all subbasins' seasonal irrigation water diversions and consumption, and the net returns of irrigated land, is presented in Table 2. There is no general trend in the amounts of water diverted and consumptively used per unit area from subbasin to subbasin; however the net returns per unit area show a decreasing trend in the downstream direction except in Hadejia Valley Subbasin. In general,

Net Returns: Comparison of Calibration with Drought Simulation, Water Years

NET RETURNS, in Naira per acre[c]					
Water			Water and Salt		
CALIB[a] (8)	MNG III[b] (9)	Change, as a percentage (10)	CALIB[a] (11)	MNG III[b] (12)	Change, as a percentage (13)
160	148	−8	160	148	−8
166	145	−13	166	145	−13
158	143	−9	158	143	−10
149	143	−4	149	143	−4
144	149	+3	144	147	+2
147	145	−1	147	134	−9
126	97	−23	126	97	−23
120	109	−9	120	106	−12
118	103	−12	118	91	−23
196	133	−32	196	131	−33
207	163	−21	207	160	−23
182	135	−26	182	103	−43
102	84	−18	102	84	−18
103	85	−17	102	81	−20
92	84	−8	92	75	−19

to obtain millimeters.

the season with the highest water diversions seems to have the highest corresponding net returns within each subbasin. The Hadejia Valley Subbasin with the highest diversions has the maximum net returns in all seasons. An examination of the salinity effects in Table 2 shows that within the same season (water year), the concentration tends to increase from subbasin to subbasin in the downstream direction except where tributaries with low salt concentration and high discharge volumes dilute the river inflows. However, the predicted soil solution concentrations produced no significant yield reductions and hardly any decline in net returns with the calibration runs.

Increasing Crop Areas.—With increases of some 59%–100% (see Table 3) in irrigated land areas of the subbasins, the amount of water diverted per unit area showed reductions from the calibration run except on the most upstream subbasin (Kano River). An evaluation of the net returns, with respect to water only, showed Kano River Subbasin with positive change (increases) in net return in all of the three growing seasons. Wudil-Dabi Subbasin had increases in net returns in two of the three growing seasons. The remaining subbasins had declines in net returns. This suggests that only the two most upstream subbasins could provide adequate water for such increases in crop areas under the present water supply situation.

Adding the effect of salinity imposes additional burdens on the water supply situation. A further look at Table 3 shows no effect of salinity on net returns

in the three upstream subbasins. However, from the second growing season on the Hadejia Valley and Burum Gana Subbasins, salinity buildup resulted in declines in net returns per unit area. The reductions in net return were slight in most cases; however it reached 11% on the Burum Gana Subbasin in the 1978 growing season.

Reducing Phreatophyte Areas.—The phreatophyte/open water areas were reduced by 50% in all the subbasins as an expected reasonable improved management practice after increasing the crop acreages to projected values. A summary of subbasin seasonal water supply and salinity effects on crop yields and net returns for water years 1976–1978 is presented in Table 4 for the management options indicated. With 50% reduction in phreatophyte areas, the model predicted up to a 42% increase in water diverted per acre in one of the subbasins; however some subbasins did not divert more water even with the increased water availability. The logical explanation for the lack of increased diversion might be water became available when not needed, i.e., more water availability when the soil moisture storage was already filled would only contribute to surface runoff and deep percolation losses. The downstream subbasins responded more favorably to water availability by diverting more water. In all subbasins, increases in water diverted per unit area resulted in from 0%–14% increases in net returns with the reduced phreatophyte areas (see Table 4). The increases in net returns are more noticeable in the downstream subbasins, slight or no increases at all are common in the upstream subbasins.

The additional effects of salinity were most noticeable in the downstream subbasin (Burum Gana River) where net returns were less for all growing seasons when salinity effects were imposed than with water alone. However, some increases in net returns were observed when the phreatophyte areas were reduced after first increasing the crop areas.

Simulated Drought.—With the exceptions of some growing seasons, the percent changes in water diverted going from calibration to the simulated drought condition are negative (see Table 5), which, as expected, indicates less water availability for crops when drought occurs. On the other hand, the amount of water diverted to Wudil-Dabi Subbasin in 1976 and 1977 growing seasons for drought simulation were actually higher than for calibration. An error (under-estimation) in the measured canal diversion used for calibration may account for this discrepancy. In general, drought simulation resulted in up to 30% decline in water supply in some subbasins and more than 15% decline in most subbasins. As a consequence, there was more than 30% cut in net revenue for most subbasins (see Table 5). The downstream subbasins (from Dabi-Marke to Burum Gana River) were the most affected since they recorded the heaviest losses in net return.

The addition of salinity effects aggravated the already bad water supply situation, the decline in net returns reached 43% on the Hadejia Valley Subbasin in 1978. As was the case for water shortages, the downstream subbasins were the most limited when salinity effects were superimposed upon that of water, resulting in further declines in net returns.

Summary and Conclusions

A hydrologic and salinity model was combined with an economic simulation model in order to predict management effects of sequential water use and salinity

by subbasins in a river basin. The sequential use model thus developed uses functions which relate seasonal crop evapotranspiration and soil solution salt concentration to yields. In essence, the outputs from the hydrologic (seasonal evapotranspiration) and salinity (calculated soil solution salt concentrations) models became inputs into the economic model.

For testing, the model was applied to an actual hydrologic unit, the Hadejia River Basin in Nigeria. The practical utility of the model was demonstrated through the predictions of crop yield and net returns from the various hydrologic and salinity conditions. Management runs of the model indicate that for Hadejia River Basin:

1. Increasing the crop areas beyond those used for model calibration resulted in increased total net return for the entire Basin area; however net returns per unit area were not as high as with the calibration runs. Declines in net returns per unit area were due to water shortages and salinity buildup in some of the subbasins.
2. Reducing the areas occupied by phreatophyte/open water indicated that water previously consumptively used by phreatophytes could be beneficially used by the crops. However, such reductions in phreatophyte/open water areas did not completely make up for water needed by the increased crop areas.
3. In the event that drought occurs, the model predicted water shortages and salinity buildup which eventually resulted in the decline of net benefits to the entire basin.

Apart from the management applications mentioned previously, the model can be useful in evaluating the crop acreage combination which will achieve maximum overall benefit in evaluating project design reservoir capacities and other facilities appropriate for the demand and available water. The model is also capable of evaluating the relative efficiency of water with respect to production or net return for several management alternatives or cropping schemes.

The sequential use model as presented in this paper would deserve increased confidence if the production functions and the salt tolerance functions had been defined more precisely. However, isolation of two factors (water and salinity) as measurements of production in the complex process of crop growth and yield is very difficult and may not represent all the factors affecting crop growth. There are other factors assumed constant in the development of this model, which in reality are not. Such "other factors" include soil fertility, infestation by pests and diseases, etc. Continued progress towards a more precise estimate of crop yields will require additional effort directed towards the quantification of the effects of these "other factors" on crop growth and yields.

Appendix I.—References

1. Bernstein, L., "Tolerance of Crops to Salinity," *Journal of the Irrigation and Drainage Division*, ASCE, Vol. 87, No. IR4, Proc. Paper 3005, Dec., 1961, pp. 1–12.
2. Doorenbos, J., Kassam, A. H., Bentrelsen, C. L. M., and Brancheid, V., "Yield Response to Water," *FAO Irrigation and Drainage Paper 33*, FAO of the United Nations, Rome, Italy, 1979.
3. Fapohunda, H. O., "River Basin Sequential Water Use and Salinity Effects on Crop Yield Economics," thesis presented to the Utah State University, at Logan, Utah,

in 1980, in partial fulfillment of the requirements for the Degree of Doctor of Philosophy.
4. Gardner, W. R., and Ehlig, C. F., "The Influence of Soil Water on Transpiration by Plants," *Journal of Geophysical Research,* Vol. 68, No. 20, 1963, pp. 5719–5724.
5. Hill, R. W., Israelsen, E. K., and Riley, J. P., "Computer Simulation of the Hydrologic and Salinity Flow System Within the Bear River Basin," *UWRL Report No. PRWG104-1,* Utah Water Research Laboratory, Utah State University, Logan, Utah, Nov., 1973.
6. Huber, A. L., Israelsen, E. K., Hill, R. W., and Riley, J. P., "Basin Simulation Assessment Model (BSAM): Documentation and User Manual," *Report No. PRWG201-1,* Utah Water Research Laboratory, Utah State University, Logan, Utah, Aug., 1976.
7. Maas, E. V., and Hoffman, G. J., "Crop Salt Tolerance—Current Assessment," *Journal of the Irrigation and Drainage Division,* ASCE, Vol. 103, No. IR2, Proc. Paper 12993, June, 1977, pp. 115–134.
8. Packer, M. R., Riley, J. P., and Israelsen, E. K., "Simulation of the Hydrologic-Economic Flow System," *Symposium, Publication No. 81: The Use of Analog and Digital Computers in Hydrology,* International Association of Scientific Hydrology, 1968, pp. 386–391.
9. Phelan, J. T., "Estimating Monthly '*k*' Values for the Blaney-Criddle Formula," presented at the March 2–6, 1972, Agriculture Research Service, Soil Conservation Service Workshop on Consumptive Use, held at Phoenix, Ariz.; also *Technical Release #21,* (Rev. 2), United States Department of Agriculture-Soil Conservation Service, Sept., 1970.

Appendix II.—Notation

The following symbols are used in this paper:

A = salinity threshold;
B = yield decrease per unit salinity increase, as a percentage;
C_{igk} = salt concentration of ground-water source, k;
C_{isj} = salt concentration of surface source, j;
C_{scp} = salt concentration associated with storage element, p;
C_{so} = salt concentration of outflow water;
CSM = critical soil moisture level below which ET is less than PET;
CSS = soil solution salt concentration (total dissolved solids);
DIFF = numerical difference between computed and measured values of a given hydrologic or salinity data;
EC_e = electrical conductivity of soil saturation extract, in millimhos per centimeter at 25° C;
ET = evapotranspiration;
ET_a = actual ET;
ET_{aL} = actual ET when water deficit exceeds 50%;
ET_b = actual ET when water deficit equals 50%;
ET_m = maximum or potential ET;
k_c = monthly crop growth coefficient;
k_t = monthly temperature coefficient;
k_y = crop yield response factor;
OBJ = objective function;
P = monthly daylight hours of year, as a percentage;
P_r = precipitation;
PET = potential evapotranspiration;
Q_{go} = subsurface outflow;
Q_{igk} = subsurface inflow from source, k;
Q_{is} = total surface inflow;

Q_{so} = total surface outflow;
SM = soil moisture level;
SMC = soil moisture capacity (root zone water storage available to plant);
SSDP = salt lost through deep percolation;
SSIR = salt applied from irrigation waters;
SSWF = salt added from weathering or fertilizer applications;
T = mean monthly temperature, in degrees Fahrenheit;
Y = relative crop yield;
Y_a = actual harvested crop yield;
Y_{aL} = actual crop yield when water deficit exceeds 50%;
Y_b = actual crop yield when water deficit equals 50%;
Y_m = maximum or potential crop yield; and
ΔS = change in storage.

JOURNAL OF THE IRRIGATION AND DRAINAGE DIVISION

Infiltration Equations Modified for Surface Effects

By Ian D. Moore[1]

Introduction

Surface sealing and mulching can significantly influence infiltration and therefore surface runoff and soil erosion. These effects have been demonstrated by numerous researchers (8,9,10,12,13,14,18,21,24). Mannering (14), e.g., showed that in many instances infiltration rates on bare soil are only 20%–30% of the rates on protected soils. Surface sealing effects can greatly overshadow other factors affecting infiltration on unprotected soils. Mulching and incorporated organic matter also have a considerable, but opposite effect. These effects have been demonstrated qualitatively, but quantitative representation of these effects in infiltration modeling is lacking. This paper shows how these effects can be incorporated into the approximate two-stage infiltration equations proposed by Mein and Larson (16,17).

Green-Ampt-Mein-Larson (GAML) Model

Green and Ampt (11) derived an infiltration equation for ponded surfaces based on Darcy's law using a capillary-tube analogy. Swartzendruber (25) pointed out that the capillary-tube model was more restrictive than needed for Green and Ampt's approach. The method assumed an initially uniform moisture content in a homogeneous soil. Philip (22) later derived the Green-Ampt equation calling it the delta-function solution. Morel-Seytoux and Khanji (20) derived an equation with the same functional form that considered air viscous effects of two-phase flow, but without many of the restrictions, including the capillary-tube analogy. Bouwer (4,5) used the Green-Ampt equation in his studies of infiltration into

[1]Asst. Prof., Dept. of Agricultural Engrg., 106 Agricultural Engrg. Building., Univ. of Kentucky, Lexington, Ky. 40546.

Note.—Discussion open until August 1, 1981. To extend the closing date one month, a written request must be filed with the Manager of Technical and Professional Publications, ASCE. Manuscript was submitted for review for possible publication on August 12, 1980. This paper is part of the Journal of the Irrigation and Drainage Division, Proceedings of the American Society of Civil Engineers, ©ASCE, Vol. 107, No. IR1, March, 1981. ISSN 0044-7978/81/0001-0071/$01.00.

nonuniform soil profiles. The Green-Ampt equation has received considerable attention in recent years and although it is an approximate equation it has been shown to have a theoretical basis, as well as measurable parameters.

If the depth of ponding is negligible, then the Green-Ampt equation can be written as

$$f = \frac{dF}{dt} = K\left(1 + \frac{S_w \Delta\theta}{F}\right) \quad \text{(1a)}$$

or in integrated form as

$$Kt = F - S_w \Delta\theta \ln\left(1 + \frac{F}{S_w \Delta\theta}\right) \quad \text{(1b)}$$

in which f = the infiltrability; F = the infiltration volume; $\Delta\theta$ = the initial moisture deficit; S_w = the capillary drive at the wetting front; K = the hydraulic conductivity in the wetted zone; and t = time. This equation is a single-stage infiltration equation because it assumes ponded conditions at all times.

Mein and Larson (16,17), utilizing concepts similar to those of Green and Ampt, developed an equation for predicting infiltration volume prior to surface ponding (assuming a uniform initial moisture profile and constant application rate). Their equation is

$$F_s = \frac{S_w \Delta\theta}{\left(\frac{I}{K}\right) - 1} \quad \text{(2)}$$

in which F_s = the volume of water infiltrated at the instant of surface ponding; and I = the application rate (constant). Mein and Larson (16,17) then modified the Green-Ampt equation to predict infiltration after surface ponding (the second stage of infiltration) by translating the time scale. This modified equation is

$$K(t - t_s + t'_s) = F - S_w \Delta\theta \ln\left(1 + \frac{F}{S_w \Delta\theta}\right) \quad \text{(3)}$$

in which t_s = the time to surface ponding (= F_s/I from Eq. 2); and t'_s = the time required to infiltrate a volume equivalent to F_s under ponded surface conditions (obtained by substituting F_s into Eq. 1 and solving for t). Eq. 2 can be solved explicitly for F_s or t_s and Eq. 3 can be solved explicitly for t or by iteration for F.

For brevity, the two-stage infiltration model defined by Eqs. 2 and 3 is termed the Green-Ampt-Mein-Larson (GAML) Model.

Derivation of GAML Model Modified for Surface Effects

Modified Green-Ampt Equation.—Fig. 1 represents the conceptual soil profile used in the following derivation of the modified Green-Ampt equation. The soil consists of a thin surface layer of thickness, L_1, with an initial moisture deficit, $\Delta\theta_1$, and characterized by a hydraulic conductivity, K_1. Below this, the soil is homogeneous and semi-infinite with an initial moisture deficit, $\Delta\theta_2$.

It is characterized by a hydraulic conductivity in the wetted zone of K_2.

If the depth of ponding is negligible, then Darcy's law can be applied to the system to give

$$f = \frac{L + S_{w2}}{\dfrac{L_1}{K_1} + \dfrac{L_2}{K_2}} \quad \text{for} \quad L \geq L_1 \quad \ldots\ldots \quad (4)$$

in which S_{w2} = the capillary drive at the wetting front in the subsurface soil; and $(L + S_{w2})$ = the potential at the wetting front if the potential at the soil

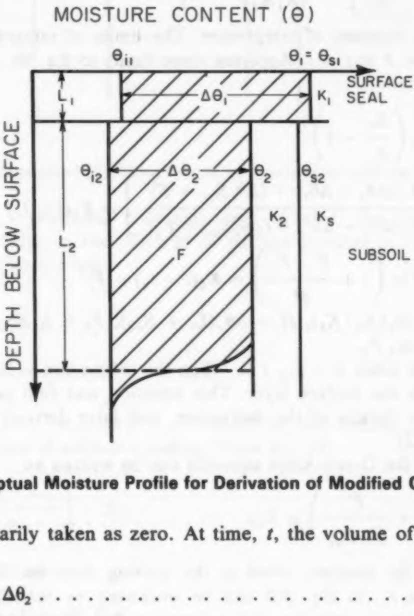

FIG. 1.—Conceptual Moisture Profile for Derivation of Modified GAML Equations

surface is arbitrarily taken as zero. At time, t, the volume of water infiltrated is

$$F = L_1 \Delta\theta_1 + L_2 \Delta\theta_2 \quad \ldots\ldots \quad (5)$$

Rearranging, we have

$$L_2 = \frac{F - L_1 \Delta\theta_1}{\Delta\theta_2} \quad \ldots\ldots \quad (6)$$

Because $f = dF/dt$; and $L = L_1 + L_2$, Eqs. 4 and 6 can be combined to yield

$$\frac{dF}{dt} = \frac{L_1 + \dfrac{F - L_1 \Delta\theta_1}{\Delta\theta_2} + S_{w2}}{\dfrac{L_1}{K_1} + \dfrac{F - L_1 \Delta\theta_1}{\Delta\theta_2 K_2}} \quad \ldots\ldots \quad (7)$$

Rearranging Eq. 7 results in

$$\frac{dF}{dt} = \frac{A + K_1 K_2 F}{B + F K_1} \quad \text{(8)}$$

in which $A = K_1 K_2 (L_1 \Delta\theta_2 - L_1 \Delta\theta_1 + \Delta\theta_2 S_{w2})$; and $B = L_1 (\Delta\theta_2 K_2 - \Delta\theta_1 K_1)$.

$$\text{Therefore} \quad \int \frac{B + F K_1}{A + K_1 K_2 F} dF = \int dt \quad \text{(9a)}$$

$$\text{or, on integrating} \quad \frac{F}{K_2} \left[\frac{B K_1 K_2 - A K_1}{(K_1 K_2)^2} \right] \ln (A + K_1 K_2 F) = t + C \quad \text{(9b)}$$

in which C = a constant of integration. The limits of integration are $F = F_1$ at $t = t_1$; and $F = F$ at $t = t$. Applying these limits to Eq. 9*b*, and substituting for A and B yields

$$F - F_1 + \left[L_1 \Delta\theta_2 \left(\frac{K_2}{K_1} - 1 \right) - \Delta\theta_2 S_{w2} \right] \ln \left[\frac{L_1 (\Delta\theta_2 - \Delta\theta_1) + (\Delta\theta_2 S_{w2} + F)}{L_1 (\Delta\theta_2 - \Delta\theta_1) + (\Delta\theta_2 S_{w2} + F_1)} \right] = K_2 (t - t_1) \quad \text{(10a)}$$

$$\text{or} \quad F + (E - H) \ln \left(1 + \frac{F - F_1}{H} \right) = K_2 (t - t_1) + F_1 \quad \text{(10b)}$$

in which $E = L_1 \Delta\theta_2 (K_2/K_1)$; $H = \Delta\theta_2 (L_1 + S_{w2})$; $F_1 = L_1 \Delta\theta_1$; and t_1 = time to infiltrate volume, F_1.

Eq. 10*b* applies when $L > L_1$, i.e., when the infiltration volume exceeds the storage volume in the surface layer. This equation was first presented by van Duin (27) without details of the derivation, and later derived by Asseed and Swartzendruber (2).

When $L \leq L_1$, the Green-Ampt equation can be written as

$$F - \Delta\theta_1 S_{w1} \ln \left(1 + \frac{F}{\Delta\theta_1 S_{w1}} \right) = K_1 t \quad \text{(10c)}$$

in which S_{w1} = the capillary drive at the wetting front in the surface layer of soil. The term t_1, in Eq. 10*b* can be evaluated by substituting F_1 for F in Eq. 10*c*. If $L_1 = 0$, then Eq. 10*b* reduces to Eq. 10*c*, written for uniform material two.

When $L > L_1$, the infiltrability is computed by Eq. 8, which can be rearranged and expressed as follows

$$f = K_2 \left(\frac{H + F - F_1}{E + F - F_1} \right) \quad \text{(11a)}$$

When $L \leq L_1$ this equation can be written as

$$f = K_1 \left(1 + \frac{\Delta\theta_1 S_{w1}}{F} \right) \quad \text{(11b)}$$

Modified Mein-Larson Equation.—At the instant surface ponding occurs, the

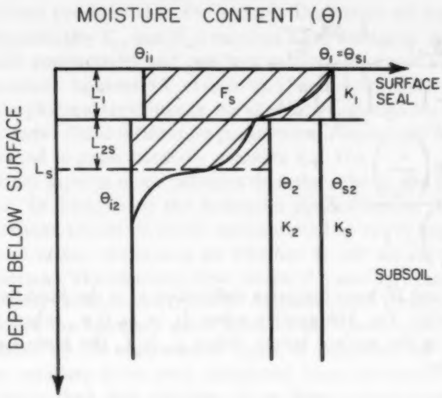

FIG. 2.—Conceptual Moisture Profile at Moment of Surface Ponding

application rate, I (assumed constant), will equal f, the infiltrability. The conceptual soil profile at the moment of surface ponding is shown in Fig. 2. Therefore, from Darcy's law:

$$I = \frac{S_{w2} + L_s}{\dfrac{L_1}{K_1} + \dfrac{L_{2s}}{K_2}} \quad \text{for} \quad L > L_1 \qquad (12)$$

in which $L_s = L_1 + L_{2s}$; and L_{2s} = depth to the wetting front below the top layer at the time of surface ponding. From Eq. 12

$$L_s = I\left(\frac{L_1}{K_1} + \frac{L_s - L_1}{K_2}\right) - S_{w2} \qquad (13a)$$

and it therefore follows that

$$L_s = \frac{I L_1 K_2 - I L_1 K_1 - K_1 K_2 S_{w2}}{K_1 K_2 - I K_1} \qquad (13b)$$

From Fig. 2 we see that $F_s = L_1 \Delta\theta_1 + L_{2s}\Delta\theta_2$ . . . . (14a)

and substituting for L_{2s} in Eq. 14a gives

$$F_s = L_1(\Delta\theta_1 - \Delta\theta_2) + L_s\Delta\theta_2 \qquad (14b)$$

which results in $L_s = \dfrac{F_s - L_1(\Delta\theta_1 - \Delta\theta_2)}{\Delta\theta_2}$ . . . . (14c)

Equating Eqs. 13b (Darcy's equation) and 14c (continuity equation) yields

$$F_s = \frac{\Delta\theta_2(L_1 + S_{w2})}{\left(\frac{I}{K_2}\right) - 1} - \frac{L_1\,\Delta\theta_2 \frac{I}{K_1}}{\left(\frac{I}{K_2}\right) - 1} + L_1\Delta\theta_1 \qquad (15a)$$

$$\text{or}\quad F_s = \frac{H - E\left(\frac{I}{K_2}\right)}{\left(\frac{I}{K_2}\right) - 1} + F_1 \qquad (15b)$$

in which E, F_1, and H, have the same definitions as in the Modified Green-Ampt equation (Eq. 10*b*). Eq. 15*b* applies when $L_s > L_1$ (i.e., when F exceeds the storage volume in the surface layer). When $L_s \leq L_1$ the Mein-Larson equation can be written as

$$F_s = \frac{\Delta\theta_1 S_{w1}}{\left(\frac{I}{K_1}\right) - 1} \qquad (15c)$$

Modified Green-Ampt Equation for Two-Stage Infiltration.—At time t, $F = F$, and at time t_s, $F = F_s$. Therefore, for two-stage infiltration when $L > L_1$ and $L_s > L_1$ Eq. 9*a* can be written as

$$\int_{F_s}^{F} \frac{B + FK_1}{A + K_1K_2F}\,dF = \int_{t_s}^{t} dt \qquad (16)$$

On integrating

$$F + (E - H)\ln\left[1 + \frac{F}{(H - F_1)}\right] = K_2(t - t_s + t'_s) \qquad (17a)$$

in which t'_s = the time required to infiltrate a volume equivalent to F_s under field saturated surface conditions (t'_s is obtained by substituting F_s for F and setting F_1 to zero in Eq. 10*b* and solving for t). When $L \leq L_1$ and $L_s \leq L_1$, the modified Green-Ampt equation for two-stage infiltration can be written as

$$F - \Delta\theta_1 S_{w1} \ln\left(1 + \frac{F}{\Delta\theta_1 S_{w1}}\right) = K_1(t - t_s + t'_s) \qquad (17b)$$

in which t'_s = obtained by substituting F_s for F in Eq. 10*c* and solving for t. When $L > L_1$ and $L_s > L_1$, Eq. 17*b* can be used for predicting F from $t = t_s$ to $t = t_1$, and Eq. 10*b* used thereafter. If $L_1 = 0$, then Eq. 17*a* reduces to Eq. 17*b*, written for uniform material two.

Eqs. 17*a* and 17*b* are used to calculate the infiltration volumes after surface ponding. The corresponding infiltrabilities are given by Eqs. 11*a* and 11*b*, respectively (for $L > L_s$ or $F > F_s$).

Parameter Evaluation for Modified GAML Equations.—The modified GAML equations can be applied to cases in which the surface layer is either: (1) More

pervious; or (2) less pervious than the subsoil. Derivation of input parameters for the model (specifically S_{w1} and S_{w2}) requires a knowledge of the relationships between hydraulic conductivity and capillary suction (K versus S), and capillary suction and moisture content (S versus θ). Parameters derived from these relationships have physical significance. An alternative, though not as theoretically satisfying, is to derive fitted infiltration parameters. Asseed and Swartzendruber (3) used this method to experimentally evaluate Eq. 17*a*.

When the surface layer is more pervious than the subsoil, the subsoil controls infiltration rates. In such cases the hydraulic conductivities, K_1 and K_2, for input to the equations should be either the saturated or rewet hydraulic conductivities in the two zones, depending on whether or not air entrapment effects are deemed important. The capillary drive terms, S_{w1} and S_{w2}, can be determined using one of several procedures (1,15,19). Aggelides and Youngs (1) found that in uniform profiles the capillary drive term in the Green and Ampt equation was best estimated by the water entry value as suggested by Bouwer (4). In their study, the capillary drive term calculated from soil-water properties was consistently greater than that obtained from direct measurements. Aggelides and Young (1) claim that these errors stem from the approximations inherent in the derivation of the Green and Ampt equation from the moisture flow equation. Detailed descriptions and analysis of the currently available methods of calculating the capillary drive terms are beyond the scope of this paper. The reader should consult the references previously mentioned for further information.

Estimation of the input parameters for Case 2, in which the surface layer is less pervious than the subsoil, is not as straight forward as for Case 1. Tagaki (26) found that when the surface layer is less pervious than the subsoil a negative pressure develops in the zone below the surface layer and remains constant for a considerable depth. Tagaki's findings imply that if the subsoil is assumed homogeneous, then the moisture content and hydraulic conductivity in this zone must also be constant and less than the values at saturation. Otherwise, a negative pressure would not develop in this zone. These assumptions of constant moisture content and hydraulic conductivity are inherent in the development of both the GAML and modified GAML equations. The equations, then are directly applicable to Case 2, of which the problem of surface sealing is probably the most important example. For Case 2, K_1 and S_{w1}, can be evaluated using the aforementioned techniques for Case 1. Variables K_2 and S_{w2}, can be evaluated by considering steady-state infiltration.

For steady-state infiltration gravity forces dominate and the capillary forces can be neglected. The hydraulic gradient approaches unity and the infiltration rate, given by Eq. 11*a*, approaches the hydraulic conductivity in the wetted (transmission) subsoil zone, K_2.

For steady-state infiltration, the flux through the restricting surface layer, q_1, must equal the flux through the subsoil transmission zone, q_2(12):

$$q_1 = q_2 \quad \text{(18a)}$$

or $$K_1\left(\frac{d\phi}{dz}\right)_1 = K_2\left(\frac{d\phi}{dz}\right)_2 \quad \text{(18b)}$$

in which ϕ = the hydraulic head. The hydraulic gradient in the subsoil transmission zone under steady-state conditions tends to unity so that

$$K_1\left(\frac{d\phi}{dz}\right)_1 = K_2 = q \quad (19)$$

If the depth of ponding on the soil surface is negligible then

$$\left(\frac{d\phi}{dz}\right)_1 = \frac{S + L_1}{L_1} \quad (20)$$

in which S = the capillary suction immediately below the surface layer; and L_1 = the thickness of the surface layer. Substituting Eq. 20 into Eq. 19 yields

$$K_1\left(\frac{S + L_1}{L_1}\right) = K_2 \quad (20a)$$

or $$\frac{K_2}{(S + L_1)} = \frac{K_1}{L_1} \quad (20b)$$

With a knowledge of the K-S relationship, and the known value of K_1/L_1, K_2 can be determined from Eq. 20*b* by trial and error. The moisture content behind the wetting front in the subsoil zone corresponds to this value of K_2 and is determined from the S-θ relationship. From these values, $\Delta\theta_2$ and S_{w2} can be directly determined.

Alternatively, the model parameters can be determined directly by employing functional relationships between capillary suction, unsaturated hydraulic conductivity and moisture content, such as those proposed by Campbell (6). These methods are only valid if a log–log plot of the moisture retention curve is a straight line, and tend to break down close to saturation. Care should therefore be exercised in using these techniques to calculate K_2 and S_{w2}.

Surface Sealing.—The modified GAML equations provide a simplified means of predicting infiltration into soils with well established, stable surface seals. In such cases, K_1 will be essentially constant, and K_2 can be determined using the aforementioned technique. Eqs. 15 and 17 can then be solved in the same

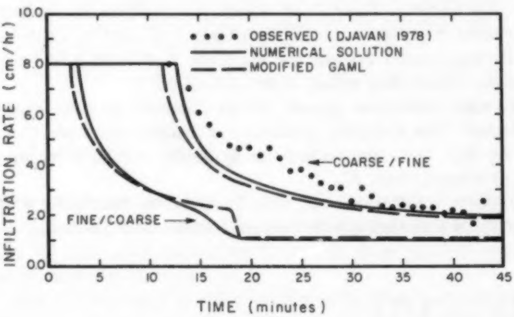

FIG. 3.—Predicted and Observed Infiltration Rates Versus Time for Coarse (Lewiston Fine Sandy Loam) Over-Fine (Millville Silt Loam) and Fine Over-Coarse Stratifications (L_1 = 5 cm)

manner as the original GAML equations using the methods suggested by Mein and Larson (16,17). That is, Eq. 15 can be solved directly for t, or by iteration for F.

In many cases, K_1 is not constant. For example, Moore et al. (19) suggest that the following equation could be used to represent the change in hydraulic conductivity of a surface seal as it develops over a period of time

$$K_1(t) = K_f + (K_i - K_f)e^{-at} \quad (21)$$

in which K_f = the final steady-state hydraulic conductivity of a stable, well-established surface seal; K_i is the initial hydraulic conductivity; and a = a constant controlling the rate of decay of the initial hydraulic conductivity. Inclusion of Eq. 21, or any other relationship to describe the change in K_1 with time, produces complicated equations that are difficult to solve (K_1, K_2, and the moisture content in the subsoil transmission zone all change with time). Examining these effects is beyond the scope of this paper.

Analysis

Djavan (7) measured infiltration rates into two-layered soil columns consisting of Lewiston fine sandy loam (coarse) overlying Millville silt loam (fine). He also measured the K-S and S-θ relationships for both soil types. These data permit the modified GAML equations to be evaluated against numerical solutions of Richards' equation and measured infiltration rates. The numerical technique used here is essentially the same as that described by Smith and Woolhiser (23). Two cases are examined; (1) Coarse over-fine; and (2) fine over-coarse stratifications.

The infiltration rates predicted by the numerical method and the modified GAML equations are shown for both Cases 1 and 2 in Fig. 3, together with observed infiltration rates (7) for Case 1. The application rate was 8.0 cm/h, and the surface layer was 5 cm thick. The calculated input parameters for the modified GAML equations are shown in Table 1.

For the coarse over-fine stratification the times to surface ponding agree very well. Predicted infiltration rates for the numerical method and the modified GAML model also agree reasonably well. The difference between the two is

TABLE 1.—Input Parameters for Modified GAML Equations for Fine[a] and Coarse[b] Soil Type

Parameter (1)	Symbol (2)	Coarse[b]/fine[a] (3)	Fine[a]/coarse[b] (4)	Units (5)
Capillary drive at	S_{w1}	4.17	22.08	centimeters of water
wetting front	S_{w2}	22.08	4.17	
Conductivity in	K_1	5.45	0.42	centimeters per hour
transmission zone	K_2	0.42	0.97	
Initial moisture	$\Delta\theta_1$	0.25	0.24	centimeters per cen-
deficit	$\Delta\theta_2$	0.24	0.163	timeter

[a]Millville silt loam.
[b]Lewiston fine sandy loam.

due to the failure of the wetting front to conform to the piston-flow assumption inherent in the derivation of the GAML equations. Observed infiltration rates are higher than predicted at intermediate times (14 min–30 min), but are in very close agreement with the predicted at larger times (>30 min).

Predictions of both the times to surface ponding and infiltration rates for the fine over-coarse stratification show close agreement, except between 12 min and 19 min from the beginning of the event. The reason for this arises, again, from the failure of the actual wetting front to conform to the piston-flow model. In the modified GAML equations the piston-type wetting front encounters the interface between the two strata at 18 min, at which time the infiltration rate drops to an approximately constant rate. The leading edge of the wetting front, as predicted by the numerical method, encounters the interface at 11 min. However, the wetting front is not as distinct as that in the modified GAML Equations and so produces a gradual reduction in the infiltration rate to a more or less constant value after it passes through the interface. The most significant result here is the fact that both the numerical method and the modified GAML equations predict this accelerated reduction of infiltration rates when the wetting front encounters the interface, though the latter predicts a much more rapid reduction. In addition, the constant infiltration rates after the wetting front

TABLE 2.—Input Parameters for GAML Equation for Ida Silt Loam Soil (16)

Parameter (1)	Symbol (2)	Value (3)	Units (4)
Total porosity	θ	0.53	centimeters per centimeter
Capillary drive at wetting front	S_w	7.43	centimeters of water
Saturated hydraulic conductivity	K_s	0.105	centimeters per hour

moves through the interface are almost identical. This tends to validate the method of calculating K_2, S_{w2}, and $\Delta\theta_2$, for fine over-coarse strata described earlier, and shows that the input parameters can be measured, and thus do not require fitting.

Asseed and Swartzendruber (3) have experimentally evaluated Eq. 10*b* for two-layered soil profiles consisting of coarse over-fine stratifications. They evaluated the parameters in the equation by fitting to infiltration data measured in both uniform and stratified profiles. For coarse over-fine stratifications their results were good. For fine over-coarse stratifications, their results were generally reasonable for predictions based on the parameter set obtained by fitting to stratified profiles. Predictions based on the parameter set obtained by fitting to uniform profiles were poor at larger times. This is expected because these parameters do not take into account the restricting effect of the fine surface layer, which prevents the coarser subsoil from reaching saturation.

In order to illustrate the magnitude of the surface effects predicted by the modified GAML equations, the following hypothetical situation is presented. The parameter set derived by Mein and Larson (16) from measured K-S and S-θ relationships, for an Ida silt loam soil will be used. The input parameter values are listed in Table 2.

In the analysis, the conductivity of the surface and subsurface layers of soil

(K_1 and K_2, respectively) was assumed constant (i.e., a well-established stable surface seal was assumed). The surface seal was assumed to be 5 mm thick (8) and the initial moisture deficit and capillary drive at the wetting front were assumed to be the same in the surface and subsurface zones. Analysis was performed for the various combinations of situations resulting from two different initial moisture contents (θ_i, three different rainfall intensity ratios (I/K_s), and four different conductivity ratios (K_s/K_1), in which K_s = the saturated hydraulic conductivity in the subsoil zone.

TABLE 3.—Predicted and Computed Cumulative Infiltration Volume at Time to Surface Ponding for $K_s/K_1 = 1$

Rainfall intensity ratio (I/K_s) (1)	Initial moisture deficit (2)	F_s (predicted), in centimeters (3)	F_s (calculated)[a], in centimeters (4)	Error, as a percentage (5)
2	0.28	2.080	1.850	−12.4
	0.13	0.968	0.727	−33.1
4	0.28	0.694	0.850	18.4
	0.13	0.322	0.315	−2.2
8	0.28	0.297	0.478	37.9
	0.13	0.138	0.163	15.3

[a]Calculated by Richards' equation (16).

TABLE 4.—Time to Surface Ponding, t_s, in minutes

Initial moisture contents (1)	Conductivity ratio, (K_s/K_1) (2)	Rainfall Intensity Ratio, (I/K_s) 2 (3)	4 (4)	8 (5)
$\theta_i = 0.40$	1	276.4	46.0	9.86
	2	222.7	32.4	4.60
	4	138.2	9.20	2.23
	8	18.4	4.45	1.10
$\theta_i = 0.25$	1	595.5	99.2	21.2
	2	478.7	69.7	9.91
	4	297.7	19.8	4.79
	8	39.6	9.58	2.36

Table 3 compares F_s predicted by the GAML model (equivalent to the modified GAML model when K_s/K_1 equals one) to values calculated from Richards' equation by Mein and Larson (16). The error, expressed as a percentage, ranges from −33%–38%. Mein and Larson (16) compared predictions of the GAML model to those of Richards' equation for four different soils. They concluded that the Ida silt loam yielded the worst results, classifying them only as "fair."

Table 4 shows the time to surface ponding, t_s, predicted by the modified GAML model. Time t_s decreases with increasing rainfall intensity ratio, increasing conductivity ratio, and increasing initial moisture content.

The cumulative infiltration volumes as functions of time for I/K_s equal to 4 are shown in Table 5. The cumulative infiltration volumes for θ_i equal to 0.40 are also shown in Fig. 4, together with the cumulative infiltration volume calculated from Richards' equation by Mein and Larson (16) for K_s/K_1 equal to one.

TABLE 5.—Cumulative Infiltration Volume, in centimeters, Versus Time for $I/K_2 = 4$

Conductivity ratio, (K_s/K_1)	Time, in hours				
	1	2	3	4	5
$\theta_i = 0.40$					
1	0.411	0.700	0.930	1.134	1.322
2	0.388	0.648	0.862	1.053	1.226
4	0.323	0.543	0.731	0.903	1.063
8	0.211	0.361	0.493	0.615	0.730
$\theta_i = 0.25$					
1	0.420	0.830	1.158	1.432	1.678
2	0.420	0.796	1.082	1.330	1.556
4	0.377	0.657	0.893	1.108	1.306
8	0.254	0.430	0.588	0.735	0.873

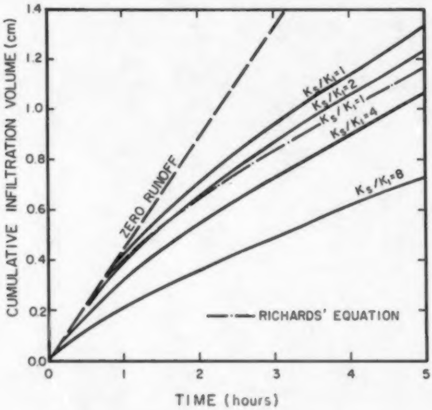

FIG. 4.—Cumulative Infiltration Volume Versus Time (Ida Silt Loam, $I/K_s = 4$; $\theta_i = 0.40$)

Figs. 5 and 6 are different ways of comparing the computed infiltration rates as functions of time. Fig. 5 clearly shows the effect that the conductivity ratio has on both the shape and position of the infiltration rate curve, as well as the time to surface ponding. In a similar way, Fig. 5 shows the effect of rainfall intensity.

The aforementioned results clearly illustrate the impact that surface effects

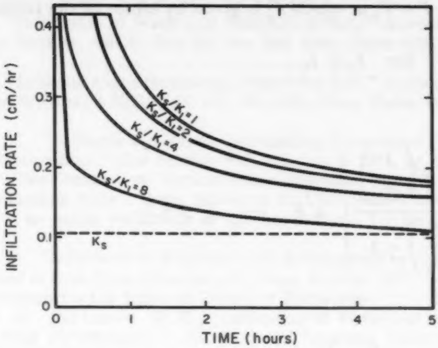

FIG. 5.—Infiltration Rate Versus Time for Four Different Conductivity Ratios (Ida Silt Loam, $I/K_s = 4$; $\theta_i = 0.40$)

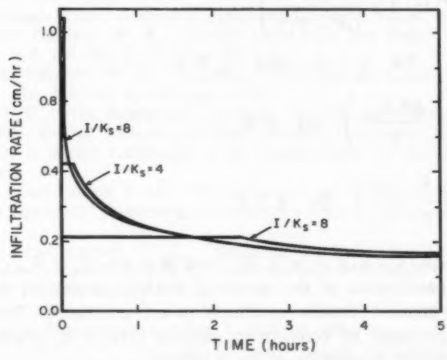

FIG. 6.—Infiltration Rate Versus Time for Three Different Intensity Ratios (Ida Silt Loam, $K_s/K_1 = 4$; $\theta_i = 0.40$)

can have on infiltration and thus, surface runoff. Reducing the hydraulic conductivity of a thin surface layer decreases the infiltrability significantly and distorts the shape of the infiltration rate curve at high conductivity ratios. The cumulative infiltration volume is reduced by 45% or more after 5 h for conductivity ratios greater than eight.

Summary and Conclusions

The GAML infiltration model was modified to include surface effects such as surface sealing. For infiltration of a constant intensity rainfall greater than the saturated hydraulic conductivity of the soil ($I > K_s$) into a soil of uniform moisture content, the governing equations can be expressed in the following

form: $f = I$ until $F = F_s$ in which F_s is given by either of the following

$$F_s = \frac{\Delta\theta_1 S_{w1}}{\left(\frac{I}{K_1}\right) - 1} \quad \text{for} \quad L_s \leq L_1 \qquad (22a)$$

$$\text{or} \quad F_s = \left[\frac{H - E\left(\frac{I}{K_2}\right)}{\left(\frac{I}{K_2}\right) - 1}\right] + F_1 \quad \text{for} \quad L_s > L_1 \qquad (22b)$$

and for $F > F_s$

$$F - \Delta\theta_1 S_{w1} \ln\left(1 + \frac{F}{\Delta\theta_1 S_{w1}}\right) = K_1(t - t_s + t'_s) \quad \text{for} \quad L \leq L_1 \qquad (23a)$$

$$\text{or} \quad F - (E - H)\ln\left[1 + \frac{F}{(H - F_1)}\right]$$

$$= K_2(t - t_s + t'_s) \quad \text{for} \quad L > L_1 \quad \text{and} \quad L_s > L_1 \qquad (23b)$$

$$\text{and} \quad f = K_1\left(1 + \frac{\Delta\theta_1 S_{w1}}{F}\right) \quad \text{for} \quad L \leq L_1 \qquad (24a)$$

$$\text{or} \quad f = K_2\left(\frac{H + F - F_1}{E + F - F_1}\right) \quad \text{for} \quad L > L_1 \qquad (24b)$$

in which $E = L_1\Delta\theta_2(K_2/K_1)$; $F_1 = L_1\Delta\theta_1$; and $H = \Delta\theta_2(L_1 + S_{w2})$.

Examples of predictions of the modified GAML model for the case of a constant surface layer hydraulic conductivity are presented. These examples illustrate the importance of considering surface effects in infiltration studies and show the potential magnitude of these effects.

Acknowledgments

This paper is published with the approval of the Director of the Kentucky Agricultural Experiment Station and designated as Paper No. 79-2-173.

Appendix I.—References

1. Aggelides, S., and Youngs, E. G., "The Dependence of the Parameters in the Green and Ampt Infiltration Equation on the Initial Water Content in Draining and Wetting States," *Water Resources Research*, Vol. 14, No. 5, 1978, pp. 857–862.
2. Asseed, M., and Swartzendruber, D., "Water Infiltration into Uniform and Stratified Soils. I. Review and Use of an Approximate Theory," *Libyan Journal of Agriculture*, Libya, Africa, Vol. 3, 1974, pp. 19–26.
3. Aseed, M., and Swartzendruber, D., "Water Infiltration into Uniform and Stratified Soils. II. Experimental Evaluation of an Approximate Theory," *Libyan Journal of*

Agriculture, Libya, Africa, Vol. 4, 1975, pp. 129–140.
4. Bouwer, H., "Infiltration of Water into Nonuniform Soil," *Journal of the Irrigation and Drainage Division,* ASCE, Vol. 95, No. IR4, Proc. Paper 6397, Dec., 1969, pp. 451–462.
5. Bouwer, H., "Infiltration into Increasingly Permeable Soil," *Journal of the Irrigation and Drainage Division,* ASCE, Vol. 102, No. IR1, Proc. Paper 11959, Mar., 1976, pp. 127–136.
6. Campbell, G. C., "A Simple Method for Determining Unsaturated Conductivity from Moisture Retention Data," *Soil Science,* Vol. 120, No. 2, 1974, pp. 92–95.
7. Djavan, M., "One-Dimensional Vertical Water Infiltration into Layered Soils Under Constant Application Rate," thesis presented to Utah State University, at Logan, Utah, in 1978, in partial fulfillment of the requirements for the degree of Doctor of Philosophy.
8. Edwards, W. M., "Infiltration of Water into Soils as Influenced by Surface Conditions," thesis presented to Iowa State University, at Ames, Iowa, in 1967, in partial fulfillment of the requirements for the degree of Doctor of Philosophy.
9. Edwards, W. M., and Larson, W. E., "Infiltration of Water into Soils as Influenced by Surface Seal Development," *Transactions,* American Society of Agricultural Engineers, Vol. 12, No. 4, 1969, pp. 463–465, 470.
10. Falayi, O., and Bouma, J., "Relationships between the Hydraulic Conductance of Surface Crusts and Soil Management in a Typic Hapludalf," *Proceedings,* Soil Science Society of America, Vol. 93, 1975, pp. 957–963.
11. Green, W. H., and Ampt, G. A., "Studies on Soil Physics—I. The Flow of Air and Water through Soils," *Journal of Agricultural Science,* Vol. 4, 1911, pp. 1–24.
12. Hillel, D., and Gardner, W. R., "Steady Infiltration into Crust-Topped Profiles," *Soil Science,* Vol. 108, No. 2, 1969, pp. 137–142.
13. Hillel, D., and Gardner, W. R., "Transient Infiltration into Crust-Topped Profiles," *Soil Science,* Vol. 109, No. 2, 1970, pp. 69–76.
14. Mannering, J. V., "The Relationship of Some Physical and Chemical Properties of Soils to Surface Sealing," thesis presented to Purdue University, at West Lafayette, Ind., in 1967, in partial fulfillment of the requirements for the degree of Doctor of Philosophy.
15. Mein, R. G., and Farrell, D. A., "Determination of Wetting Front Suction in the Green-Ampt Equation," *Proceedings,* Soil Science Society of America, Vol. 38, 1974, pp. 872–876.
16. Mein, R. G., and Larson, C. L., "Modeling the Infiltration Component of the Rainfall-Runoff Process," *Bulletin 43,* Water Resources Research Center, University of Minnesota, St. Paul, Minn., 1971.
17. Mein, R. G., and Larson, C. L., "Modeling Infiltration During a Steady Rain," *Water Resources Research,* Vol. 9, No. 2, 1973, pp. 384–394.
18. Moore, I. D., Larson, C. L., and Slack, D. C., "Predicting Infiltration and Micro-Relief Surface Storage for Cultivated Soils," *Bulletin 102,* Water Resources Research Center, University of Minnesota, St. Paul, Minn., 1980.
19. Moore, I. D., Larson, C. L., Slack, D. C., Wilson, B. N., Idike, F., and Hirschi, M., "Modeling Infiltration; A Measurable Parameter Approach," *Journal of Agricultural Engineering Research,* 1981.
20. Morel-Seytoux, H. J., and Khanji, J., "Derivation of an Equation of Infiltration," *Water Resources Research,* Vol. 10, No. 4, 1974, pp. 794–800.
21. Morin, J., and Benyamini, Y., "Rainfall Infiltration into Bare Soil," *Water Resources Research,* Vol. 13, No. 5, 1977, pp. 813–817.
22. Philip, J. R., "An Infiltration Equation with Physical Significance," *Soil Science,* Vol. 77, 1954, pp. 152–157.
23. Smith, R. E., and Woolhiser, D. A., "Mathematical Simulation of Infiltrating Watersheds," *Hydrology Paper No. 47,* Colorado State University, Fort Collins, Colo., 1971.
24. Steichen, J. M., Nail, M. E., and Gregory, J. M., "Infiltration Influenced by Tillage—Part I. Experimental Results," presented at the 1979, American Society of Agricultural Engineers-Canadian Society of Agricultural Engineers Summer Meeting, held at Winnipeg, Manitoba, Canada (Paper No. 79-2042).
25. Swartzendruber, D., "Infiltration of Constant-Flux Rainfall into Soils as Analyzed

by the Approach of Green and Ampt," *Soil Science*, Vol. 117, No. 5, 1974, pp. 272–281.
26. Tagaki, S., "Analysis of the Vertical Downward Flow of Water Through a Two-Layered Soil," *Soil Science*, Vol. 90, 1960, pp. 98–103.
27. van Duin, R. H. A., "Tillage in Relation to Rainfall Intensity and Infiltration Capacity of Soils," *Netherlands Journal of Agricultural Science*, The Netherlands, Vol. 3, 1955, pp. 182–191.

Appendix II.—Notation

The following symbols are used in this paper:

a, E, H = constants;
F = infiltration volume;
f = infiltrability;
I = uniform application rate;
K = hydraulic conductivity;
L = distance of wetting front below surface;
q = soil water flux;
S = capillary suction;
S_w = capillary suction at wetting front;
t = time;
t'_s = equivalent time to infiltrate volume, F_s, under ponded surface conditions;
z = vertical distance from soil surface;
$\Delta\theta$ = initial moisture deficit; and
ϕ = hydraulic head.

Subscripts

f = steady state;
i = initial condition;
s = conditions at instant surface ponding begins;
1 = surface soil layer; and
2 = subsoil layer.

JOURNAL OF
THE IRRIGATION
AND DRAINAGE DIVISION

Required Head Loss over Long-Throated Flumes

By Marinus G. Bos[1] and Yvonne Reinink[2]

Introduction

In the management of an irrigation project, it is important that the flow at canal bifurcations be measured accurately, for only in this way can the efficiency of irrigation water use be calculated. Accurate flow measurements are also important in drainage system management since they are the only means of assessing a reliable water balance upon which drainage criteria can be based.

In many irrigation or drainage systems, however, the available energy headloss over a discharge measurement structure is limited. For accurate flow measurement in such channels, the long-throated flume is the most promising structure (2,3) because it can be tailored to fit the stage-discharge curve of the channel in which it is to be placed, it is relatively easy and cheap to construct (2) and, for large flumes, the critical submergence ratio can be as high as 0.95 (1,2,4,5,7).

To obtain more data on this critical submergence ratio, as a function of the degree of downstream expansion, we ran extensive laboratory tests on two trapezoïdal flumes. We also tested the influence of the slope of the entrance transition on the flume calibration.

Description of Model

In a concrete-lined canal section, with bottom width, $b_1 = 0.50$ m, and a side slope of 1 to 1, a trapezoïdal long-throated flume was placed (Fig. 1). The flume-throat was made of polyvinyl chloride (PVC) and had a length, $L = 0.60$ m, width, $b = 0.20$ m, and a side slope ratio of 1 to 1. The bottom

[1] Civ. Engr., Irrigation and Water Management, International Inst. for Land Reclamation (ILRI), Wageningen, The Netherlands.

[2] Formerly Research Asst., International Inst. for Land Reclamation and Improvement, Wageningen, The Netherlands.

Note.—Discussion open until August 1, 1981. To extend the closing date one month, a written request must be filed with the Manager of Technical and Professional Publications, ASCE. Manuscript was submitted for review for possible publication on February 27, 1980. This paper is part of the Journal of the Irrigation and Drainage Division, Proceedings of the American Society of Civil Engineers, ©ASCE, Vol. 107, No. IR1, March, 1981. ISSN 0044-7978/81/0001-0087/$01.00.

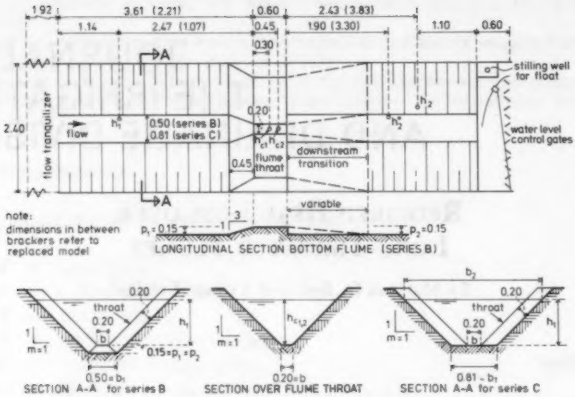

FIG. 1.—Dimensions of Model, in meters, 1 m = 3.2808 ft

of the throat was placed 0.15 m above the bottom of the approach channel so that $p_1 = p_2 = 0.15$ m (Fig. 1).

For individual series of tests, we fitted this throat section with the following entrance and downstream transitions:

1. A concrete entrance transition, the bottom of which converged 1 to 2. The transition of the side slopes started at the same distance upstream of the throat entrance (0.30 m) as did the bottom transition. The sides thus converged 1 to 1.5. Two downstream transitions were fitted to this flume, the angles of divergence being 1:0 (Test A1) and 1:6 (Test A5). We used these tests to test the influence of the short (1:2) entrance transition on the discharge coefficient C_d.
2. As basic flume in the test series B, the entrance transition was changed so that the bottom slope became 1 to 3 (sides 1 to 2.25). This flume was tested with the downstream transitions shown in Table 1. During test B4 we encountered some difficulties with the measurement of a stable tailwater level h_2. To solve this problem, we first placed a pressure tap for h_2 and for test B5 we moved the flume 1.40 m upstream (see Fig. 1).
3. For the C-series, the bottom of the approach and tailwater canals were raised by 0.15 m so that $p_1 = p_2 = 0$. In this series the flat-bottomed flume thus needed no transition on the bottom. The angles of divergence α of the side wall transition are the same as used in the B-series.

Discharge was measured by a magnetic flow meter that was calibrated, before the tests started, against a gaged volumetric tank. This calibration was repeated three times in between the tests. As a result, the error in the measured discharge is less than 1%. Heads were measured by point gages that can be read to the nearest 0.1 mm. Each head given in this paper is the average of five readings.

Head-Discharge Relationship

The head-discharge equation for trapezoïdal long-throated flumes was given by the first author (2,3) as:

$$Q = C_d(by_c + m_c^2)[2g(H_1 - y_c)]^{1/2} \quad \text{. . . . . (1)}$$

in which Q = discharge in cubic meters per second (Q in cubic seconds if United States Customary units are used in the equation); C_d = discharge coefficient (dimensionless); b = bottom width of flume throat, in meters; m = side slope ratio of flume throat, horizontal to vertical; g = acceleration due to gravity, 9.81 m/s^2; H_1 = upstream energy head with respect to bottom of flume throat, in meters; and y_c = critical depth in the flume throat, in meters. The last mentioned is a function of H_1, b, and m. For the tested flumes m = 1; y_c-values can be obtained from Table 2.

The discharge coefficient C_d has a predictable value provided that no separation of flow occurs at the boundary in the entrance transition. With a curved entrance transition, e.g., cylindrical surfaces with sufficiently large radii, flow separation will not occur. Construction costs, however, are lower with a plane surface entrance transition. After a study by Wells and Gotaas (8), it became common

TABLE 1.—Downstream Transitions Test Series B

Variable (1)	Test Number B1 (2)	B2 (3)	B3 (4)	B4 (5)	B5 (6)	B6 (7)
Bottom slope	1:0	1:1	1:2	1:4	1:6	1:10
Side wall slope	1:0	1:0.75	1:1.5	1:3	1:4.5	1:7.5

practice to use transitions of which the convergence of each plane wall does not exceed 1:3 relative to the flume center line.

To check this figure we tested two flumes, A1 and A5, the bottom of which converged 1:2 and the side walls 1:1.5. The C_d-values for these flumes are shown in Fig. 2. Also shown are the C_d-values for two flumes, B_1 and B_5, for which the bottom entrance convergence is 1:3 and side wall convergence 1:2.25, and for one flume, C6, whose flat bottom plus side wall convergence is 1:2.25. For H_1/L-ratios greater than 0.5, the C_d-values of the A-series are about 0.01 less than the C_d-values of the B-series, but equal to the C_d-values of the C6-flume. All C_d-values, however, are well within the range of values derived from literature by the first writer (3). This range, which has a 95% confidence level, is shown in Fig. 2.

On the basis of the aforementioned data, there would seem to be little objection in practice to using plane transitions, provided that the convergence of each wall does not exceed 1:2 relative to the flume center line. A typical flow pattern along the flume boundary is shown in Fig. 3.

If the streamlines at the control section in the flume throat are straight and parallel and the flow is critical, the C_d-value is independent of flow patterns downstream of the throat. For ratio's of H_1/L greater than 0.5, however,

TABLE 2.—Values of Ratio y_c/H_1 as Function of H_1/b for Trapezoïdal Control with 1:1 Side Slope

H_1/b (1)	y_c/H_1 (2)
0.00	0.667
0.01	0.668
0.02	0.670
0.03	0.671
0.04	0.672
0.05	0.674
0.06	0.675
0.07	0.676
0.08	0.678
0.09	0.679
0.10	0.680
0.12	0.684
0.14	0.686
0.16	0.687
0.18	0.690
0.20	0.692
0.22	0.694
0.24	0.696
0.26	0.698
0.28	0.699
0.30	0.701
0.32	0.703
0.34	0.705
0.36	0.706
0.38	0.708
0.40	0.709
0.42	0.711
0.44	0.712
0.46	0.714
0.48	0.715
0.5	0.717
0.6	0.723
0.7	0.728
0.8	0.732
0.9	0.737
1.0	0.740
1.2	0.747
1.4	0.752
1.6	0.756
1.8	0.759
2	0.762
3	0.773
4	0.778
5	0.782
10	0.791
∞	0.800

streamlines become increasingly curved, resulting in slightly increasing C_d-values for higher values of H_1/L. In flat-bottomed flumes, ($p_1 = p_2 = 0$) the discharging jet is supported by the bottom of the downstream transition, and streamline curvature is thus less than in flumes with elevated throats. This difference

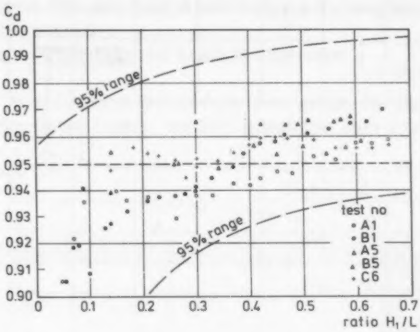

FIG. 2.—C_d-Values as Function of H_1/L and Entrance Transition

FIG. 3.—Typical Flow Pattern Along Flume (A1) boundary, $Q = 0.160\ m^3/s$

in C_d-values is shown in Fig. 4 for H_1/L-values of 0.6. The flare angle of the transition seems to have no significant influence on C_d.

The random distribution of C_d-values for low values of H_1/L (<0.03) can be attributed to viscous effects, to the changing velocity distribution in approach

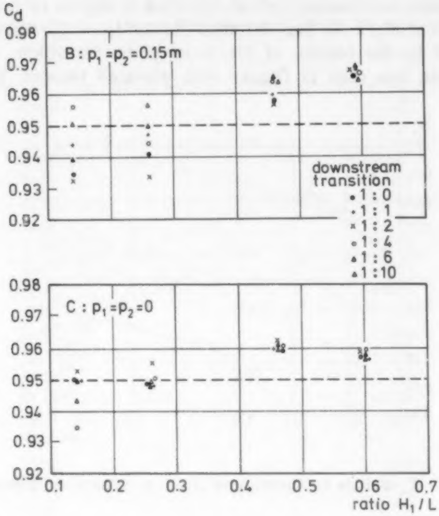

FIG. 4.—C_d-Values as Function of Downstream Transition and H_1/L

canal and flume throat, and to minor errors in the determination of Q and h_1, all of which have a relatively great influence on C_d-values if H_1/L is small.

Modular Limit

If the water level downstream of the flume is sufficiently low, flow at the control section (in the throat) is supercritical and the discharge through the flume, Q, depends on H_1 only. This flow is referred to as free or modular. With rising downstream water level, however, flow at the control section becomes subcritical and Q depends also on the downstream energy head, H_2. The modular limit is defined as the value of the submergence ratio, H_2/H_1, at which the real discharge deviates by 1% from the discharge calculated by the head-discharge equation (Eq. 1). For higher values of H_2/H_1, Eq. 1 must be expanded to read:

$$Q = f C_d (by_c + my_c^2) [2g(H_1 - y_c)]^{1/2} \quad \ldots\ldots\ldots\ldots \quad (2)$$

in which f = drowned flow reduction factor, being less than unity.

Fig. 5 shows a typical curve giving f-values as a function of the submergence ratio. The higher the value of the modular limit, the more the curve will move into the top right corner of this figure. In fact, we do not recommend submerged flumes for measuring discharge and for the following reasons:

1. Errors in the determination of both H_1 and H_2 propagate into H_2/H_1. In the example of Fig. 5, an error of about 3% in the submergence ratio causes

the f-value to vary from 0.82–0.94. In practice the error in H_2/H_1 often exceeds 3%. If in addition the submergence ratio and the modular limit are higher, the f-value is so inaccurate that the true discharge can only be estimated.

2. If a flume is submerged (H_2/H_1 exceeds the modular limit) while the discharge is constant and H_2 rises, the upstream head must rise greatly to allow the discharge to pass. This may lead to overstopping of the upstream embankment unless freeboard is excessive.

3. Determining and handling two heads is expensive.

If a flume is to be designed in the modular flow range, the modular limit must be known. For the tested flumes, we determined this limit firstly by generating

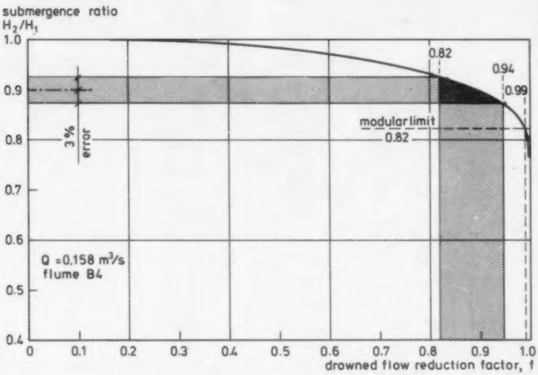

FIG. 5.—Typical Values of Drowned Flow Reduction Factor as Function of Submergence Ratio

a Q-H_1 relationship of a very general from:

$$Q = KH_1^u \qquad (3)$$

in which K = a coefficient depending on the size and the shape of the flume (variable dimension depends on u); and u = a dimensionless power depending on the cross section of the flume throat. And secondly by calculating the head $H_{1(101)}$ at which the calculated discharge deviates by 1% from the actually measured discharge, or:

$$\frac{Q_{(101)}}{Q_{(100)}} = \frac{KH^u_{1(101)}}{KH^u_{1(100)}} \qquad (4)$$

$$H^u_{1(101)} = 1.01\, H^u_{1(100)} \qquad (5)$$

$$u \log H_{1(101)} = \log 1.01 \times H^u_{1(100)} \qquad (6)$$

From this equation we calculated $H_{1(101)}$, and $h_{1(101)} = H_{1(101)} - v_1^2/2g$.

For each flume we set the measured discharge at 0.010 m³/s, 0.030 m³/s, 0.090 m³/s, and 0.160 m³/s, and raised the downstream water level stepwise.

TABLE 3.—Modular Limits and Energy Losses for Tested Flumes as Function of Discharge, in meters

Tested flume (1)	Data (2)	Discharge, in cubic meters per second 0.010 (3)	0.030 (4)	0.090 (5)	0.160 (6)
B1	h_2/h_1	0.7564	0.8288	0.7885	0.7075
B1	H_2/H_1	0.7615	0.8353	0.8006	0.7293
B1	ΔH	0.0203	0.0253	0.0549	0.0963
B2	h_2/h_1	0.7758	0.8178	0.7987	0.7020
B2	H_2/H_1	0.7812	0.8242	0.8104	0.7241
B2	ΔH	0.0184	0.0269	0.0522	0.0981
B3	h_2/h_1	0.7927	0.8292	0.8023	0.7183
B3	H_2/H_1	0.7980	0.8354	0.8138	0.7391
B3	ΔH	0.0171	0.0253	0.0513	0.0927
B4	h_2/h_1	0.8176	0.8548	0.8136	0.7717
B4	H_2/H_1	0.8230	0.8607	0.8246	0.7901
B4	ΔH	0.0148	0.0214	0.0483	0.0745
B5	h_2/h_1	0.8145	0.8567	0.8503	0.8216
B5	H_2/H_1	0.8218	0.8629	0.8599	0.8355
B5	ΔH	0.0152	0.0211	0.0385	0.0584
B6	h_2/h_1	0.8361	0.8757	0.8705	0.8416
B6	H_2/H_1	0.8414	0.8874	0.8796	0.8543
B6	ΔH	0.0135	0.0173	0.0331	0.0519
C1	h_2/h_1	0.7730	0.8087	0.8906	0.8309
C1	H_2/H_1	0.7873	0.8232	0.9030	0.8519
C1	ΔH	0.0184	0.0275	0.0268	0.0531
C2	h_2/h_1	0.7860	0.8222	0.8855	0.8333
C2	H_2/H_1	0.7991	0.8367	0.8983	0.8537
C2	ΔH	0.0173	0.0254	0.0281	0.0525
C3	h_2/h_1	0.7937	0.8390	0.8739	0.8301
C3	H_2/H_1	0.8068	0.8527	0.8880	0.8509
C3	ΔH	0.0166	0.0228	0.0309	0.0533
C4	h_2/h_1	0.8113	0.8497	0.8689	0.8402
C4	H_2/H_1	0.8231	0.8620	0.8850	0.8602
C4	ΔH	0.0152	0.0231	0.0321	0.0501
C5	h_2/h_1	0.8271	0.8702	0.8528	0.8654
C5	H_2/H_1	0.8388	0.8812	0.8690	0.8824
C5	ΔH	0.0138	0.0183	0.0360	0.0421
C6	h_2/h_1	0.8436	0.8901	0.8642	0.8827
C6	H_2/H_1	0.8541	0.9002	0.8790	0.8978
C6	ΔH	0.0124	0.0154	0.0334	0.0366

Note: 1 m^3/s = 35.3145 sec-ft, and 1 m = 3.2808 ft. With flumes B1, B2, and B3 the h_2-value was measured at 1.90 m downstream of the throat. For flume B4 this value was 2.43 m and for the other flumes 3.83 m (see Fig. 1).

Upon stabilization of the flow pattern we measured all heads and found $h_{1(101)}$ and the matching h_2. Table 3 lists the modular limits for each flume and discharge in terms of both water levels, h_2/h_1 and energy heads, H_2/H_1.

Whether flow through the flume is modular or submerged can usually be seen from the way the jet leaves the flume throat. For modular flow the flow pattern is almost symmetrical with respect to the center line of the flume. If the flume is submerged, the jet moves either to the right or to the left, as shown in Fig. 6. The side to which the jet moves can easily be influenced by disturbing or changing the flow pattern in the approach channel to the flume.

FIG. 6.—Here Jet has Moved to Left; Flume is Submerged

With submerged flumes in earthen channels, this unstable jet can erode the side slopes.

Estimating Modular Limit

As can be seen from Table 3, the modular limit for the tested trapezoïdal flume throat varies from about 0.70–0.90. Some general conclusions that can be drawn from this table are:

1. Downstream transitions with a ratio of expansion of 1:1, 1:2, and (to some extent) 1:4, raise the modular limit only slightly.
2. Flat bottomed flumes, because of less streamline curvature, have a higher modular limit than flumes with elevated throats.
3. For the higher discharge range the modular limit is improved considerably for flumes B3–B6. For flat-bottom flumes (C3–C6) the modular limit varies only from 0.85–0.90. This is because most of the energy is lost in the eddy

between the jet from the throat and the bottom of the expansion. If this jet does not separate from the bottom (B5, B6, and C-flumes) this single most important cause of energy losses does not exist.

Although the aforementioned conclusions give some support in estimating the modular limit of a (trapezoïdal) long-throated flume, we still needed a generally applicable method of estimating the modular limit, and thus the energy head loss over a flume. In our search for such a method, we divided the loss of (energy) head into: (1) The head loss between the upstream head measurement section and the control section in the flume throat; (2) the losses due to friction between the control section and the downstream head measurement section; and (3) the losses due to energy conversion over the downstream transition.

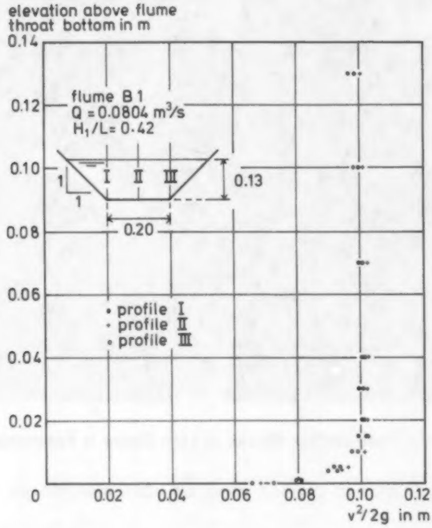

FIG. 7.—Velocity Profiles in Flume Throat in Section at h_{c2}, 1 m = 3.2808 ft

Ad (1).—The energy losses over the section upstream of the control were given by the first writer (2) as

$$H_1 - H_c = H_1(1 - C_d^{1/u}) \quad (7)$$

in which

$$H_c = \beta y_c + \frac{\alpha v_c^2}{2g} \quad (8)$$

for the control section in which flow is critical. In Eq. 8: α = the energy coefficient that takes into account the nonuniform distribution of velocities across the section; and β = a coefficient depending on the mean curvature of the stream lines, and thus on the pressure distribution. The y_c-value can be calculated by using Table 2, after which v_c can be derived from the measured discharge.

For values of $H_1/L <$ about 0.4, the streamlines at the control section are straight and the velocity distribution is uniform, as is shown in Fig. 7. Thus, it may be assumed that $\alpha = 1$ and $\beta = 1$. Eq. 7 then gives a good estimate of the energy head loss upstream of the control section, as is shown in Fig. 8. If the ratio, H_1/L, increases, streamlines at the control section become increasingly curved, thereby influencing the values of α, β, and C_d. However, within the limits of application of H_1/L for long-throated flumes (2), $0.1 < H_1/L < 1.0$, Eq. 7 gives a good estimate of the energy head loss upstream of the control section.

Ad (2).—Although flow is nonuniform in the downstream transition, we calculated the energy losses due to friction by applying the equation of Manning to three reaches: (1) Reach of the flume throat downstream of the control

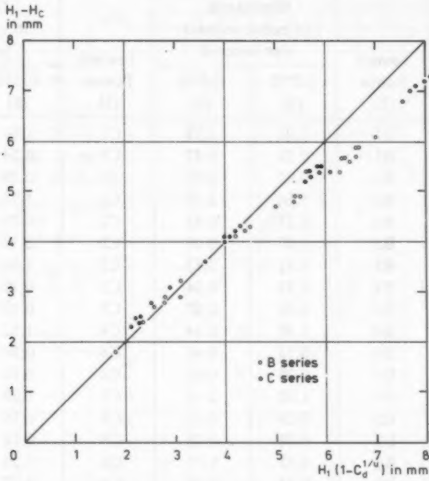

FIG. 8.—Energy Losses over Entrance Transition. (1 mm = 0.03937 in.)

section, which approximates (1/3) $L = 0.20$ m; (2) length of reach of the actual transition of (bottom and) side walls; and (3) length of canal reach from transition to measurement section of h_2. (In our calculations, we used values of $n = 0.011$ for PVC, $n = 0.013$ for plywood, and $n = 0.015$ for concrete.)

The total energy loss due to friction, ΔH_f, between the control section and the section where h_2 is measured then equals the sum of the losses over the three reaches, or:

$$\Delta H_f = \Delta H_{\text{throat}} + \Delta H_{\text{trans}} + \Delta H_{\text{canal}} \quad (9)$$

Table 4 lists the calculated values of ΔH_f, together with values of ΔH and of H_1-H_c.

As can be seen in Table 4, the energy loss due to friction, $H_1 - H_c + \Delta H_f$, expressed as a percentage of the total energy loss over the flume, ΔH, increases

with increasing length of the downstream transition. For a flat-bottomed flume with 1:10 transition (C6), this percentage is already larger than 35. Because of the relatively high flow velocities in the transition, the percentage of energy loss due to friction is larger in a flat-bottomed flume (C-series) than in a flume with an elevated throat (B-series). In the latter type, a gradual expansion can thus save more energy.

Ad (3).—The losses due to energy conversion over the downstream transition are assumed to equal the total energy losses minus all losses due to friction.

TABLE 4.—Energy Losses over Flumes Flowing at their Modular Limit, in centimeters

Given data per row, in centimeters (1)	Tested flume (2)	Discharge, in cubic meters per second		Tested flume (5)	Discharge, in cubic meters per second	
		0.010 (3)	0.030 (4)		0.010 (6)	0.030 (7)
$\Delta H = H_1 - H_2$	B1	2.03	2.53	C1	1.84	2.75
$H_1 - H_c$	B1	0.29	0.47	C1	0.24	0.42
ΔH_f	B1	0.07	0.07	C1	0.19	0.18
ΔH	B2	1.84	2.69	C2	1.73	2.54
$H_1 - H_c$	B2	0.27	0.43	C2	0.25	0.43
ΔH_f	B2	0.07	0.07	C2	0.19	0.18
ΔH	B3	1.71	2.53	C3	1.66	2.28
$H_1 - H_c$	B3	0.32	0.54	C3	0.23	0.36
ΔH_f	B3	0.07	0.07	C3	0.19	0.18
ΔH	B4	1.48	2.14	C4	1.52	2.31
$H_1 - H_c$	B4	0.18	0.46	C4	0.31	0.40
ΔH_f	B4	0.08	0.08	C4	0.18	0.18
ΔH	B5	1.52	2.11	C5	1.38	1.83
$H_1 - H_c$	B5	0.29	0.41	C5	0.25	0.41
ΔH_f	B5	0.08	0.08	C5	0.18	0.17
ΔH	B6	1.35	1.73	C6	1.24	1.54
$H_1 - H_c$	B6	0.24	0.28	C6	0.27	0.41
ΔH_f	B6	0.08	0.09	C6	0.17	0.16

Note: 1 m^3/s = 35.3145 sec-ft, 1 cm = 0.032808 ft.

These losses were analyzed with the generally known equation:

$$H_c - H_2 - \Delta H_f = \xi \frac{(v_c - v_2)^2}{2g} \quad (10)$$

in which ξ = the energy loss coefficient, a function of the angle of expansion of the downstream transition; v_c = average velocity in that section of the throat where flow is critical; and v_2 = average velocity in the section in which h_2 is measured.

We calculated values of ξ for each flume and plotted them in Fig. 9 as a function of the angle of expansion of the transition. As expected, the ξ-values decrease with decreasing angle of expansion. They are, however, well above

the values of Formica (6) for transitions with subcritical flow both upstream and downstream of the expansion.

International literature contains few data that allow the total energy loss over flumes to be analyzed and ξ-values to be calculated. We could, however, use data from Blau (1), Engel (4), Inglis (7), and Fane (5). The ξ-values we obtained in this way are shown in Fig. 9. They correspond reasonably with the ξ-values for the series B and C.

To estimate the energy losses due to conversion of kinetic into potential energy over the downstream transition, we recommend the use of the envelope of Fig. 9 to find on ξ-value for use in Eq. 10.

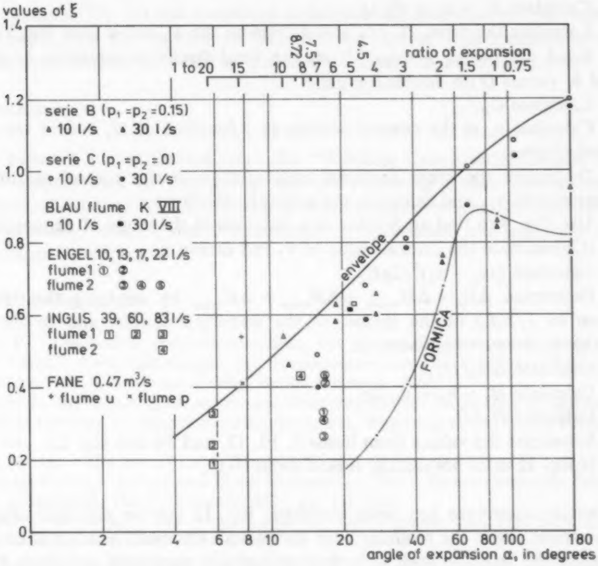

FIG. 9.—Values of ξ as Function of Angle of Divergence of Downstream Transition

The total energy loss over the flume at the modular limit can now be calculated by adding Eq. 7, 9, and 10, which yields:

$$H_1 - H_2 = H_1 - H_1 C_d^{1/u} + \Delta H_f + \frac{\xi(v_c - v_2)^2}{2g} \qquad (11)$$

The modular limit can be found by dividing both sides of this equation by H_1, giving:

$$\frac{H_2}{H_1} = C_d^{1/u} - \frac{\Delta H_f}{H_1} - \frac{\xi(v_c - v_2)^2}{2gH_1} \qquad (12)$$

Eq. 12 is a general expression for the modular limit of any long-throated flume and can also be used for the, hydraulically similar, broad-crested weir.

Procedure to Estimate Modular Limit

To find the modular limit of a flume discharging Q at an upstream head, h_1, both sides of Eq. 12 have to be equalized by trial and error. The procedure is as follows:

1. Determine the cross-sectional area of flow at the station where h_1 is measured, and calculate the average velocity, v_1.
2. Calculate $H_1 = h_1 + v_1^2/2g$.
3. Calculate the ratio, H_1/L, and determine the C_d-value (see Fig. 2).
4. Read the power u direct from the head-discharge equation or from a plot of h_1 versus Q on double-log paper.
5. Calculate $C_d^{1/u}$.
6. Calculate y_c at the control section as a function of H_1 and of the throat size and shape.
7. Determine the cross sectional area of flow at the control section with the waterdepth, y_c, and calculate the average velocity v_c.
8. Use Fig. 9 to find an ξ-value as a function of the angle of expansion.
9. (Gu)estimate the critical value of h_2 and derive v_2.
10. Calculate $\xi(v_c - v_2)^2/2gH_1$.
11. Determine $\Delta H_f = \Delta H_{throat} + \Delta H_{trans} + \Delta H_{canal}$ by applying the Manning equation to $1/3(L)$ of the throat, to the transition length, and to the canal up to the h_2 measurement section.
12. Calculate $\Delta H_f/H_1$.
13. Calculate $H_2 = h_2 + v_2^2/2g$.
14. Calculate H_2/H_1.
15. Substitute the values from items 5, 10, 12, and 14 into Eq. 12.
16. If Eq. 12 does not match, repeat items 9–15.

Once some experience has been acquired, Eq. 12 can be matched after two or three trials. Since the modular limit varies with upstream head, it is advisable to estimate the modular limit at both minimum and maximum anticipated heads and to check if sufficient head loss, $H_1 - H_2$ is available in both cases.

Conclusions

Long-throated flumes with a prismatic throat cross section are very suitable for the accurate measurement of flows in irrigation and drainage canals. These flumes can be tailored to fit almost any range of discharge while the head loss they require over the flume to ensure modular flow is less than that of all other known structures (2).

Extensive laboratory tests on the influence of the upstream and downstream transition on the value of the discharge coefficient have shown that upstream a plane transition can be used, provides the convergence of each wall does not exceed 1:2 relative to the flume center line. An analysis of modular limit values and energy losses for the tested flumes shows that:

1. Downstream transitions with a ratio of expansion of 1:1, 1:2, and 1:4 raise the modular limit only slightly.
2. Flat-bottomed flumes, because of less streamline curvature, have a higher modular limit than flumes with an elevated throat.
3. Because most energy is lost beneath the jet separating downstream of the elevated throat, and because the energy losses due to friction in a flat-bottomed flume may approach 40% of the total energy loss, a downstream transition, ratio 1:6, for a flume with elevated throat improves the modular limit significantly. Downstream of a flat-bottomed flume an expansion only slightly improves the modular limit.

The equation (Eq. 12) and procedure to estimate the modular limit, as presented in this paper, can be used for all long-throated flumes with a prismatic throat cross section, and also for the, hydraulically similar, broad-crested weir.

Acknowledgments

This paper is a contribution from the "Working Group on Hydraulic Structures." Represented in this group are the following Dutch institutions: (1) International Institute for Land Reclamation and Improvement; (2) Delft Hydraulics Laboratory; and (3) the Departments of Hydraulics and Irrigation of the Agricultural University.

Appendix I.—References

1. Blau, E., "Die modellmässige Untersuchung von Venturi Kanälen verschiedener Grösse und Form," *Veröffentlichungen der Forschungsanstalt für Schiffahrt,* Wasser und Grundbau, Nr. 8, Akademie Verlag, Berlin, Germany, 1960.
2. Bos, M. G., ed., *Discharge Measurement Structures,* 2nd ed., Publication 20, International Institute for Land Reclamation and Improvement, Wageningen, The Netherlands, 1978, pp. 464.
3. Bos, M. G., "The use of Long-Throated Flumes to Measure Flows in Irrigation and Drainage Canals," *Agricultural Water Management,* No. 1, Elsevier Scientific Publishing Co., Amsterdam, The Netherlands, 1977, pp. 111–126.
4. Engel, F. V. A. E., "The Venturi Flume," *The Engineer,* No. 158, 1934, London, England, Aug. 3, pp. 104–107 and, Aug. 10, pp. 131–133.
5. Fane, A. G. C., "Report on Flume Experiments on Sirhind Canal," *Paper No. 110,* Punjab Engineering Congress, Punjab Irrigation Branch, 1927.
6. Formica, G., "Esperienze Preliminari sulle Perdite di Carico nei Canali Dovute a Cambiamenti di Sezione," *L'Energia Electrica,* Vol. 32, No. 7, Milano, Italy, July, 1955, pp. 554–568.
7. Inglis, G. C., "Notes on Standing Wave Flumes and Flume Meter Falls," *Technical Paper No. 15,* Public Works Department, Bombay, India, 1929.
8. Wells, E. A., and Gotaas, H. B., "Design of Venturi Flumes in Circular Conduits," *Journal of the Sanitary Engineering Division,* ASCE, Vol. 82, No. SA2, Proc. Paper 928, Apr., 1956, pp. 1–34.

Appendix II.—Notation

The following symbols are used in this paper:

A = cross-sectional area of flow (L^2);
B = water surface width (L);

b = bottom width (L);
C_d = discharge coefficient (dimensionless);
f = drowned flow reduction factor (dimensionless);
g = acceleration due to gravity (LT^{-2});
H = total energy head with respect to throat level (L);
h = piezometric head with respect to throat level (L);
K = coefficient;
L = length of throat in direction of flow (L);
m = side slope ratio, horizontal to vertical (dimensionless);
p = height of bottom hump (L);
Q = discharge (L^3T^{-1});
u = power of head (dimensionless);
v = average flow velocity (LT^{-1});
y = water depth (L);
α = angle of divergence in degrees; velocity distribution coefficient (dimensionless);
β = pressure distribution coefficient (dimensionless);
ΔH = total energy loss over flume (L);
ΔH_f = energy loss due to friction downstream of control (L); and
ξ = energy loss coefficient (dimensionless).

Subscripts

c = critical flow conditions;
1 = head measurement section; and
2 = downstream section.

JOURNAL OF
THE IRRIGATION
AND DRAINAGE DIVISION

DISCUSSION

Note.—This paper is part of the Journal of the Irrigation and Drainage Division, Proceedings of the American Society of Civil Engineers, ©ASCE, Vol. 107, No. IR1, March, 1981. ISSN 0044-7978/81/0001-0105/$01.00.

DISCUSSIONS

Discussions may be submitted on any Proceedings paper or technical note published in any *Journal* or on any paper presented at any Specialty Conference or other meeting, the *Proceedings* of which have been published by ASCE. Discussion of a paper/technical note is open to anyone who has significant comments or questions regarding the content of the paper/technical note. Discussions are accepted for a period of 4 months following the date of publication of a paper/technical note and they should be sent to the Manager of Technical and Professional Publications, ASCE, 345 East 47th Street, New York, N.Y. 10017. The discussion period may be extended by a written request from a discusser.

The original and three copies of the Discussion should be submitted on 8-1/2-in. (220-mm) by 11-in. (280-mm) white bond paper, typed double-spaced with wide margins. The length of a Discussion is restricted to two *Journal* pages (about four typewritten double-spaced pages of manuscript including figures and tables); the editors will delete matter extraneous to the subject under discussion. If a Discussion is over two pages long it will be returned for shortening. All Discussions will be reviewed by the editors and the Division's or Council's Publications Committees. In some cases, Discussions will be returned to discussers for rewriting, or they may be encouraged to submit a paper or technical note rather than a Discussion.

Standards for Discussions are the same as those for Proceedings Papers. A Discussion is subject to rejection if it contains matter readily found elsewhere, advocates special interests, is carelessly prepared, controverts established fact, is purely speculative, introduces personalities, or is foreign to the purposes of the Society. All Discussions should be written in the third person, and the discusser should use the term "the writer" when referring to himself. The author of the original paper/technical note is referred to as "the author."

Discussions have a specific format. The title of the original paper/technical note appears at the top of the first page with a superscript that corresponds to a footnote indicating the month, year, author(s), and number of the original paper/technical note. The discusser's full name should be indicated below the title (see Discussions herein as an example) together with his ASCE membership grade (if applicable).

The discusser's title, company affiliation, and business address should appear on the first page of the manuscript, along with the *Proceedings* paper number of the original paper/technical note, the date and name of the *Journal* in which it appeared, and the original author's name.

Note that the discusser's identification footnote should follow consecutively from the original paper/technical note. If the paper/technical note under discussion contained footnote numbers 1 and 2, the first Discussion would begin with footnote 3, and subsequent Discussions would continue in sequence.

Figures supplied by the discusser should be designated by letters, starting with A. This also applies separately to tables and references. In referring to a figure, table, or reference that appeared in the original paper/technical note use the same number used in the original.

It is suggested that potential discussers request a copy of the *ASCE Authors' Guide to the Publications of ASCE* for more detailed information on preparation and submission of manuscripts.

STORAGE COEFFICIENTS FROM GROUND-WATER MAPS[a]

Closure by Brij M. Sahni[5] and Harbhajan S. Seth[6]

The writers would like to thank Jones and Soliman for their valuable comments. The discussers are in general agreement with the writers with regard to the practical utility and potential of the method which uses readily obtainable data without incurring extra time and cost in drilling observation wells for preliminary assessment of aquifer parameters. The basic principle in writing the flow equation in a simplified form in Refs. 4 and 8 is essentially the same as used by the writers, namely, reducing the differential equation to a simple finite difference algebraic equation. However, it was the intent of the writers to emphasize the assumptions involved first in writing a general flow equation

$$\nabla \cdot (\rho k \nabla h) = S_s \rho \frac{\partial h}{\partial t} \quad (9)$$

in which S_s = specific storage coefficient, as

$$\nabla^2 h = \frac{S}{T} \frac{\partial h}{\partial t} \quad (10)$$

and then in reducing it to Eq. 2 and finally, in arriving at the finite difference, Eq. 4.

It is important to appreciate the restrictions imposed by each of the mathematical steps involved for, as discussed at length by the writers, the practical utility and validity of the method is dependent to a great extent on whether or not all these restrictions are satisfied within acceptable limits in a given field situation. For instance, on page 161, the discusser, Soliman, states that

> Flow through aquifers may be considered a two-dimensional problem when the aquifer thickness is nearly uniform. For an aquifer strip of finite width, along a flow path, the piezometric head fluctuation, h, can be considered as a function of distance x and time t

It should be noted here that even under these conditions stated by Soliman the flow may not be unidirectional, for instance, as also discussed in the original paper, at points close to any natural or artificial sources and sinks.

---

[a]June, 1979, by Brij M. Sahni and Harbhajan S. Seth (Proc. Paper 14658).

[5]Postdoctoral Fellow, Dept. of Irrigation Water Management, International Rice Research Inst., P.O. Box 933, Manila, Philippines.

[6]Prof. and Head, Dept. of Civ. Engrg., G. B. Pant Univ. of Agr. & Tech., Pantnagar, India.

It is also important to note that in Eq. 7 of Soliman's discussion, S and T cannot and should not be always taken as constants. For example, even if the aquifer thickness were uniform, the lithology of the aquifer material may change, or the aquifer nature may change from a nonleaky artesian to a leaky one within a certain distance. In the latter case the flow in the aquifer is augmented by vertical leakage through other strata. Under these conditions neither S and T may be constants nor the assumption of unidirectional flow of Eq. 6 of Soliman would be valid. Such situations in the field are not uncommon.

Development of Eq. 4 by the writers clearly brings out the limitations imposed on the choice of finite space and time elements Δs and Δt. A judicious choice of these parameters based on *actual* observations rather than on guessing is very essential for the success of determination of S using groundwater maps. Soliman (4) recommends a water level record from a *single* well and ground-water piezometric map drawn from a *single* set of observations. Though a continuous record of ground water level at *a* point would give more details regarding fluctuations at *that* point, it cannot help verify whether Δs and Δt chosen for calculation of $\Delta I/\Delta s$ and $\Delta h/\Delta t$ do meet the requirements for validity of Eq. 4 or Eq. 8. The four piezometric contour maps drawn by the writers for the same study area for four different dates (Fig. 4) clearly show that it is not justified to assume $\Delta h/\Delta t$ over an *arbitrarily chosen* Δx to be the same as that observed at one single point as was done in Soliman's study. On the other hand, following the procedure described in steps 2 and 3 by the writers (p. 207) it is possible to make judicious selection of the finite difference values of s and t to meet the requirements of Eq. 4 as closely as desired.

Ideally, if the resources available permit automatic recorder readings at a number of points scattered over the study area, more detailed data could be obtained making possible even preparation of daily piezometric contour maps. However, where that is not possible and the observations have to be made manually at a large number of points spread over an extensive area, a weekly or semiweekly (or more frequent, depending on the manhours available) collection of piezometric data would be adequate. But one ground-water map prepared from one-time observations and thereafter observing fluctuations of ground water level only at a single point to obtain $\Delta h/\Delta t$ for the entire area as proposed by Soliman is certainly not appropriate.

Errata.—The following corrections should be made to the original paper:

Page 209, paragraph 2, subheading: Should read **Case I (Fig. 3*a*)** instead of **Case I (Fig. 3)**

Page 211, paragraph 1, subheading: Should read **Case II (Fig. 3*b*)** instead of **Case II (Fig. 4)**

Crop Response Information for Water Institutions[a]

Closure by Gary D. Lynne[6] and Roy R. Carriker[7]

The discussion by Hatchett, Stevens, and Vaux on the original paper expresses concern that the writers misunderstand the economic concept of scarcity, that the writers fail to appreciate difficulties associated with development and use of crop response information, and that the writers advocate emulation of markets by government agencies "when markets themselves can accomplish the job." However, these concerns are not substantiated, either by the intent of the writers or by the content of the article.

The need to distinguish "scarcity" and "shortage," as expressed by the discussers reflects primarily a semantic difficulty. "Shortage" need not be temporary, self-correcting, or relevant only in the context of markets. Nonmarket mechanisms for resource allocation do exist, and shortages can occur and persist in the context of the nonmarket allocation of resources. In any case, ". . . existing terms of trade . . ." need not carry short-term or long-term connotations, and need not presume a particular form of organization for resource allocation. The relevant point is that a decision framework of some kind is needed whenever resources are limited, demands appear unlimited, and choice is necessary. Making an issue of the definition of scarcity, and the need to distinguish "shortage" as a separate concept, invites protracted debate over a point which is not at all crucial to the subject of the article or to the context within which the subject of scarcity is raised.

Estimation of water demand functions is costly and complex. The discussers emphasize this point and provide a useful clarification of the manner in which r_{wid} in Eq. 2, is derived. This process for calculating the MVP of water is appropriate for short-run planning horizons (wherein all inputs but water are invariant) and competitive market conditions. The long run marginal value of irrigation water, as depicted by r_{wid} in Eq. 1, is not simply $P_y(\partial Y/\partial W)$, however. Rather, r_{wid} in Eq. 1 represents the marginal value of irrigation water as all other inputs and water are varied simultaneously along the long-run, optimal expansion path. The discussers' description of $r_{wid} = P_y(\partial Y/\partial W)$ is strictly correct only for Eq. 2.

The term r_{wid} is referred to advisedly as ". . . marginal ability to pay . . .," and not as "marginal willingness to pay," since the demand for irrigation water is a derived demand—derived from the demand for the products of irrigated agriculture. "Marginal willingness to pay" is more appropriate with reference to measures of the utility-based demand of consumers.

The discussers assert that crop response information is difficult and costly

---

[a]September, 1979, by Gary D. Lynne and Roy R. Carriker (Proc. Paper 14814).

[6]Assoc. Prof., Food and Resource Economics Dept., G099 McCarty Hall, Inst. of Food and Agricultural Sci., Univ. of Florida, Gainesville, Fla. 32611.

[7]Asst. Prof., Food and Resource Economics Dept., G099 McCarty Hall, Inst. of Food and Agricultural Sci., Univ. of Florida, Gainesville, Fla. 32611.

to obtain, and that water allocation institutions are unlikely to have the budget and expertise to acquire such data. To this extent the discussers apparently concur with points made by the writers.

The "comparability" of the marginal value of water for irrigation to other values requires some clarification. The intended message was that estimates of net value for irrigation water could be compared with estimates of net value in other uses. If there were a highly competitive market for water, the net marginal values would be equal.

The institutional setting does affect water demand. The effects of price support programs would be reflected in the demand models through higher levels of product price (p in Eqs. 1 and 2). Restrictions on production practices would affect the level of, and nature of, the inputs used and the character of the underlying production functions. Restrictions on crop type simply eliminate some of the possible water demand functions. All of these refinements can be handled within the conceptual framework provided by the writers.

It is difficult to develop an ". . . abiding faith in the ability of government agencies to emulate markets administratively." Certainly, nothing in the article should be construed as such. However, administrative water law is a reality in Florida. The purpose of the article, as stated in the introduction, was to outline a conceptual basis for integrating crop-water response information into the decision-making process for water allocation with particular reference to the Florida system. That system does not currently involve any form of transferable water right.

The Model Water Code (29), which served as the model for the Florida Water Resources Act of 1972 (57), has been thoughtfully critiqued elsewhere (see, e.g., Ref. 62). Alternative approaches to allocation was the subject of two articles by Kiker and Lynne (58,59), and included discussions of market approaches as well as other approaches to water allocation. A thorough discussion of the subject must await another forum. Three points are worth noting, however. First, evaluation of alternative institutional forms, be they market, nonmarket, or some other form, requires some concept of what institutions are supposed to achieve and some criterion for evaluation. Proposals for market solutions, as well as other proposals, must be subjected to this criterion. Analytical approaches to institutional design are the subject of several interesting articles [see, e.g., Ciriacy-Wantrup (56), Schmid (61), Randall (60), and Bromley (55)]. Second, the likelihood that a particular institutional alternative can be adopted depends upon how that alternative is assessed by those who are empowered to effect institutional change. The socio-political climate may be such that markets will never be allowed and used for the allocation of water, not withstanding the elegance of market approaches to resource allocation and the fact that regulatory approaches entail a ". . . costly and unnecessary burden" to develop value information. Finally, even if some form of market for water or water rights were designed and implemented, the importance of ". . . taking care in each case to protect third parties and nonefficiency objectives . . ." will still leave unresolved questions about how much the public sector should pay to protect third party interests, or about the level at which such interests should be supported. These demand elements are real, even if they cannot be reflected in the market. Thus, the writers see a role for both market and nonmarket institutions in water management and allocation.

Appendix.—References

55. Bromley, D. W., "On Appraising Environmental Institutions: Comment," *American Journal of Agricultural Economics,* Vol. 56, No. 4, Nov., 1974, pp. 819–822.
56. Ciriacy-Wantrup, S. V., "Water Policy and Economic Optimizing: Some Conceptual Problems in Water Research," *American Economic Review,* Vol. 57, No. 2, May, 1967, pp. 179–189.
57. *Fla. Stat.*, ch. 373.013 et. seq., 1975.
58. Kiker, C., and Lynne, G. D., "Water Allocation Under Administrative Regulation: Some Economic Considerations," *Southern Journal of Agricultural Economics,* Vol. 8, No. 2, Dec., 1976, pp. 57–63.
59. Kiker, C., and Lynne, G. D., "Economic Impacts of Administrative Water Law Systems," *Transactions, of the American Society of Agricultural Engineers,* Vol. 22, No. 1, 1979, pp. 115–129.
60. Randall, A., "On Appraising Environmental Institutions: Comment," *American Journal of Agricultural Economics,* Vol. 56, No. 4, Nov., 1974, pp. 823–825.
61. Schmid, A. Allan, "Analytical Institutional Economics: Challenging Problems in the Economics of Resources for a New Environment," *American Journal of Agricultural Economics,* Vol. 54, No. 5, Dec., 1972, pp. 893–901.
62. Trelease, Frank J., "The Model Water Code, the Wise Administrator, and the Goddam Bureaucrat," *Natural Resources Journal,* Vol. 14, No. 2, Apr., 1974, pp. 207–229.

Modeling Rill Density[a]

Discussion by George R. Foster[4] and Leonard J. Lane, A. M. ASCE[5]

The authors contributed to rill erosion modeling for agricultural land by applying concepts from channel morphology and sediment transport theory for noncohesive channels. This discussion describes the writers' analysis of field measurements of rill erosion on agricultural lands.

The authors assumed that agricultural soils are noncohesive when they suggested that critical shear stress for agricultural soils could be estimated from Shields criterion (4). However, this estimate of critical shear stress for erosion of agricultural soils is much too small, as the writers will show from analysis of field data (7). Critical shear stress was obtained (Fig. 2) from these data by plotting observed erosion rate versus shear stress estimated from observed data for discharge, velocity, slope, and unreported measured cross-sectional elevations. Hydraulic geometry from these data and data from a similar study (6) are described by:

$$R_o = 0.50\, A_o^{0.64} \quad \quad (23)$$

in which R_o = hydraulic radius, in feet; and A_o = flow area, in square feet. An estimate of critical shear stress from Fig. 2 is 0.06 psf.

---

[a]March, 1980, by Ruh-Ming Li, Victor Miguel Ponce, and Daryl B. Simons (Proc. Paper 15230).

[4]Hydr. Engr., U.S. Dept. of Agr., Science and Education Administration, Agricultural Research, Dept. of Agricultural Engrg., Purdue Univ., Lafayette, Ind.

[5]Hydro., U.S. Dept. of Agr., Science and Education Administration, Agricultural Research, Western Region, Southwest Watershed Research Center, 442 E. Seventh St., Tucson, Ariz. 85705.

Critical shear stress from the Shields criterion is plotted as a function of D_{84} (Fig. 3), assuming a shear velocity of 0.23 fps [corresponding to the second level discharge of Meyer, et al. (7) study], and a specific gravity of 2.65 for sediment particles. Meyer, et al. (7) observed that aggregates greater than 1 mm accounted for 14% of the sediment coming from the rills (7). From Fig. 3, 1 mm for D_{84} gives a critical shear stress of 0.013 psf, significantly less than the observed value of 0.06 psf. The actual D_{84} of the soil was much smaller, which gives an even smaller critical shear stress from the Shields criterion. Therefore, the Shields criterion using D_{84} for primary particles making up tilled agricultural soils like Russell silt loam significantly underestimates critical shear stress for rill erosion. The Shields criterion has proven satisfactory for estimating critical shear stress for transport of aggregates (specific gravity of approx 1.8) and primary particles (specific gravity of 2.65) by flow in rills (5).

Many agricultural soils do not armor. Certainly those studied by Meyer, et

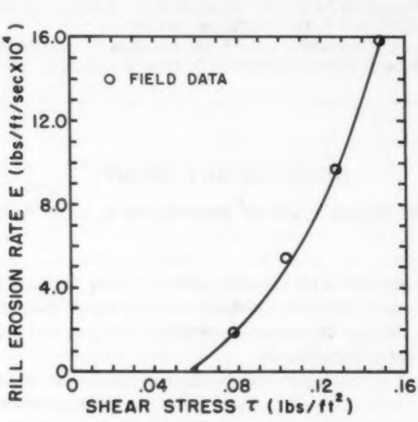

FIG. 2.—Erosion Rate in Rills on Tilled Agricultural Soil, Russell Silt Loam, as Function of Shear Stress of Flow; Data from Ref. 7

al. (3,7) did not armor during their tests. The shear stress required to detach particles is greater than the shear stress required to transport coarse sand that might armor these soils. Usually not enough gravel is available in many highly productive midwestern soils to armor during an annual cropping cycle. Land in cultivated agriculture is usually tilled for seedbed preparation, and sometimes for weed control at least once each year. Tillage buries most of the armor of coarse particles. If armoring does occur, more than a year is usually needed for a complete armor to develop.

Tillage may be the single most important factor related to critical shear stress and rill erosion. Foster (5) measured rill erosion on a cropland soil that had consolidated and had not been tilled for a year. The soil was tilled and the measurements repeated. Rill erosion following tillage was five times the rate before tillage.

Rills in the Meyer, et al. (7) study, unlike the authors' assumption, did not reach a geomorphic equilibrium where shear stress of flow in the channel equals the critical shear stress of the channel boundary. If this type of equilibrium is reached, rill erosion ceases. Rill erosion rates were essentially constant for the duration of both Meyer et al. (3,7) tests.

If any restricting layer is deep, the apparent equilibrium is one where the cross sections of rills erode to an equilibrium shape that erodes downward at an equilibrium rate for steady flow. If a rill reaches a nonerodible layer, it widens and eventually reaches a final width when rill erosion ceases. The time required to reach a final width depends on depth to the nonerodible layer, discharge, critical shear stress, and slope (6).

The authors' channel geometric properties a, T_o, and A_o are functions of discharge Q_o, slope S_o, and soil properties (8). These functions could and should

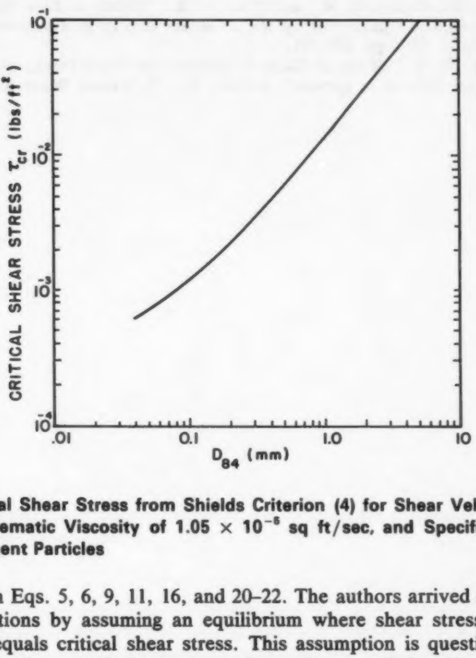

FIG. 3.—Critical Shear Stress from Shields Criterion (4) for Shear Velocity of 0.23 sq ft/sec, Kinematic Viscosity of 1.05 × 10^{-5} sq ft/sec, and Specific Gravity of 2.65 for Sediment Particles

be included in Eqs. 5, 6, 9, 11, 16, and 20–22. The authors arrived at a solution to their equations by assuming an equilibrium where shear stress of flow in the channel equals critical shear stress. This assumption is questionable, and another concept is needed. Given channel morphology relationships for erosion of cohesive soils, rill widths could be determined if Q_o could be estimated (6).

Discharge, Q_o, in each rill is often an independent hydraulic variable and is a function of rilling patterns which may be primarily deterministic rather than random. Microtopography and macrotopography as affected by tillage, land form, and crop, influence rill frequency and discharge in each rill.

Future research on rill density should include studies on rill frequency and

the fraction of total discharge in each rill. Also, study of rill morphology relationships as a function of properties of tilled, cohesive agricultural soils as they are affected by tillage, management, and cropping is another important research area.

Appendix.—References

5. Foster, G. R., "Modeling the Erosion Process," *Hydrologic Modeling of Small Watersheds,* Monograph, Chap. 8, American Society of Agricultural Engineering, St. Joseph, Mich., 1980.
6. Lane, L. J., and Foster, G. R., "Concentrated Flow Relationships," *CREAMS—A Field Scale Model for Chemicals, Runoff, and Erosion from Agricultural Management Systems,* W. G. Knisel, ed., Vol. III: Supporting Documentation; *Conservation Research Report No. 26,* U.S. Department of Agriculture, Science and Education Administration, Chap. 11, pp. 474–485, 1980.
7. Meyer, L. D., Foster, G. R., and Nikolov, S., "Effect of Flow Rate and Canopy on Rill Erosion," *Transactions of the American Society of Agricultural Engineering,* Vol. 18, No. 5, 1975, pp. 905–911.
8. Osterkamp, W. R. "Effect of Channel Sediment on Width-Discharge Relations, with Emphasis on Streams in Kansas," *Bulletin No. 21,* Kansas Water Resources Board, 1977.